Optimal Use of Distributed Energy Resources in Microgrids

By

Ramón A. Reyes Colón

A thesis submitted in partial fulfillment of the requirements for the degree of:

MASTER OF SCIENCE

In

ELECTRICAL ENGINEERING

University of Puerto Rico

Mayagüez Campus

2018

Approved by:

_____   _____
Agustín A. Irizarry Rivera, PhD.   Date
Member, Graduate Committee

_____   _____
Fabio Andrade Rengifo, PhD.   Date
Member, Graduate Committee

_____   _____
Efraín O'Neill Carrillo, PhD.   Date
President, Graduate Committee

_____   _____
Mauricio Cabrera Rios, PhD.   Date
Representative of Graduate Studies

_____   _____
José Colom Ustáriz, PhD.   Date
Chairperson of ECE Department

Abstract

Distributed generation has important advantages that must be exploited. In order to maximize the benefits, distributed energy resources (DERs) must be managed and controlled properly, especially to minimize power fluctuations from renewable energy sources. Therefore, the optimal use of distributed energy resources is an important topic, in particular within microgrids. Due to the high integration and variety of resources in a microgrids, conventional methods to optimize power systems fall short; modern methods and techniques are needed to find efficient configurations. This thesis presents an optimization algorithm developed to find efficient and stable configurations of distributed energy resources in a microgrid in different time periods, to maximize the benefits, to comply with the system constraints while considering sustainability objectives (economic, social and environmental aspects).

Resumen

La generación distribuida posee muchas ventajas importantes que deben ser explotadas. Para maximizar sus beneficios, los recursos energéticos distribuidos deben ser manejados y controlados apropiadamente, especialmente para minimizar fluctuaciones de potencia causadas por recursos energéticos renovables. Por lo tanto, el uso óptimo de recursos energéticos distribuidos es un tema importante, particularmente dentro de las microredes. Dada la alta integración y variedad de recursos en microredes, métodos convencionales para resolver problemas de optimización en sistemas de potencia no logran resolverlo; técnicas modernas de optimización son necesarias para encontrar configuraciones eficientes de recursos en una microred. Esta tesis presenta un algoritmo el cual fue desarrollado para encontrar configuraciones eficientes y estables de recursos distribuidos en una microred en diferentes periodos de tiempo, para maximizar sus beneficios, cumpliendo con las restricciones del sistema y considerando objetivos de sustentabilidad (aspectos económicos, sociales y ambientales).

"Tutto è possibile; l'impossibile richiede soltanto più tempo."

— *Dan Brown, "Crypto"*

Acknowledgement

Table of Contents

List of Figures

xiii

List of Tables

List of Abbreviations

MG	Microgrid
DG	Distributed Generation
DERs	Distributed Energy Resources
PVs	Photo-Voltaic Systems
BSS	Battery Storage Systems
OPF	Optimal Power Flow
MOPF	Microgrids Optimal Power Flow (Algorithm)
GPS	General Pattern Search (Algorithm)
EPA	Environmental Protection Agency (USA)
pu	Per Unit
EMS	Energy Management System
TES	Transactive Energy System
DSO	Distribution System Operator
SOC	State of Charge
AC	Alternating Current
DC	Direct Current
PPA	Power Purchase Agreement

Chapter 1:   Introduction

1.1 Overview

Renewable energy resources could represent a cleaner alternative to generate electric power, and to develop local socio-economic development. Their integration to conventional power systems represent a challenge because the grid was designed to operate with controllable and constant-output generators. Thus, most of the research on renewable energy integration has been based on dealing with the power fluctuations produced in conventional power systems [1]. Renewables are low inertia systems, that means they can respond fast to disturbances on the system; unlike the centralized generation with high inertia generators and limited ramp rates such as the Utility [2]. On one hand, this can be an advantage because they can respond faster to a disturbance, but on the other hand, the variabilities produced by renewables can affect the system's reliability and could cause power quality issues (voltage and frequency regulation violations). With optimization techniques, those disturbances, variances or intermittencies could be handled by compensating energy shortages with other resources. For example, if a PV system is injecting a determined amount of energy and suddenly a cloud passes-by and the PV drop its power injection, demand response (DR) could be applied to compensate this energy variance or a storage system could inject power to compensate as well. This coordination and management of resources could be achieved though optimization techniques or an advanced and controlled Energy Management System (EMS), increasing the use of renewable sources in a power system.

In the optimization procedure, there are several computational burdens and limitations such as problem's convergence, optimization time, and resources (hardware/software) needed to reach an

optimal solution in a multidimensional search space (multiple decision variables). The search space size is proportional to the number of decision variables in the problem. The following examples show the size of a search space depending on the number of decision variables:

- Example #1:

  A variable can take a discrete value from the range [0, 0.25, 0.5, 0.75, 1]; thus, this variable can take five possible values with a step of 0.25. If there are two variables with the same range, the number of possible configurations on the search space are given by the following equation:

  $$\text{\# of configurations} = \left(\frac{1}{step} + 1\right)^{(\text{\# of variables})} = \left(\frac{1}{0.25} + 1\right)^{2} = 25$$

  Therefore, there are 25 possible configurations in the search space with two variables with a 0.25 step.

- Example #2:

  160 variables with a $1 * E^{-5}$ step. The total number of possible configurations are:

  $$\text{\# of configurations} = \left(\frac{1}{step} + 1\right)^{(\text{\# of variables})} = \left(\frac{1}{1 * E^{-5}} + 1\right)^{160} \approx 1 * E^{800}$$

  Therefore, there are $1 * E^{800}$ possible configurations on the search space with 160 variables with a $1 * E^{-5}$ step; an enormous search space, thus, very difficult to find a solution. This is part of the several computational burdens and limitations to find a global or local optimum for the problem to be solved and one of the reasons traditional optimization methods fell short; thus, modern optimization methods are required.

  Renewable energy's intermittency will cause an impact on the utility's load factor; which is the ratio of the average energy in a determined period divided by the total peak energy that could

have been used in this period [3], [4]. The following figure shows a graphical example to determine the load factor:
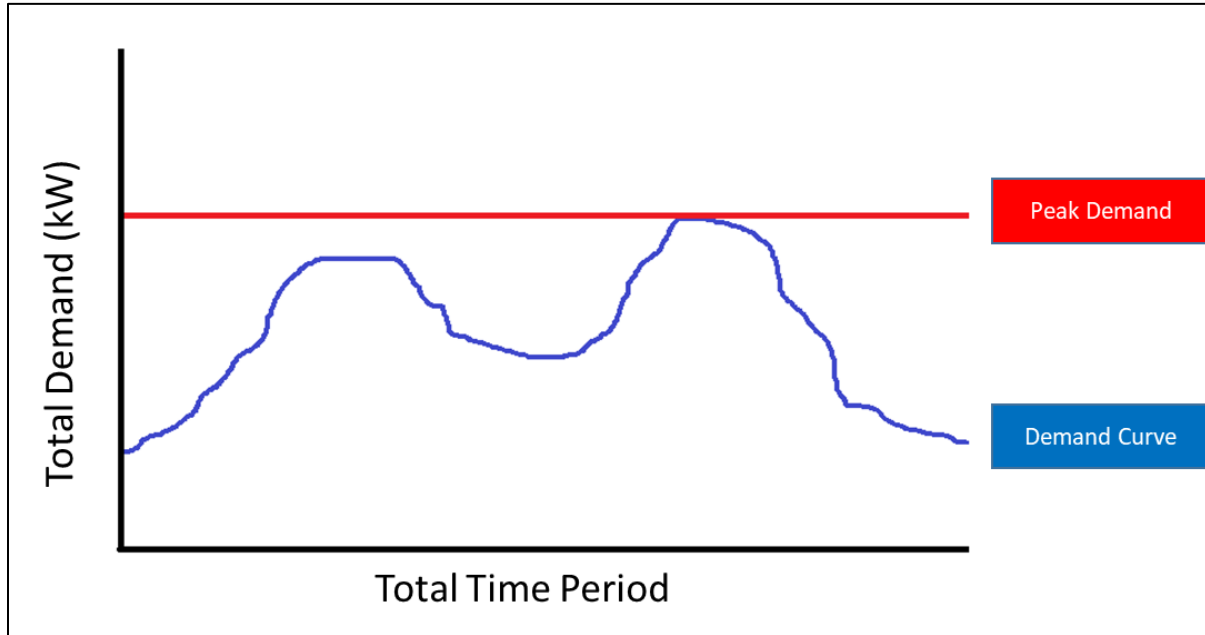
Figure 1: Demand curve for LF calculation.

In this figure, the load factor is the ratio of the area under the blue curve and the area under the red curve. The following expression can be used to calculate the load factor [3], [4]:

$$Load\ Factor = \frac{Average\ Energy\ (kWh)}{Peak\ (kW) * T} \ ; \ \text{T} = \text{time period}$$

A high load factor can decrease the total energy production costs. As presented in [5], Austin Energy stated that a 25% load factor has an average cost per kWh of 13.2 cents, while an 80% load factor has an average cost of 7.9 cents per kWh; this is one of the economic benefits of a having high load factor. The following graph show the cost per kWh as a function of the load factor:
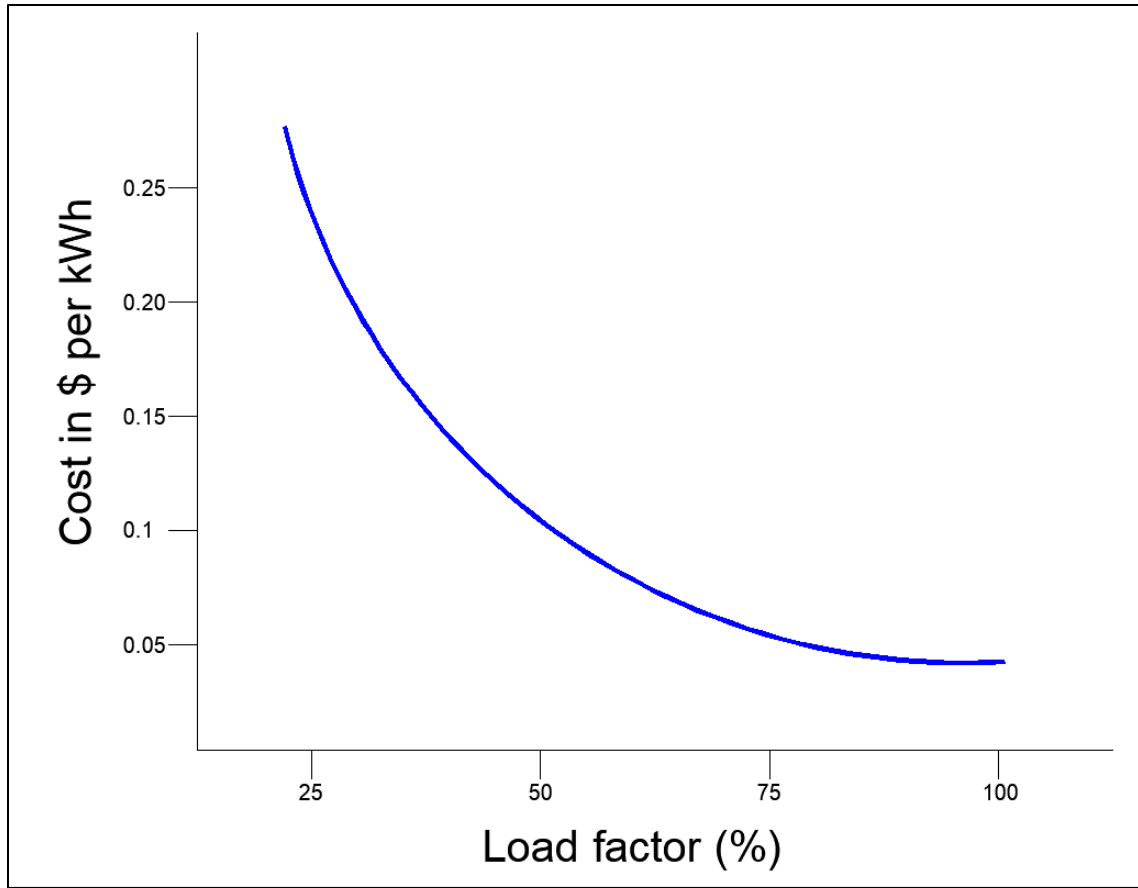
Figure 2: Cost per kWh as a function of the load factor % (Modified from [6])

From the previous graph, it can be seen that a high load factor can decrease the cost per kWh, on the other hand, a low load factor could increase the cost significantly. As presented in [7], a low load factor (below 40%) could contribute significantly on the customer's electric bill in the form of demand charges. The management and control of intermittent resources must be addressed in order to achieve a high load factor in a distribution system with a high participation of DERs. Besides economic benefits, a high load factor will allow a higher integration of renewables in the distribution system since the energy variances are being controlled and managed; thus, there is a positive environmental impact (more renewables into the system).

4

1.2 Justification

Based on the issues presented previously, regarding MGs with DERs, this thesis will address the following questions:

1) How to use available resources in order to satisfy the energy demand plus system's losses complying with the system's physical and operational constraints?

2) How to maximize the benefits provided by those DERs?

3) How DERs behave in a MG?

4) Can a multi-objective optimization achieve a zero or low net energy MG that has enough resources to minimize the impact to the grid?

5) How the interaction of DERs affects the system's operational constraints (e.g. voltage and frequency regulation)?

6) How can DERs intermittency be handled?

7) How the value provided by a MG with DERs be determined or measured?

8) How can sustainability be considered and achieved on a MG?

9) Can a multi-objective optimization support the possible creation of an energy market at the distribution level?

.

1.3 Objectives and Contributions of the Thesis

The main objective of this thesis was to develop an algorithm implementing a modern optimization method to find efficient and stable configurations of DERs, in different time periods, to take advantage and maximize the benefits provided by a MG. An Optimal Power Flow (OPF) for MGs was performed considering the system constraints. The result of the work is a stable and efficient configuration of the resources on a grid-tied (connected to the grid) or islanded (disconnected from the grid) MG in order to achieve a low dispatch cost to supply the energy demand and covering the system losses while taking in consideration physical and operation constraints. In this optimization, besides minimizing costs, other objectives can be achieved such as: maximizing the use of renewable resources (e.g., PVs) minimize the use of storage resources (e.g., BSS), minimize the use of non-renewable resources (e.g., fossil-fuel generators), minimizing system losses as well as considering environmental, social and other aspects defined by the user.

There are some optimization methods and algorithms presented in literature, some of them consider several system constraints and different resources, but not all of them possess the flexibility to apply them on every problem (they were designed for a specific system), to consider system unbalances (most of them are designed for a single-phase system or a balanced three-phase system), to add new resources such as DR, or to add new objectives functions and constraints desired by the user. In order to consider all the things mentioned before at once, a flexible and enhanced algorithm using modern optimization methods was needed. Therefore, a key contribution of this thesis was a new algorithm with such flexibility.

Another contribution is that the optimization achieved does not focus only on economic costs, it also considers broader sustainability concerns such as environmental and social aspects, as well as other values provided by MG services and its resources. The work in this thesis resulted

in the creation of a sustainable microgrid analysis and design framework that includes social, economic and environmental objectives using a multi-objective optimization approach. The framework was designed to ensure efficient and feasible configurations from the search space as long as the system's constraints, conditions and topology allow it. With the results obtained in this optimization possible estimates of the value provided by MG services and recommendations were made to answer the questions presented in Section 1.2.

1.4 Thesis Outline

The contents of this thesis are organized as follows:

- Chapter 2: Overview of DG, MGs, DERs, Optimization and Energy Markets
- Chapter 3: MG and DERs mathematical model used in MOPF Algorithm
- Chapter 4: MOPF Algorithm development and description
- Chapter 5: Case study parameters and defined data
- Chapter 6: Case study results and discussion
- Chapter 7: Conclusions and future work

Chapter 2: Distributed Energy Resources and Optimization

2.1 Microgrids and Distributed Energy Resources

A MG is a small electrical system with local distributed energy resources (DERs) and loads with the capability of operating connected to the main grid (grid-tied) or disconnected (islanded) from the main grid. The DERs could be fossil-fuel generators, PV systems, wind systems, storage systems, and several load categories [8]. Another resource could be demand response (DR) techniques used to balance the power generation and demand by changing a customer's energy-use patterns. Consumers who participate in DR may receive an incentive, but there are some regulatory concerns to be addressed first to determine how this is going to work and how feasible it is [9].

Over the past decades, policies have been established to promote the development and deployment of distributed energy resources (DERs). Nowadays, the cost of renewables and more efficient technologies are decreasing and they are becoming an affordable and attractive option for end-customers at the distribution level. Among the potential benefits provided by a MG with DERs are [8], [10]:

1) Increase of the electric system's reliability.

2) Reduction of energy production costs.

3) Improvement of economic competitiveness.

4) An emergency backup of energy supply and capacity.

5) Reduction of peak demand.

6) Capacity to provide ancillary services such as voltage and frequency regulation.

7) Power quality improvements on the grid.

8) Reduction of system's losses.

9) Management and control of energy variances produced by renewable resources (manage intermittency).

DERs are decentralized, which means they are distributed on multiple locations, unlike a utility with centralized generation, and this makes them more flexible and efficient. End-customers have the option to purchase and install DERs in their facilities or lease them from a third-party owner, commonly known as a power purchase agreement (PPA) [11]. DERs can interconnect with the main grid and use it for both purposes; buy electric energy from the utility or sell it. In this scenario, the distribution network will be the platform to accomplish those transactions. It is important to establish policies related to these transactions and how to manage the resources [12], [13]. The following figure illustrates a MG structure with its possible resources:
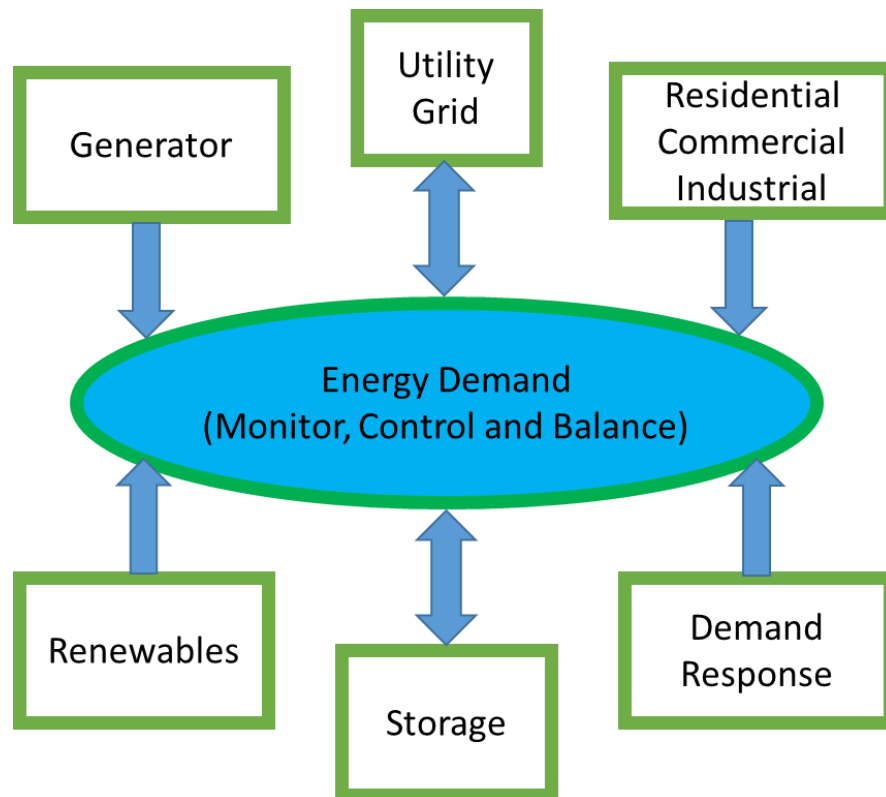
Figure 3: MG Structure (Modified from [8]*)*

9

Within this structure, local users can have more control of their resources and they could be optimized to take advantage of the benefits provided by DERs.

2.2 Optimization in Microgrids

2.2.1 Optimization Problem Definition and Methods

Any problem in engineering, physics, economics and other sciences were the main goal is to minimize or maximize something, could be expressed as an optimization problem. Optimization is a mathematical process to find the best value, point or configuration of a specific problem known as the objective function (fitness function for other methods). An optimization problem consists of minimizing or maximizing the objective by selecting values on a decision variable vector in a constrained or unconstrained search space (the problem's domain). The optimization problem can be represented as follows [14]:

$$\min \{F(x)\}$$

$$\max \{F(x)\}$$

Where:

- $F(x)$ is the objective function which can be a single objective $f(x)$ or the weighted sum of several objectives $F(x) = w_1 * f_1(x) + w_2 * f_2(x) + w_n * f_n(x)$.
- In this formulation w_i is the weight for each objective.

Optimization is often referred to as minimization and most available tools are made only to minimize. To maximize a function the problem can be written as $\min \{-F(x)\}$, which is equivalent to $\max \{F(x)\}$, and then the objective's value will be the negative of this result. Therefore, a maximization problem can be reformulated as a minimization problem [14]. In a minimization problem, the search space may have more than one or even infinite possible optimal

10

solutions (which are also feasible solutions for the problem), known as local minima or relative minimum points of the objective function. However only one global or absolute minimum value exists which is the minimum point in the whole search space. There are several methods developed by mathematicians to solve different optimization problems depending on the objective function, problem constraints and characteristics. Some of these methods are able to reach and can also guarantee a global solution, but others do not. There are methods that get caught on a local solution and others can even diverge. The achievability of a solution (global or local) will depend on the selected method, objective function, constraints and other characteristics of the problem to be optimized. These constraints and characteristics must be modeled with mathematical equations which can be convex, concave, non-convex, linear or non-linear [14]; a description of a convex and non-convex problem is available in Appendix F. Optimization methods can be deterministic, heuristic or stochastic. In this particular optimization for MGs these three kinds will be considered and tested to see which one can be applied to Optimal Power Flow (OPF) problems and which one yields better results. The different methods considered in this Thesis are representative of each kind:

- Deterministic methods (Traditional Methods)

  1) Linear/Quadratic Programming (Interior-Point Method, Simplex method)

  2) Non-linear Programming (Interior-Point Method, Sequential Quadratic Programming, Trust-Region)

- Heuristic and Stochastic methods (Modern methods of Evolutionary Programming):

  1) Swarm Intelligence Algorithms (Particle Swarm Optimization (PSO))

  2) Genetic Algorithms (Non-Sorting Genetic Algoritm-2 (NSGA-2))

  3) Pattern Search Polling Algorithms (GPSPositiveBasis2N)

A general constrained minimization problem can be written as follows [14]:

$$\min\{F(x)\}; x \in \sigma$$

Subject to: $c(x) \leq 0$; $ceq(x) = 0$

Where:

- $F(x)$ is the objective function

- x is the vector of decision variables

- σ is the search space or domain of the problem

- $c(x)$ are the problem's inequality constraints

- $ceq(x)$ are the problem's equality constraints

A constrained optimization problem can be converted into an unconstrained problem by using penalty methods. This is done by adding a term (penalty) in the objective function. In general, an unconstrained minimization problem with a penalty has the following form [15]:

$$min\left\{F(x) + \alpha_i(x) \sum c_i(x) + \beta(x) \sum ceq_i(x)\right\}; x \in \sigma$$

Where:

- $F(x)$ is the objective function

- x is the vector of decision variables

- σ is the search space or domain of the problem

- α is the penalty vector for inequality constraints

- β is the penalty vector for equality constraints

- $c(x)$ are the problem's inequality constraints

- $ceq(x)$ are the problem's equality constraints

On Chapter 3, the implementation and modeling of the problem for MG optimization using this general form of unconstrained minimization is discussed in more detail.

2.2.2 Centralized and Decentralized Optimization

Transactive energy refers to market transactions between electric energy producers and consumers, usually at distribution voltage levels. It entails economic control techniques to manage the interchange of electric energy generation and demand, for example in a MG. As presented in [16], there are currently two paradigms for how a Transactive Energy System (TES) with DERs can be designed and operated. The first one is based on a centralized, whole-system optimization performed by the transmission system operator (TSO), which needs detailed information and visibility into all levels of the system in order to be able to optimize the system and its resources and is technically an extension of the wholesale market structure that exists today but with DERs participating on it.

The second one is based on a decentralized, layered optimization structure were the system operator (DSO or TSO) only requires visibility to the interface point layers and does not need visibility to what is inside those other layers. Therefore, it will only see a single resource at each layer or the aggregated value of the individual DERs below that layer. In this paradigm the distributed system operator (DSO) will aggregate all DERs on each area and provide a single bid at the transmission and distribution (T-D) interface. Those areas are called local distribution areas (LDAs) which are defined as the distribution infrastructure and connected DERs. Thus, this might be a MG or a community at distribution level.

The centralized optimization paradigm can have disadvantages since visibility of the whole distribution system is needed for the MG optimization problem and must be considered at once.

This can become a difficult problem which can have severe computational problems and its most likely to divergence while using the methods presented previously. Furthermore, the centralized approach can require a very long time for the optimization procedure or algorithm to reach an optimal solution to the problem. On the other hand, the decentralized optimization paradigm poses great advantages over the centralized one since it can be divided into smaller problems and solved independently from one another. In the case of a bulk distribution system, MGs with DERs interconnected could be treated as LDAs, therefore they can be optimized independently. Then, the result obtained after optimizing each LDA would be used to optimize the bulk distribution system.

2.2.3 Hierarchical Energy Management System

With the decentralized paradigm, a Transactive Energy Management System could be developed and optimized in a hierarchical fashion. In [17] is presented a hierarchical Transactive Energy Management System framework for MGs to share energy excess with neighbors consisting of a three-level structure as presented in the following figure:
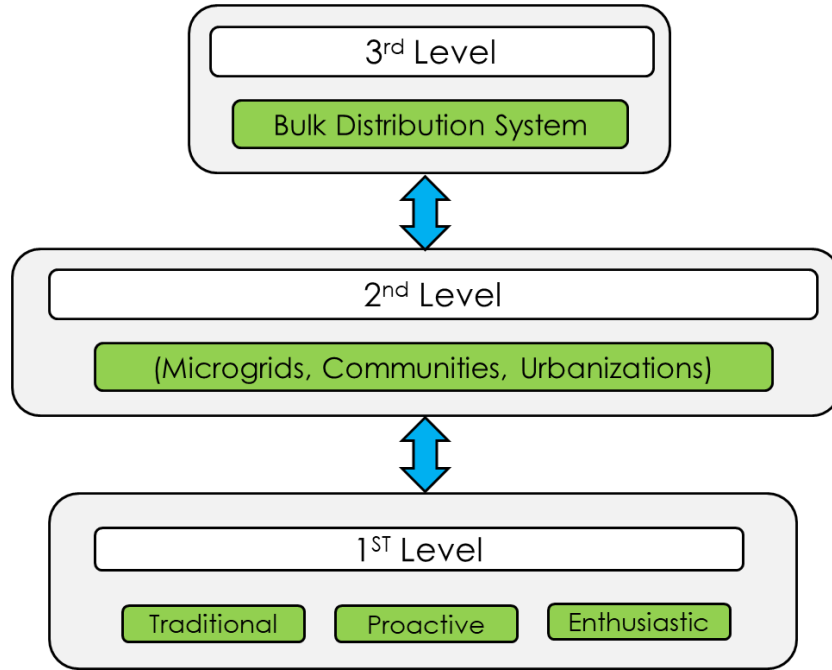
Figure 4: Hierarchical Energy Management System (Modified from [17]*)*

In the previous figure the resources have three classifications:

1) Traditional: Those are energy consumers that do not produce electricity, but they can participate with demand response (DR); nevertheless, they are not required to participate.

2) Proactive: Those are energy consumers who possess DERs and produce electricity. They can also participate in demand response (DR).

3) Enthusiastic: Same as Proactive, but also possesses storage resources such as BSS.

The whole system will be optimized following the steps shown below:

1) Apply optimization in the 1st layer at secondary distribution voltage, where the resources are connected (local resource optimization, home level).

2) Apply optimization in the 2st layer at secondary distribution voltage. At this level the output obtained in the 1st layer optimization will be used to optimize the MG, community or subdivision where DERs are interconnected.

15

3) Apply optimization in the 3nd layer at primary distribution voltage. At this level the bulk distribution system will be optimized using the output obtained in the 2st layer optimization.

2.2.4 Microgrids Control Levels

On [18] a hierarchical control framework for a MG is presented. The framework consists of three levels and each one is implemented to give support to different functions in a MG. The following table summarized the tasks in each level:

Control Level	Time required	Function support	Control components
Primary	micro/milliseconds	- Switching logic (PWM) - Protection - Local DERs control (PVs, BSS, etc.)	- Inverter controller - Storage controller - Protection relays - Generator Governor
Secondary	seconds	- Supervisory control (SCADA) - Load control (DR resources)	- MG controller - Automation system
Tertiary	minutes/hours	- Optimal Dispatch (OPF) - System Modeling - Load forecast	Software (MATLAB, GAMS, PYTHON, C++, etc.)

		▪ DERs forecast	

Table 1: Microgrids control levels (Modified from [18]*)*

The objective in the first level is to balance the energy generation with the demand. At this level, voltage and current control is performed. The most common method used to achieve the balance is the droop control due to its fast response, resiliency and needless of communication with other resources (communication in not needed) [19]. At the secondary level, voltage and frequency mismatches from the first control are corrected, by creating set-points and comparing them with the resources available; can be done using centralized or decentralized architectures. The main objective in this level is to return the system to its nominal frequency or an acceptable frequency range. A good communication structure is needed in this secondary level to receive information from all resources available and maintain the system's stability. In the tertiary control, advance functions based in models are managed. Among these functions are: economical dispatch, optimal power flow, environmental optimization, loads optimization and any other kind of optimization to be performed. To achieve this, advanced and/or complex algorithms are needed; this thesis will present an algorithm to optimize the use of DERs in a MG at this tertiary level of control.

2.3 Transactive Energy and Energy Markets at the Distribution Level

The following figure illustrates the structure of the energy markets at distribution and transmission levels.
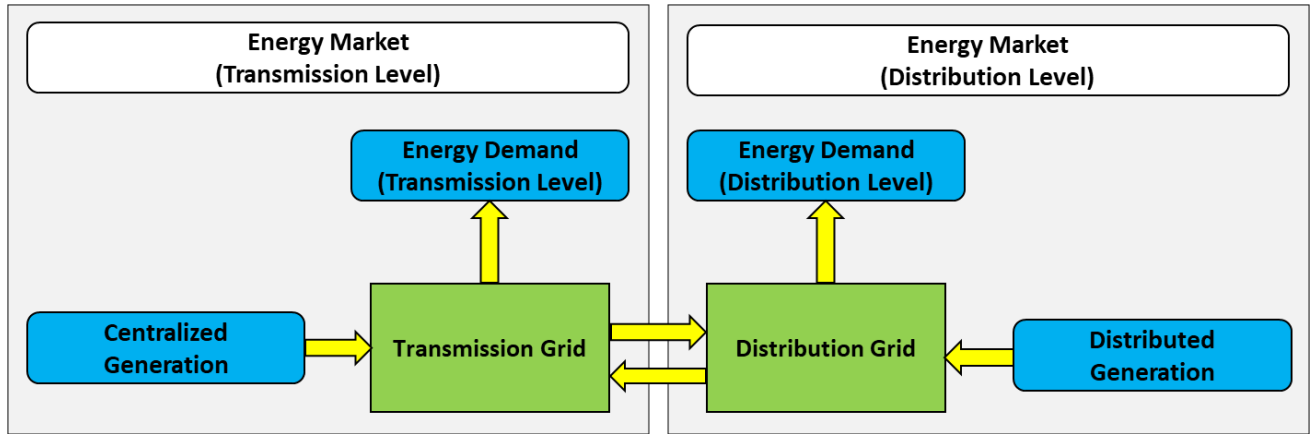
Figure 5: Energy Markets; Transmission and Distribution

On this structure both markets can be interconnected and interchange energy. At the distribution level, the energy demand could be supplied by the distributed generation or the centralized generation. Transactive Energy could enable an energy market at the distribution level with DERs; end-users could buy or sell electric energy from their resources [20].

There are some phases that need to be followed in order to achieve a market at the distribution level as presented in [21]. The following figure illustrates those steps.

Steps to Reach a Market at Distribution Level

DERs Level (vertical axis)

Time (horizontal axis)

Stage 1:
Grid
Modernization

Low DER Adoption — NY, PR and others

Infrastructure update and investment

Stage 2:
DER Integration

Moderate to high DER Adoption — CA, HI and others

DERs Integration

Distribution platform development

Stage 3:
Distributed Market

Very High DER adoption

Energy market Multi-party transactions

5% penetration

Figure 6: Distribution Market Steps (Modified from [21]*)*

Based on the previous figure, it can be seen that a very high integration of DERs and a developed distribution platform are needed to achieve a market at the distribution level, as well as an optimal coordination and control of these resources due to their high energy penetration on the electric system.

In a transactive energy system (TES), the distribution system operator (DSO), is in charge of the system's security, reliability and efficiency; its goal is to ensure that the electric energy generation and the demand are balanced and to make the system sustainable. A detailed TES with a case study is presented in [22].

19

2.4 Value of Microgrid Services

A MG with renewable-based DERs can provide many benefits among them [23], [24]:

1) Renewable Energy Integration- A Microgrid with DERs such as renewable technologies, BSS and load management (e.g., DR) can manage and reduce the variability produced by high penetrations of solar and wind power systems. Therefore, an improvement on the system's power quality and stability can be achieved.

2) System's Reliability: Power system's disturbances are mostly caused by disturbances in the distribution system. Normally, users with high reliability needs have local energy systems in their facilities. Therefore, a good approach is to place DERs at the end-user's location. This will provide a cleaner and more efficient system and, with an optimal control and management of the resources.

3) Fuel Savings: If based on renewables integration, the system will rely less on fossil-fuels and will rely more on these renewables resources. Therefore, it provides an economic reduction on fuel costs.

4) Environmental benefits (Emissions reduction): Due to renewables integration and fuel savings, there will be a reduction on emissions such as and greenhouse gasses (GHG). Therefore, the environmental impact will be less.

5) Emergency Services: MGs could serve as a backup in case of an emergency such as outages. It could also act as a backup after natural disasters, such as hurricanes, where the main electric grid may be damaged and rendered inoperable for an undetermined time period.

6) Electrification in developing countries or small islands: In the world, there are places that have no access to electric energy from a utility due to several limitations such as remote

location, size (number of customers), service viability or regulatory policies. A MG with DERs could provide electric service for those areas.

7) Ancillary services: Those services are required to maintain the grid in balance and comply with power quality standards. A MG could provide these services by dispatching reactive power (VAR) and providing support from DERs to increase the power factor of the system.

2.5 Sustainability

The United States Environmental Protection Agency (EPA) states that "Sustainability is based on a simple principle: Everything that we need for our survival and well-being depends, either directly or indirectly, on our natural environment. To pursue sustainability is to create and maintain the conditions under which humans and nature can exist in productive harmony to support present and future generations." [25]. Figure 7 shows the three pillars of sustainability:
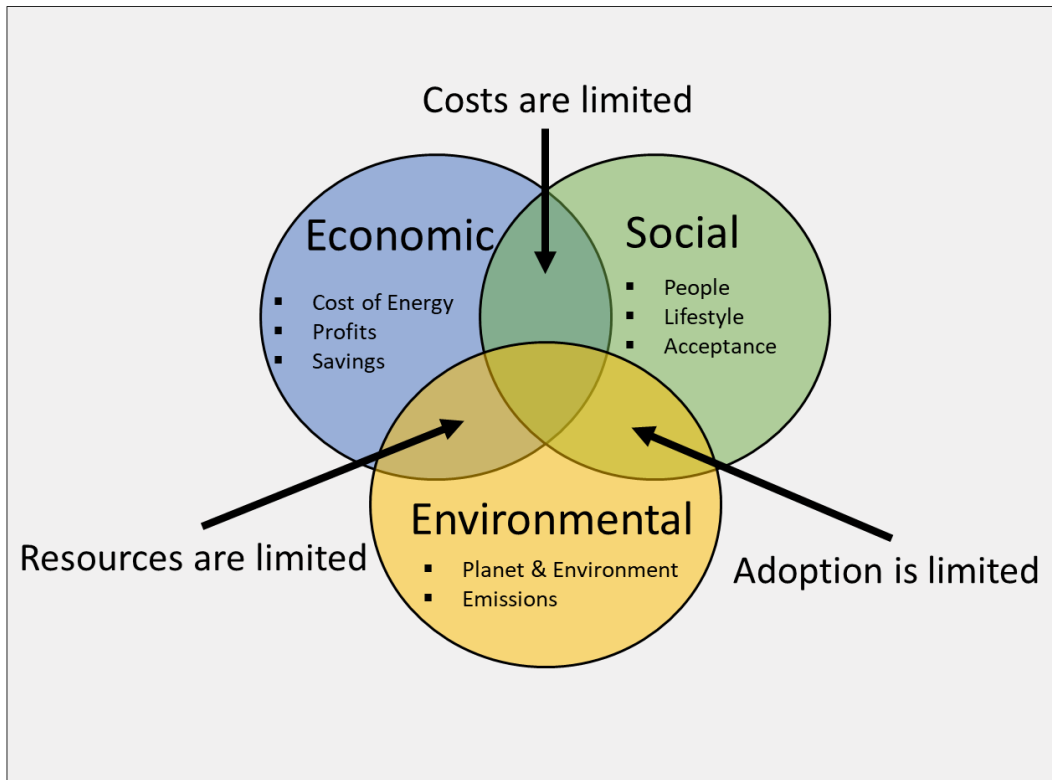
Figure 7: The Three Pillars of Sustainability (Modified from [26]*)*

On the figure, sustainability is achieved at the center of the diagram, which is held by the three pillars. It can be seen that there are economic, environmental and social limitations to achieve sustainability. Sustainable energy can be defined as an energy system capable of supplying the energy demand of a population (end-users) with energy resources that can be used without depleting them and cause little or no harm to the environment [27]. This encompasses aspects such as economics (e.g., cost of energy generation and supply), environmental issues (e.g., CO_2 emissions), and social issues (e.g., policies and regulations, customer's acceptance and willingness to contribute).

Based on Figure 7 and the statement from EPA, some questions to be asked are:

1) How can sustainability be achieved in a MG and how feasible it is?

2) Does the optimization help in any way to achieve this?

22

A planning tool for the development of sustainable MGs in remote communities with renewable energy resources is presented in [27]. It is an optimization tool to find the optimal sizing and location of DERs, considering economic, social and environmental aspects, using a modern method of evolutionary programming (NSGA-2 algorithm) with several objectives. This can be a useful tool to be used in the MGs field, but it is not enough. The optimal sizing and location of DERs is an important issue to be addressed in order to achieve sustainability. But it is also necessary to find the optimal use (optimal dispatch) of those DERs in different time periods, which was not achieved with this tool. If the resources available are not managed and controlled properly, a sustainable MG could not be achieved; or will be very difficult. In this thesis, the sustainability concept was used to give a possible answer to the questions posed in section 1.2, and an algorithm to find efficient and stable configurations of DERs considering sustainability objectives.

Chapter 3: Mathematical modeling of a Microgrid with DERs

3.1 MG and DERs modeling with their physical and operational constraints

In order to optimize a MG with DERs, the system with its constraints and resources must be modeled mathematically. Several equations are needed to model the MG components and its physical and operational constraints such as losses, capacities, transformers, etc. Resources such as photovoltaic (PV) systems, battery banks, demand response and non-renewable resources need to be modeled as well. The mathematical representation of MGs developed for this thesis is:

Cost objective function ($):

$$\min\left\{f = \sum_{t}^{T}\left(\sum_{s=1}^{S}w_s * F(P_s(t)) + \sum_{b=1}^{B}w_b * F(P_b(t)) + \sum_{dr=1}^{Dr}w_{dr} * F(P_{dr}(t)) + \sum_{u=1}^{U}w_u * F(P_u(t))\right) * \Delta t\right\}$$

Where:

- $F(P_s(t))$, $F(P_b(t))$, $F(P_{Dr}(t)))$ and $F(P_u(t))$ are the PVs, BSS, DR, and fossil-fuel resources cost functions, respectively.

- T is the time period (24-hour period).

- S, B, Dr and U are the PVs, BSS, DR and fossil-fuel resources quantity.

- w_s, w_b, w_{dr} and w_u are the PVs, BSS, DR and fossil-fuel resources cost function weight.

- Δt is the time step.

Equality constraints (Energy conservation):

$$\sum_{t=1}^{T}\left(\sum_{l=1}^{L}Pload_l(t) + Ploss\right) = \sum_{t=1}^{T}\left(\sum_{s=1}^{S}(P_s(t)) + \sum_{b=1}^{B}(P_b(t)) + \sum_{u=1}^{U}(P_u(t)) + \sum_{dr=1}^{DR}P_{dr}(t)\right)$$

Where:

- $Pload_l(t)$ are the individual loads connected in the system.

- $P_{dr}(t)$ are the clients with DR.

- $P_s(t)$, $P_b(t)$ and $P_u(t)$ is the power injected to the MG provided by PVs, BSS and fossil-fuel resources, respectively.

- $Ploss$ are the total system losses.

Penalty Functions:

$$Sl = \sum_{t=1}^{T} (w_{slack} * P_{slack}(t))$$

$$Vl = \sum_{t=1}^{T} w_{viol} * (viol(t))$$

Where:

- $P_{slack}(t)$ is the slack's power injection.

- $w_{slack}(t)$ is the slack's penalty weight (defined by the user).

- $viol(t)$ is the number of voltage and current violations (values outside the defined bounds) in the system.

- w_{viol} is the violation's function penalty weight.

Main Objective Function

$$min \left\{ F = \sum_{t=1}^{T} f + Sl + Vl \right\}$$

Where:

- f is the cost objective function.

- Sl is the slack's injection penalty function.

- Vl is the violation's penalty function.

PVs equations:

$$P_s(t) \; ; 0 \le P_s(t) \le Pmax_s$$

$$F\big(P_s(t)\big) = rate_s(t) * P_s(t)$$

Where:

- $P_s(t)$ is the PV system power output (inverter's s output) in kW at time t.

- $rate_s(t) = $ PV system rate in $\frac{\$}{kWh}$.

- $F\big(P_s(t)\big)$ is the cost function for the PV systems.

BSS equations:

$$P_b(t), \qquad Pmin_b \le P_b(t) \le Pmax_b \;\; (kW)$$

$$F\big(P_b(t)\big) = rate_b(t) * P_b(t)$$

$$discharging: \;\; Q_b^{t+1} = Q_b^t - \eta_b P_b(t) * \Delta t; \;\; \eta_b * P_b(t) \le \; Q_b(t)$$

$$charging: \;\; Q_b^{t+1} = Q_b^t + \eta_b * P_b(t) * \Delta t; \;\; \eta_b * P_b(t) \le \; Q_b(t)$$

Where:

- $P_b(t)$ is the BSS input/output power (charging or discharging)

- Q_b^{t+1} is the charge state at time t+1 (new state of charge)

- Q_b^t is the charge state at time t (current state of charge)

- η_d is the BSS charge/discharge efficiency

- $F\big(P_b(t)\big)$ is the BSS cost function

- Δt is the time step

Demand response equations:

$$P_{dr}(t) = \lambda_{dr}(t) * Pload_l(t)$$

$$F\big(P_{dr}(t)\big) = rate_{dr}(t) * P_{dr}(t)$$

Where:

- $P_{dr}(t)$ is the total DR contributed.

- λ_{dr} is the demand reduction percentage.

Utility and fossil fuel generators equation:

$$\mathrm{F}\big(P_u(t)\big) = a * P_u(t)^2 + b * P_u(t) + c; \; Pmin_u \leq P_u(t) \leq Pmax_u$$

Where:

- $P_u(t)$ is the power generated by the fossil generator or the utility.

- a, b and c are the generator's cost function coefficients (some of these coefficients can have a value equal to zero).

Loads (Real and Reactive Power Demands) equations:

$$Pload_l(t) = P_l(t)$$

$$Qload_l(t) = Q_l(t)$$

Where:

- $P_l(t)$ is the load real power consumption in kW at time t

- $Q_l(t)$ is the load reactive power consumption in kVar at time t

The equations used to model a MG with DERs that describe the system and resource's behavior were appropriate for the scenarios simulated [15]. Nevertheless, the user could consider more details in any particular equation to describe other behavior of interest.

3.2 Social aspects to consider in the model

There are social aspects that might affect the MG with DERs optimization results and should be considered:

- The energy use patterns of the customers.

- The willingness of customers to change their energy use habits.

In a MG, there may be different types of customers with different social classes and behaviors. There are some customers that can afford and invest in PV systems and storage devices (Enthusiast customers), others who can only afford PV systems (Proactive customers) and others who cannot afford or are not willing to invest on DERs (Traditional customers with or without DR) [17]. There are also different customer willingness levels to contribute with DR that must considered. The maximum amount of DR contribution will depend on the customer's willingness to change their energy consumption behavior. A flexible client may contribute with more DR than a less flexible one [28], [29]. The social and/or economic position of a customer could be a factor that affects the maximum DR contribution. As an example, an affluent customer could afford to pay high energy rates, therefore, his demand elasticity could have a low value (his demand will not change significantly when the rate per kWh increases). On the other hand, an economically-challenged customer could react to price signals by changing his/her energy demand pattern; thus, demand elasticity could be higher than other types of customers. Furthermore, there could be skeptical customers that simply do not support DR and prefer to remain as traditional customers with no DR contribution. Some considerations when the optimization is taking place include:

- Percentage of customers with PVs in each busbar.

- Percentage of customers with storage resources in each busbar.

- Number of customers contributing with DR in each busbar.

- Demand elasticity of these customers with DR, as a function of price signals in order to determine the maximum DR percentage available in each busbar.

Demand elasticity is basically the relation between the demand change percentage and a price change percentage. A general expression to determine the demand elasticity can be expressed as follows [30]–[32]:

$$Demand\ elasticity = \frac{Demand\ change\ percentage}{Price\ change\ percentage}$$

When this relation gives a value less than 1 pu, it is said to be an inelastic demand (demand will not change significantly when price increases); for values greater than 1, it is said to be an elastic demand (demand will change significantly when price increases); and if this relation gives a value equal to 1, it is said to be a unitary elastic demand (demand will change proportionally, 1:1 proportion, when price increases) [30]. Since a demand change percentage can be interpreted as an energy demand percentage reduction in a power system, which is equivalent to the DR contributed by a customer, the demand change percentage in the previous relation can be rewritten as:

$$DR(percentage) = Demand\ elasticity\ (pu) * Price\ change(percentage)$$

For this thesis, four customer categories with different demand elasticities were considered. Assuming an elasticity range between [0,1] pu, an elasticity allocation for each category was made. This allocation is basically a third fraction of this [0,1] range for each category, were category 3 have a demand elasticity greater than category 2, and category 2 have a demand elasticity greater than category 1. Customers who does not contribute with DR will be classified as category 4. The allocation was done as follows:

- Category 1 – [0, 0.333] pu
- Category 2 – [0, 0.667] pu
- Category 3 – [0, 1] pu

- Category 4 – 0 pu

Using the elasticity allocation values and a $price\ change(percentage) = 25\%$, the maximum

DR percentage range per category was calculated as follows:

- $DR_{cat1}(\%) = [0, 0.333] * 25\% = [0, 8.33]\%$

- $DR_{cat\ 2}(\%) = [0, 0.667] * 25\% = [0, 16.67]\%$

- $DR_{cat\ 3}(\%) = [0, 1] * 25\% = [0, 25]\%$

- $DR_{cat\ 4}(\%) = 0 * 25\% = 0\%$

Therefore, category 1 could contribute with a maximum DR of 8.33%; category 2 could

contribute with a maximum DR of 16.67%; category 3 could contribute with a maximum DR of

25%; and category 4 will not contribute with DR. It is important to emphasize that these values

may change if the assumptions made are different or if actual data is obtained from surveys on

customer willingness and habits. The assumptions used are meant to include social aspects that

could impact the maximum DR available in the optimization results (since DR is considered an

energy resource).

The following table shows an example of the total DR available in a busbar, assuming that five

of these ten customers are willing to contribute with DR and the other five customers do not. In

this example, two of them are category 1, two of them are category 2, and just one of them is

category 3.

	# of customers	Maximum DR contribution (per customer)
DR with Category 1	2	8.33%
DR with Category 2	2	16.67%

DR with Category 3	1	25%
DR with Category 4	5	0%
Total DR available (aggregated) $= \dfrac{2*8.33\% + 2*16.67\% + 1*25\% + 5*0\%}{10\ customers} = \mathbf{7.5\%}$		

Table 2: Example of total DR available in a busbar.

In this example, the maximum DR available is 7.5% of the total energy demand in the busbar. A general expression to calculate the maximum DR available in a busbar can be expressed as follows:

$$DR(\%) = \frac{\left(\left(\sum_{i=1}^{3} (\#\ of\ customers\ with\ category_i\ ) * (maximum\ DR_{cat\ i}\ contribution(\%)) \right) \right)}{Total\ \#\ of\ customers}$$

3.3 Environmental aspects to consider in the model

On the scenarios simulated, the resources being optimized are PVs, BSS, DR and they are considered to be environmentally friendly, therefore none on them will produce emissions and cause environmental harms. In this analysis, BSS were considered "friendly" as an enabling technology that allows a reduction of fossil-fuel use. However, BSS could have negative environmental impact if not properly disposed [33], [34]. It was assumed that the only resource in a MG that can produce emissions is the utility, since it is considered to be a fossil-fuel generator. The amount of emissions produced by the utility will depend on the energy demanded from the MG, the contracted energy and the fossil-fuel resource used by this generator. The following table show emission rates ($\frac{kg\ CO_2}{kWh}$) based on different fossil-fuels [35].

Generator fossil-fuel	CO_2 Emissions rate $\left(\dfrac{kg\ CO_2}{kWh}\right)$
Coal, steam generator	0.9606
Petroleum, steam generator	0.7434
Natural gas, combustion turbine	0.6042
Natural gas, combined cycle	0.4066

Table 3: Emission rates for fossil generators [5].

As presented in [35], the total emissions ($kg\ CO_2$) issued by fossil-fuel generators can be expressed as follows:

$$Emissions(kg\ CO_2) = Energy\ production(kWh) * emmision\ rate\left(\frac{kg\ CO_2}{kWh}\right)$$

For the scenarios in this thesis, the utility will use different percentages of each fossil-fuel resource. Those percentages are: 10% of coal, steam generator; 20% of petroleum, steam generator; 30% of natural gas, combustion turbine; and 40% of natural gas, combined cycle.

Chapter 4:   Microgrids Optimal Power Flow

4.1 Optimization Approaches for MGs

There are several approaches presented in literature to optimize MGs with DERs. Most of these approaches try to optimize MGs considering economical aspects and some physical and operational constraints of the system, but there are other important aspects, constraints and condition in the system that may affect the optimization results. For example, in [36] a genetic algorithm (Fuzzy-GA) is presented to improve the MG's economic efficiency and ensure cost savings for customers, but it does not consider restrictions such as voltage regulation (upper and lower voltage bounds), nor load unbalances which are very common on distribution systems. On [37], the authors formulated the MG's energy management as an optimal power flow (OPF) problem. They considered several constraints in the system, but they assumed renewables as a non-dispatchable resources (they always inject their maximum energy available into the system). Nowadays renewables technologies are evolving, those resources can be dispatchable (their power output can be controlled) and they could also contribute with reactive power as well. DR is another resource that was not considered and can change the optimization results. On [15], an Energy Management Strategy using enhanced the Bee Colony Optimization (BCO) is presented. It has a very good mathematical model for the energy resources and the system's constraints, but renewables are not-dispatchable and DR in not considered as an energy resource. There are also other software such as Matpower [38], but this software is used to optimize just in a particular time, not for several time periods, or, as in this thesis, a day ahead optimization. Thus, in order to consider other constraints that may affect the system, to consider sustainability considerations such

as social and environmental aspects, and also to consider other resources such as DR, a new method

or algorithm that considers all these aspects and elements was needed.

4.2 General Pattern Search (GPS) and Back/Forward Sweep Algorithms

In order to develop an algorithm to optimize a MG with multiple DERs, an algorithm to

select decision variables in a search space was needed. For this selection, the methods presented

in section 2.2.1 (Optimization Problem Definition and Methods) were tested. During this testing,

the algorithm that showed the best behavior and results for this particular problem was the pattern

search method with the "GPSPositiveBasis2N" algorithm (constant power demanded from the

utility, reasonable convergence time, low penalty value, solutions with sense, high load factor

achieved on the simulations, etc.). This method was also compared with other ones, as presented

in [39] and Appendix E. Methods such as genetic algorithms (GA) and particle swarm

optimization (PSO) converged very slowly (too much time to reach a solution) and did not achieve

the same high load factor as the one obtained with the pattern search algorithm. Traditional

methods, such as the interior-point method, yielded a low-value objective function, but the power

demanded by the utility did not meet the target and the penalty value was high. Those traditional

methods can yield better results for problems with a small quantity of variables (In a MG, there

is a large quantity of variables). On the other hand, the GPS algorithm has a heuristic nature, thus

a global solution (which is the optimal solution) cannot be guaranteed; a local solution is more

likely. Nevertheless, a local solution (which is a good solution) from the search space is an

efficient and stable configuration that comply with the simulation goals and the system

constraints. The pattern search algorithm is a polling method which starts at an initial point x_0

defined by the user (flat-start point) [40]. More detailed information about how a pattern search polling works is presented in [41] as well as in Appendix E.

The MG's optimization algorithm also needed an unbalanced load flow algorithm. For this, the back/forward sweep algorithm was selected (presented and adapted from [42]). This algorithm is commonly used for three-phase load-flow analysis of radial distribution systems. More detailed information about how the back/forward sweep method works is presented in [43] as well as in Appendix E.

4.3 Microgrids Optimal Power Flow (MOPF) Algorithm

An algorithm to optimize MGs with DERs was developed implementing the mathematical model of a MG with DERs presented in the previous section, the "GPSPositivebasis2N" algorithm for the decision variables selection and the back/forward sweep algorithm for the unbalanced load flow. This algorithm was named Microgrids Optimal Power Flow (MOPF), and it follows a sequence of steps as presented in Figure 8.

It is important to emphasize that this is an initial version of the algorithm. It can be modified and enhanced to better address different optimization problems or other objectives need by the user. Since it was written in MATLAB, it is very flexible and changes such as replacing the load flow algorithm, the random decision variables selection algorithm, the input data, objectives and penalty functions can be done easily (knowledge in power systems, DERs, optimization and programming in MATLAB are required). For example, during Spring 2018 undergraduate students from a Senior design course at UPRM were able to modify and use the algorithm in the analysis and design of a community microgrid. In addition, the user can also put priorities to the resources available. For example, if the user desires to use and dispatch the resources in the following order:

PVs (1st), DR (2nd), BSS (3rd), weights can be assigned to each resource to establish this priority. It is important to emphasize as well that the algorithm cannot guarantee a global solution to any type of problem because that would depend on the nature of the problem being solved and the limitations of the methods and routines being used. However, even in those cases the solutions could be local solutions, which are good solutions. On this thesis, the algorithm was used as a tool to make analyses and reach conclusions regarding DERs optimization and the value of MG services. Through the scenarios developed and studied, the author of this thesis proved that this MOPF algorithm is indeed a framework that can be used for the analysis and design of sustainable microgrids.
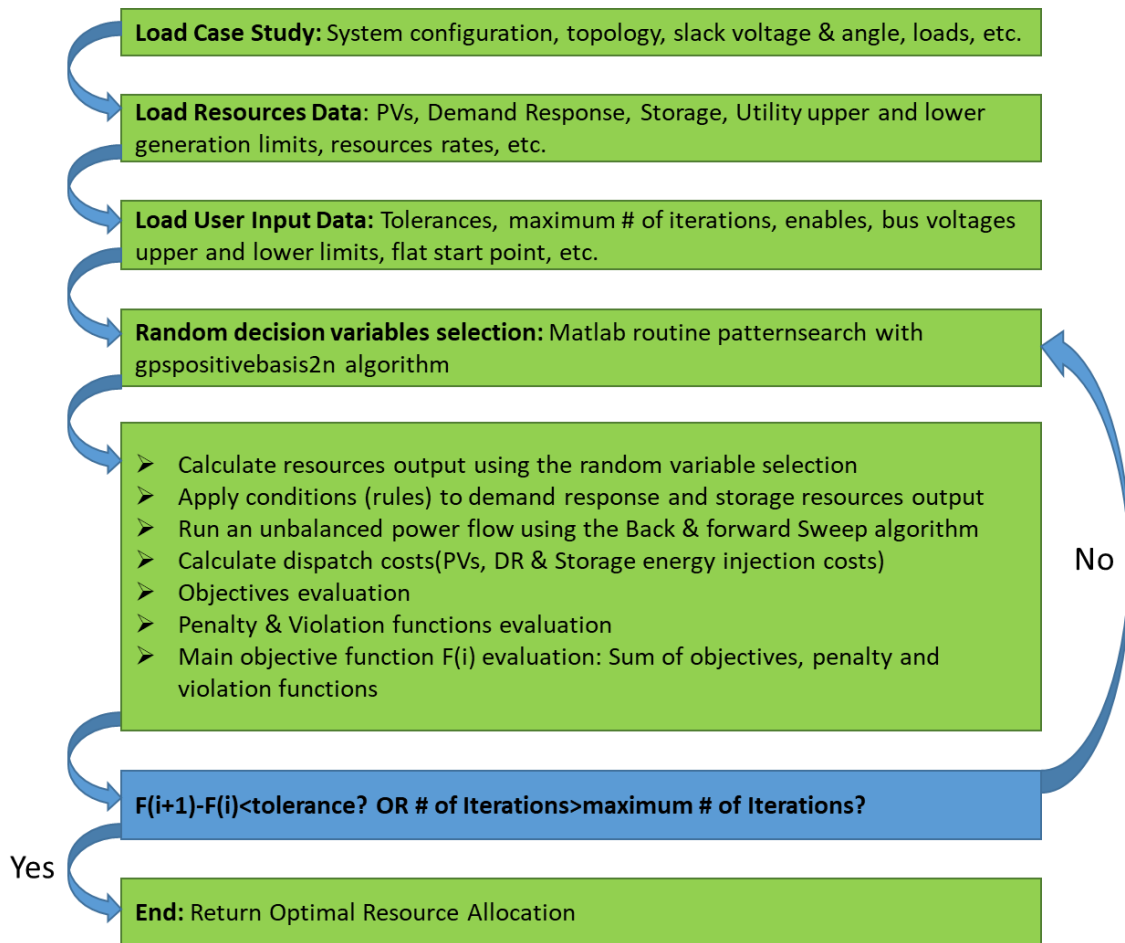
Figure 8: MOPF Algorithm Flowchart

36

Chapter 5:   Analysis of Sustainable Microgrids

5.1 Case Study Topology

An actual power system was used to create analysis scenarios to test the MOPF algorithm. The case study was based on a subset of a community in Southern Puerto Rico, which was also used in [44]. The scenarios developed had different types and levels of DER participation in a MG, so that effects on the utility system could be studied. This case study consisted of 20 groups of 10 houses, all of them with PVs, BSS, loads and DR. The whole community was modeled with a 45-bus system as presented in Appendix C. The assumptions and data values for the scenarios are presented next.

5.2 Simulation Assumptions, Data Values and Summary of Cases

Demand curves per busbar:

- 20 demand curves were generated based on three basic profiles for 20 buses (10 residential clients per busbar) [44]. Each generated curve is based on a percentage of one of those three curves. The percentage for each demand profile were generated randomly and the sum of these percentages equals 100% (e.g., 30% of profile 1, 40 % of profile 2 and 30 % of profile 3).

- The end-users are connected to single-phase distribution transformers. The power demand is supplied through two phases. Since it is common to find unbalance in a power system, the total demand is divided in the two phases with a maximum load unbalance of 20% (e.g., 40% of demand in phase 1 and 60% of demand in phase 2). The allocation of this unbalance is generated randomly, considering this maximum unbalance between phases.

- All loads have a 0.9 power factor (pf); thus, they consume reactive power as well.

  Given that: $\cos(\theta) = pf$ and $\tan(\theta) = \frac{Q(t)}{P(t)}$, the reactive power demanded in each time

  step is calculated as: $Q(t) = P(t) * \tan(\cos^{-1}(pf)) = 0.4843 * P(t)$. The reactive power

  demanded will be a fraction of the real power demanded, but this could be changed if the

  use needs to study a more fluctuating reactive power demand.

Demand response (DR):

- DR percentages were calculated based on the three categories presented previously with

  different demand elasticities and a 25% price change. The assumptions and equations

  presented in section 3.2 were used (social aspects to consider in the model).

Solar Irradiation Curves:

- Solar Irradiation curves from [44] were discretized every 15 minutes and every 1 hour. The

  15-minute discretized curves (sunny96.mat and cloudy96.mat) have 96 data points and the

  hourly discretized curves (sunny24.mat and cloudy24.mat) have 24 data points. For the

  cases simulated, the 15-minute discretized curves were used. To run simulations with these

  96-point curves, good computational resources (hardware) were needed due to

  computational burdens and long simulation time (hours). For this thesis, simulations were

  done using an Intel(R) Core(TM) i7-4702MQ CPU (Quad-core processor) and 16GB of

  RAM. To run simulations with a smaller time step (e.g., 5 minutes, 1 minute or real-time)

  better resources are needed (an i7 processor with 16GB of RAM are not enough;

  simulations could last days).

- The irradiation curves are normalized (values between 0 and 1) and are multiplied by the

  PVs maximum capacity (inverter's maximum capacity) in each time step. Therefore, when

the time step reaches the maximum irradiance point in the curve, the PVs will produce their maximum power generation.

PV systems:

- A 3-kW PV system will be used for all end-users. Therefore, since there are 10 clients per busbar, a 30-kW aggregated PV system will be available in each busbar. The PVs power output will follow the solar irradiation curves defined previously.

- Those PVs can supply energy with a 0.8 power factor, therefore, they can supply reactive power (Var) as well.

Storage:

- The LG RESU10H (Li-ion technology) was used to simulate the storage devices. This battery has a maximum capacity of 9.8-kWh and a maximum charge/discharge rate of 5-kW. However, LG recommends a 3.3-kW charge/discharge rate for maximum battery life [45]. Thus, a 3.3-kW discharge rate and a 1.1-kW (1/3 of discharge rate) charge rate was set for all storage devices to maximize their life expectancy. Since there are 10 of these resources in each bus bar, each one has an aggregated BSS of 98-kWh with a 33-kW discharge rate and 11-kW charge rate.

- At the beginning of the simulations, all BSS were assumed to have a 70% state of charge (SOC), equivalent to 68.6-kWh of energy stored, and a 40% minimum SOC, equivalent to 39.2-kWh of reserved energy; unless otherwise noted.

Utility:

- The utility will supply a predefined energy amount, representing a contract between the MG and the utility for a constant demand of electric energy. For example, on cases 4 and 5, it will deliver 30-kW per phase (90-kW in total) in each time step.

Energy production cost rates (Appendix H provides more detailed information and justification of the rates set):

- The rates for PV resources were set to $0.10 \frac{\$}{kWh}$.

- Reactive power rates will be $\frac{1}{10}$ of the real power rates of each resource (e.g., $0.01 \frac{\$}{kVarh}$).

- DR rates will be the utility's price change percentage; e.g., if the utility's rate is $0.20 \frac{\$}{kWh}$ and there is a price change of 25%, equivalent to $0.05 \frac{\$}{kWh}$, DR rates will be $0.05 \frac{\$}{kWh}$.

- The rate for storage resources are set to $0.30 \frac{\$}{kWh}$; storage resources are more expensive than the other resources.

- The utility's rate was set to $0.20 \frac{\$}{kWh}$; A common bill/rate value in Puerto Rico in 2017 [46].

The previous assumptions will be used on all cases unless otherwise noted. Table 4 shows a summary of the cases simulated:

For the grid-tie mode, the MG will be demanding or selling a predefined power contracted from the utility. For the islanded, stand-alone or zero-power mode, the utility will deliver/sell zero-power to the MG. Zero-power means the MG is connected to the utility, but will demand or sell zero power from it. Islanded means the MG is disconnected from the utility, but if the resources are not enough to balance the demand it will need to interconnect with the utility and buy power

from it. In a practical application of the stand-alone case, the utility would charge for back-up or emergency services provided. That discussion was not part of the scope of this thesis.

Table 4: Summary of cases

Case	Optimization Applied	DERs	Utility	Solar Irradiance	Microgrid Mode
1	No	None	Acting as a Slack	*Not apply	Grid-Tie
2	No	Only PVs injecting their maximum energy available	Acting as a Slack	Sunny Day	Grid-Tie
3	No	Only PVs injecting their maximum energy available	Acting as a Slack	Cloudy Day	Grid-Tie
4	Yes	All available (PVs, DR and BSS)	Supplying 90-kW on each time step	Sunny Day	Grid-Tie
5	Yes	All available (PVs, DR and BSS)	Supplying 90-kW on each time step	Cloudy Day	Grid-Tie
6	Yes	All available (PVs, DR and BSS)	Supplying 0-kW on each time step	Sunny Day	Islanded or Zero-Power (Grid-Tie)
7	Yes	All available (PVs, DR and BSS)	Supplying 0-kW on each time step	Cloudy Day	Islanded or

					Zero-Power (Grid-Tie)
8	Yes	All available (PVs, DR and BSS), but with less resources	Supplying 90-kW on each time step	Sunny Day	Grid-Tie
9	Yes	All available (PVs, DR and BSS), but with less resources	Supplying 90-kW on each time step	Cloudy Day	Grid-Tie
10	Yes	All available (PVs, DR and BSS), with higher BSS capacity	Supplying 0-kW on each time step	Sunny Day	Islanded or Zero-Power (Grid-Tie)
11	Yes	All available (PVs, DR and BSS), with higher BSS capacity	Supplying 0-kW on each time step	Cloudy Day	Islanded or Zero-Power (Grid-Tie)
12	Yes	All available (PVs, DR and BSS); with higher BSS capacity	Buying 90-kW on each time step	Sunny Day	Grid-Tie
13	Yes	All available (PVs, DR and BSS), with higher BSS capacity	Buying 90-kW on each time step	Cloudy Day	Grid-Tie
14	Yes	All available (PVs, DR and BSS), with a lead-acid BSS	Supplying 0-kW on each time step	Sunny Day	Islanded or Zero-Power (Grid-Tie)

Chapter 6: Results and Discussion

6.1 Case #1: Utility/Slack with no optimization

This was a base case, with no optimization and no DERs. The only resource available to supply the energy demanded is the utility. The following graphs were obtained after simulating case 1. The load factor obtained in this case was 43.14 %, which can be considered a low value.
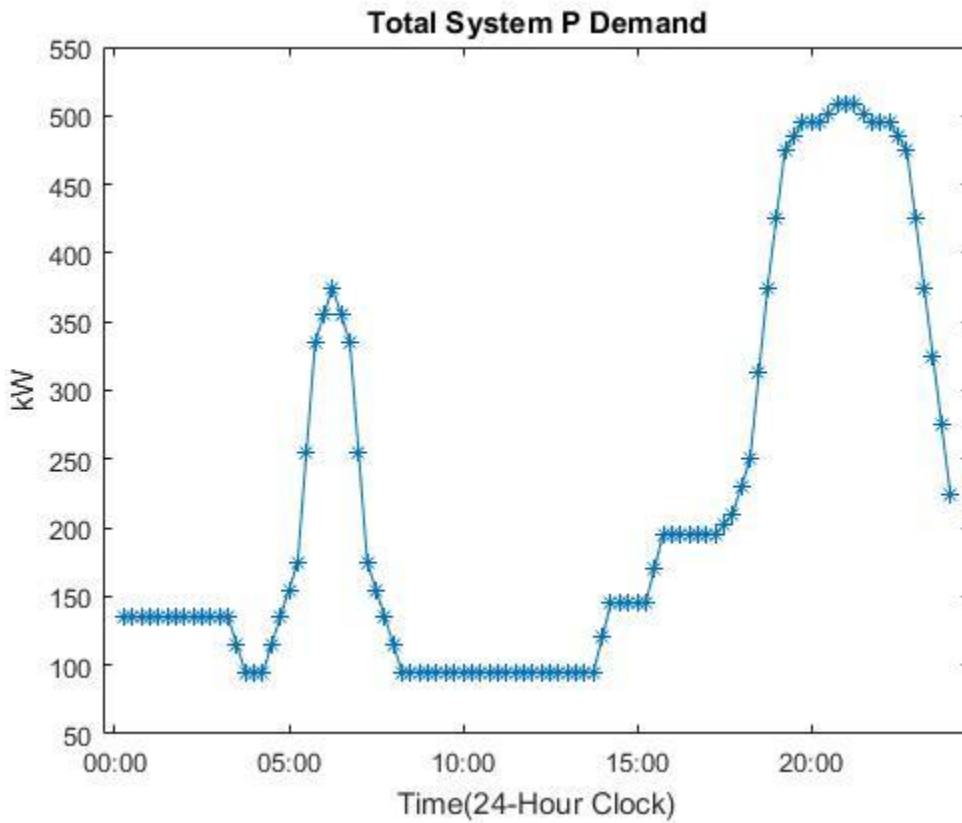
Figure 9: Total real power demanded in each time step (Case #1).
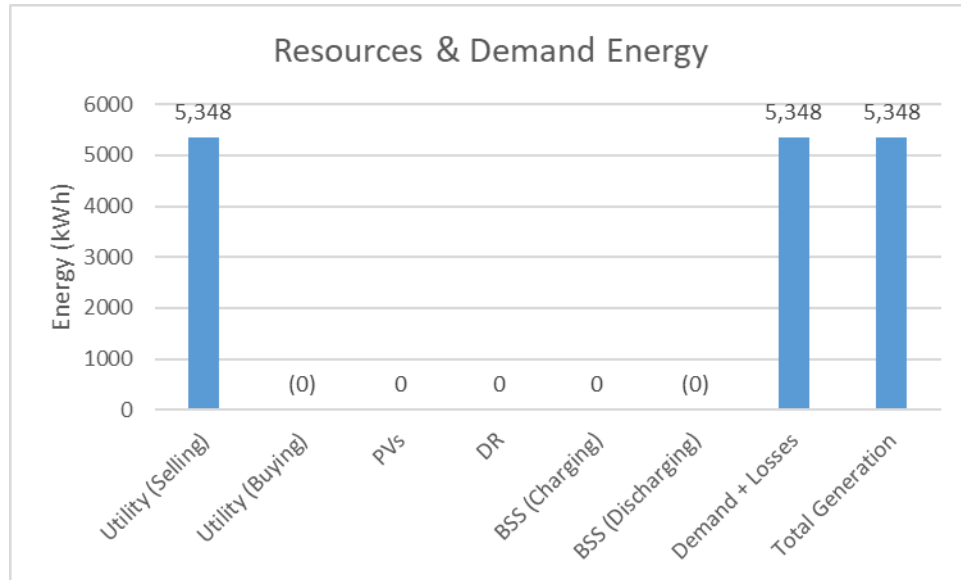
Figure 10: Resources and Demand Energy (Case #1).

6.2 Case #2: Utility/Slack and PVs (Sunny day) with no optimization

On this case, there are two energy resources that can supply the energy demand; the PVs and the utility. This case had no optimization but the PV systems inject their maximum energy available, during a sunny day. The utility acts as a slack (providing any electric energy deficiency). The following graphs were obtained after simulating case 2:
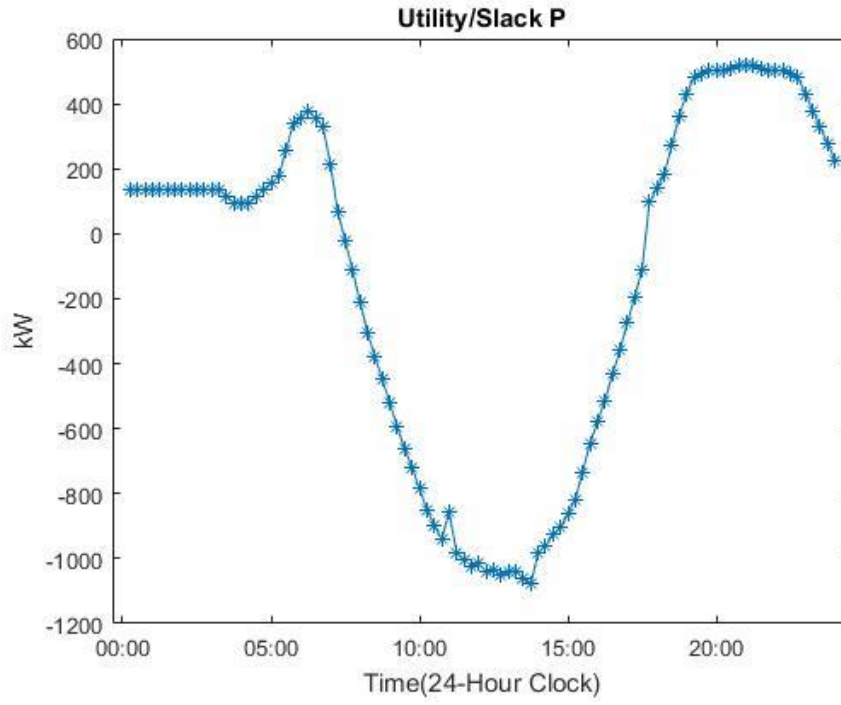
Figure 11: Utility real power (P) injection in each time step (Case #2).

Figure 12: Utility reactive power (Q) injection in each time step (Case #2).

45
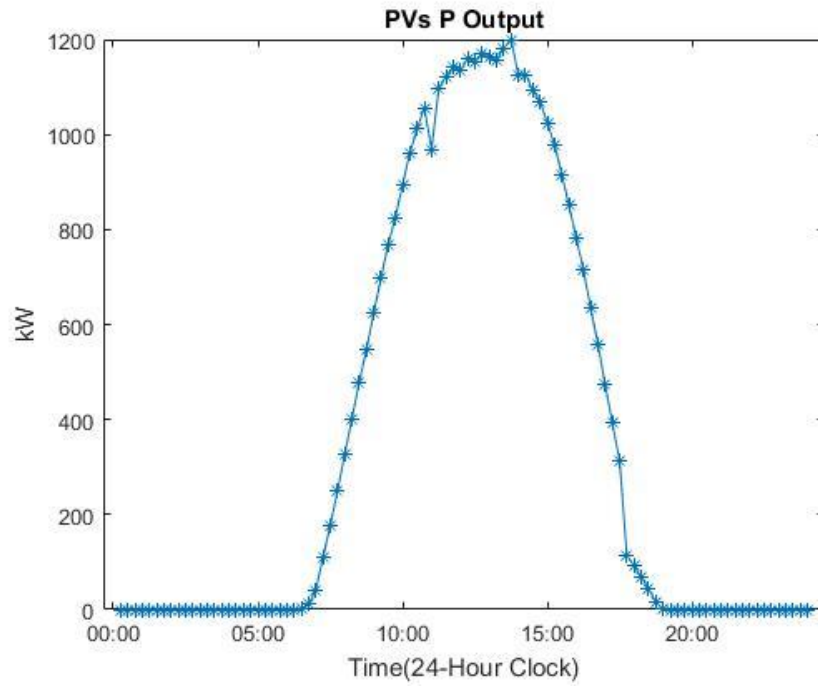
Figure 13: PVs real power output in each time step (Case #2).
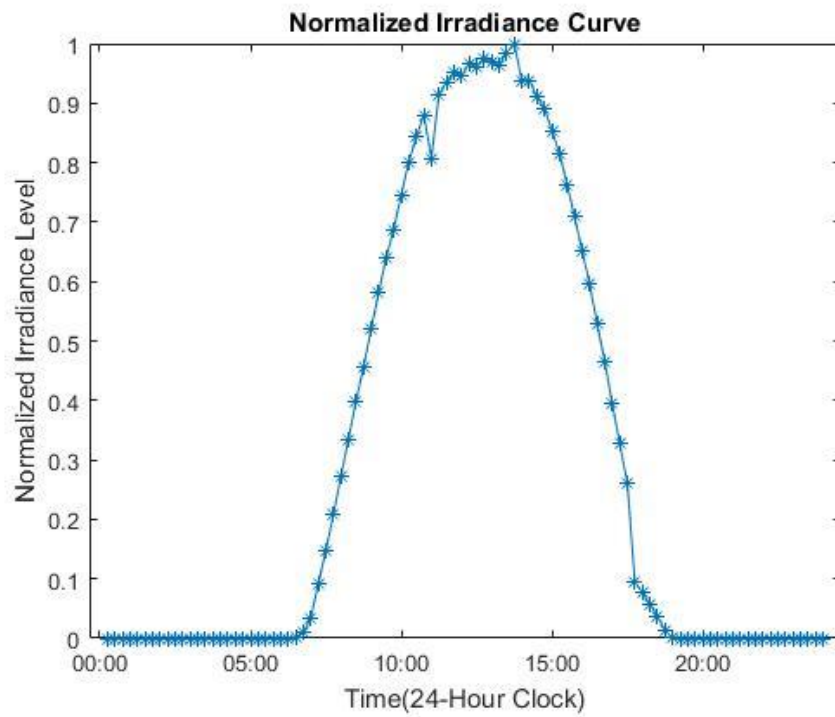
Figure 14: Normalized solar irradiance curve for a sunny day (Case #2).

46
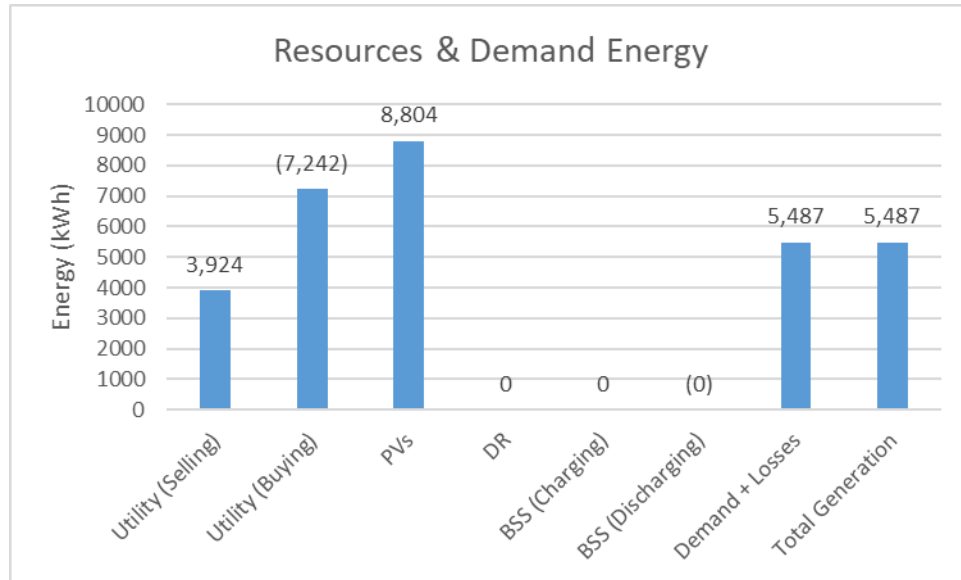
Figure 15: Resources and Demand Energy (Case #2).

Since the PVs are injecting their maximum energy available, the solar irradiation curve and the PVs real power curve have the same shape. The utility's real power curve has negatives values; which means a power flow in the utility's direction, in other words, sending or selling power to the utility. This also explains why the cost of energy production curve has negative values as well (A positive value means selling power and a negative value means buying power). The load factor obtained in this case was 12.82%; a very low value, therefore, the PVs do not improve the load factor if they are not controlled or managed properly.

6.3 Case #3: Utility/Slack and PVs (Cloudy day) with no optimization

This case is the same as case 2, the only difference is the solar irradiation curve (a sunny day for case 2 and a cloudy day for case 3). This case had no optimization, PVs injecting their maximum energy available in a cloudy day, and the utility acting as a slack. The following graphs were obtained after simulating case 3.
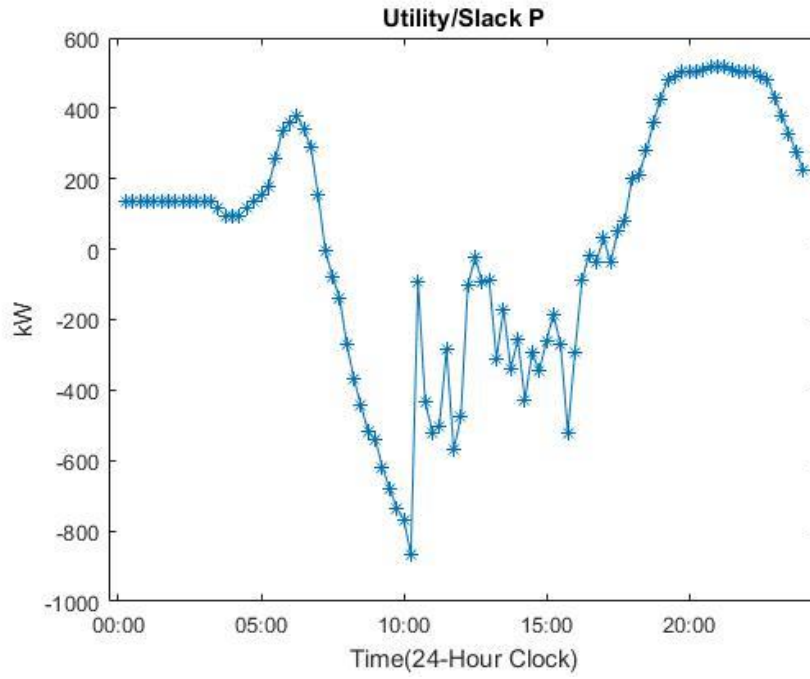
Figure 16: Utility/Slack real power (P) injection in each time step (Case #3).
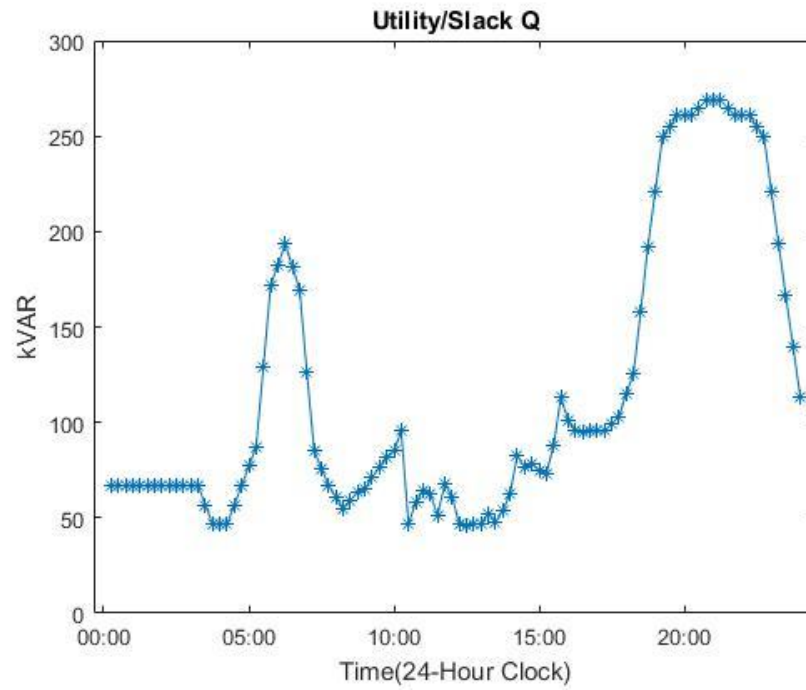
Figure 17: Utility/Slack reactive power (Q) injection in each time step (Case #3).
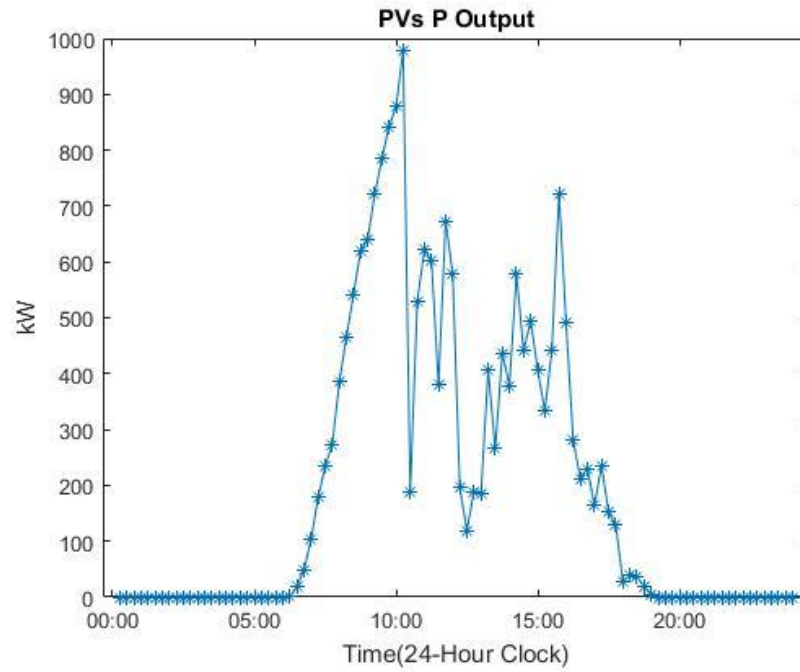
Figure 18: PVs real power output in each time step (Case #3).
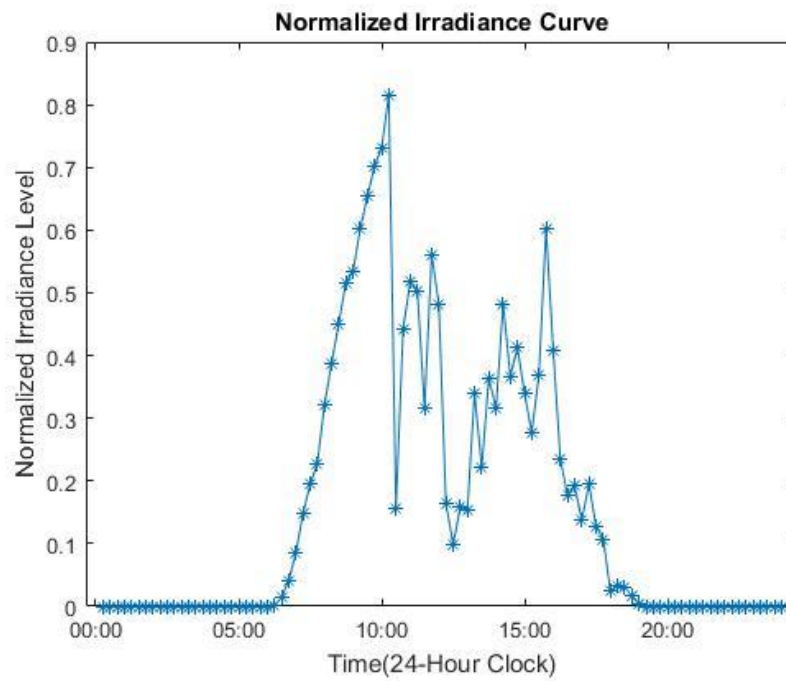
Figure 19:Normalized solar irradiance curve for a cloudy day (Case #3).
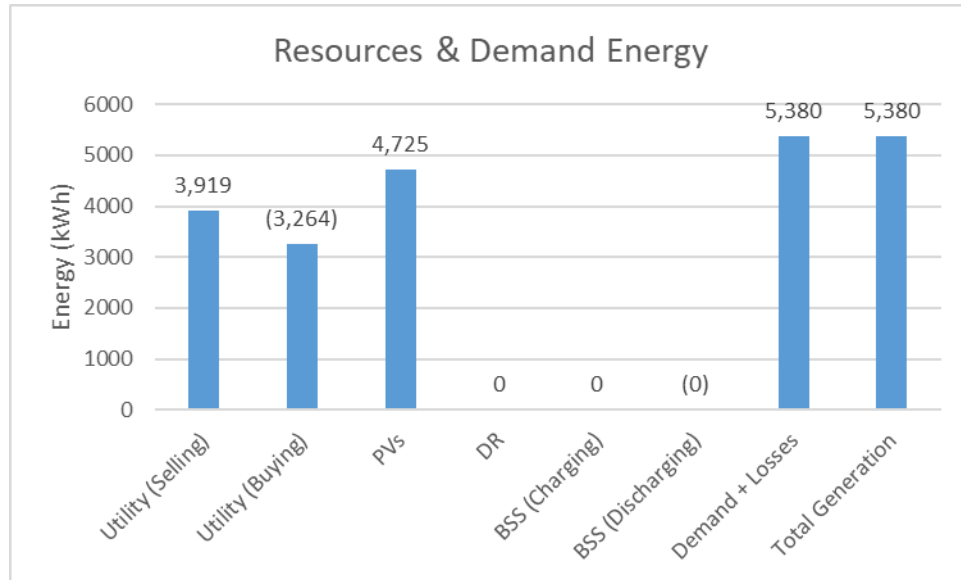
Figure 20: Resources and Demand Energy (Case #3).

On this simulation, since the only difference (with respect to case 2), is the solar irradiation curve, the main noticeable differences are the PV's and the utility's real power injection curves. A cloudy day produces more energy variances in the system, thus, the load factor obtained in this case was 3.15%; even lower than the value obtained in case 2.

6.4 Case #4: All DERs (Sunny day) with optimization

This was a case with all DERs available, a sunny day and applying optimization (the MOPF algorithm). The irradiation curve is the same as the one presented in case 2 (sunny day). In this simulation, the algorithm found an efficient allocation of the resources to supply the energy demand at the lowest cost possible while complying with the utility's power contract; the goal was to obtain the highest load factor as possible. The following graphs were obtained after simulating case 4.

Figure 21: Utility/Slack real power (P) injection in each time step (Case #4).

Figure 22: Utility/Slack reactive power (Q) injection in each time step (Case #4).

51

Figure 23: PVs real power output in each time step (Case #4).

Figure 24: Demand response applied in each time step (Case #4).
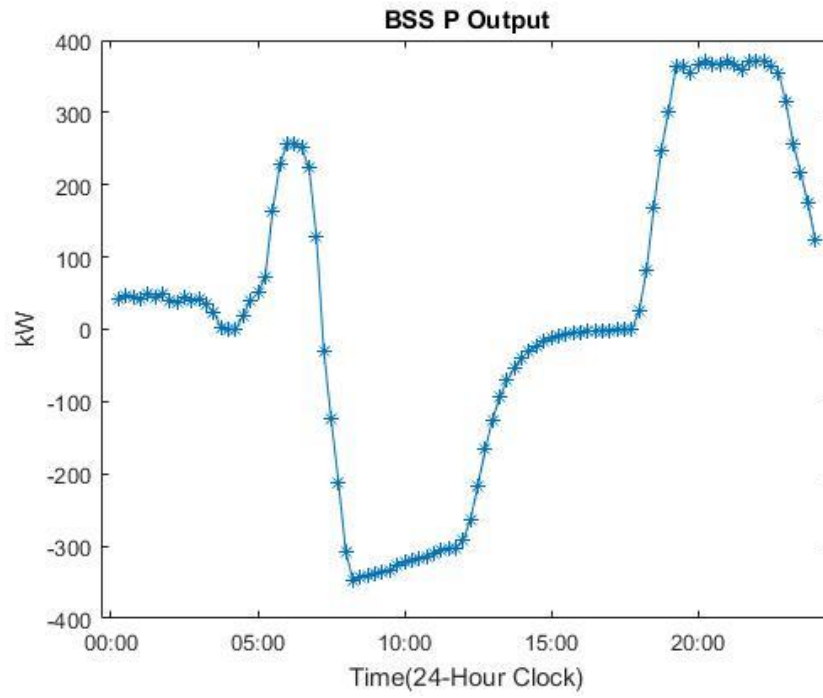
Figure 25: BSS power output/input in each time step (Case #4).

Figure 26: PVs reactive power output in each time step (Case #4).

53
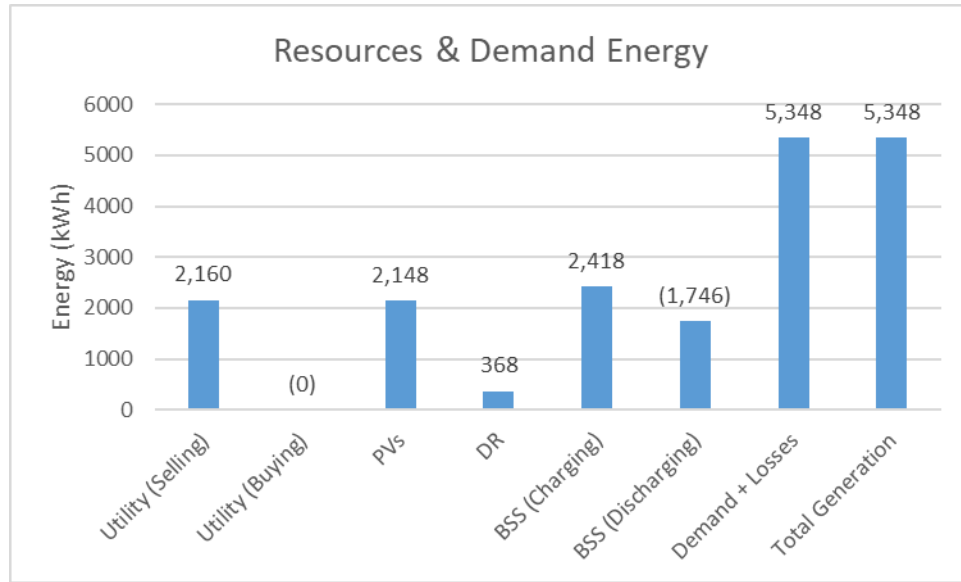
Figure 27: Resources and Demand Energy (Case #4).

On this simulation, since all DERs are available and are being optimized, the utility's real power curve is smoother (compared with the previous base cases). Since the PVs are being optimized (managed and controlled), they do not inject their maximum energy available all the time, and the PVs real power curve does not necessarily have the same shape as the solar irradiance curve (as in case 2). Moreover, since the PVs can also provide and supply reactive power, the utility does not need to supply all the reactive power demanded. For this particular scenario, the reactive power injection from the utility is very low (those values could be tolerance errors and thus can be neglected and considered as zero). Therefore, the PVs could supply the whole reactive power demanded. The BSS curve have positive and negative values; positive values means discharging and negative values means charging; the algorithm determined the best times to charge and discharge the BSS. The highest discharge values were obtained close to the demand peaks (morning and afternoon peaks), and the highest charge values were obtained when the solar irradiation curve was reaching its maximum. The DR resources were applied when the algorithm

54

determined it was necessary. It can be seen from the demand response curve that DR was mostly applied on the demand peaks. The load factor obtained in this case was 99.99 %; a much higher value than the ones obtained on the previous base cases. Therefore, the algorithm was successful and helped to achieve a very high load factor value by optimizing the use of available resources.

6.5 Case #5: All DERs (Cloudy day) with optimization

This case is the same as case 4, the only difference is the solar irradiance curve (a sunny day for case 4 and a cloudy day for case 5); the solar irradiation curve is the same as the one presented in case 3. The following graphs were obtained after simulating case 5.

Figure 28: Utility/Slack real power (P) injection in each time step (Case #5).

55

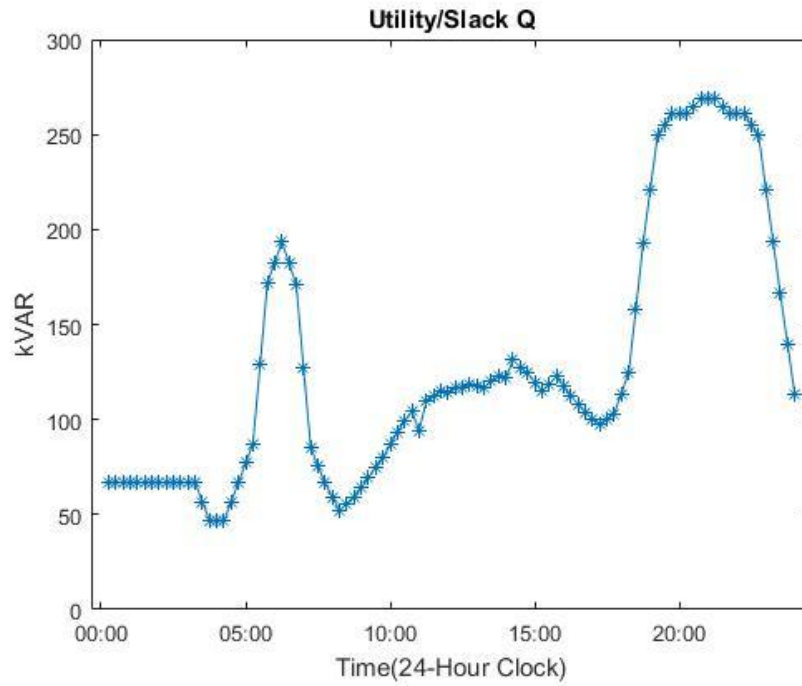*Figure 29: Utility/Slack reactive power (Q) injection in each time step (Case #5).*
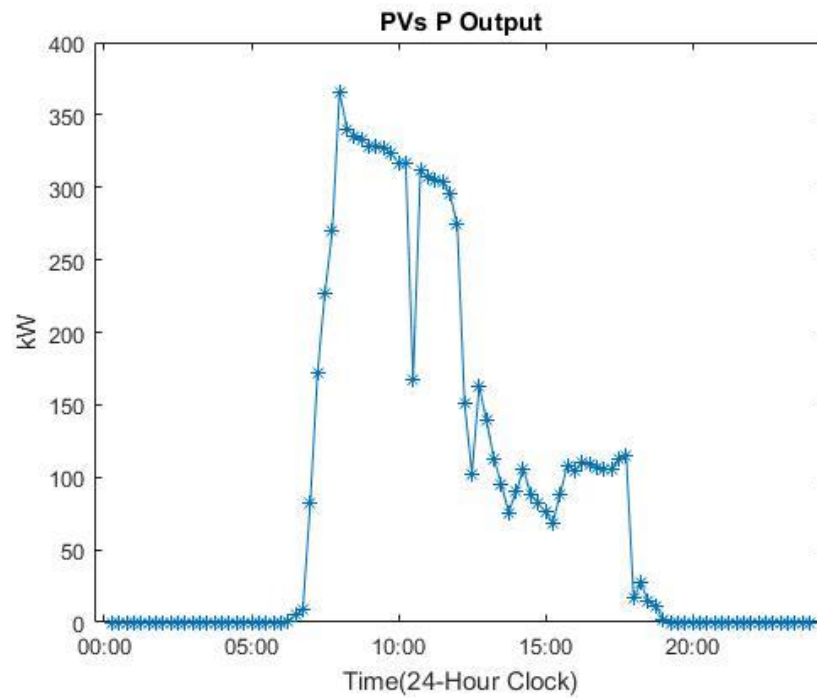
Figure 30: PVs real power output in each time step (Case #5).

56

*Figure 31: Demand response applied in each time step (Case #5).*
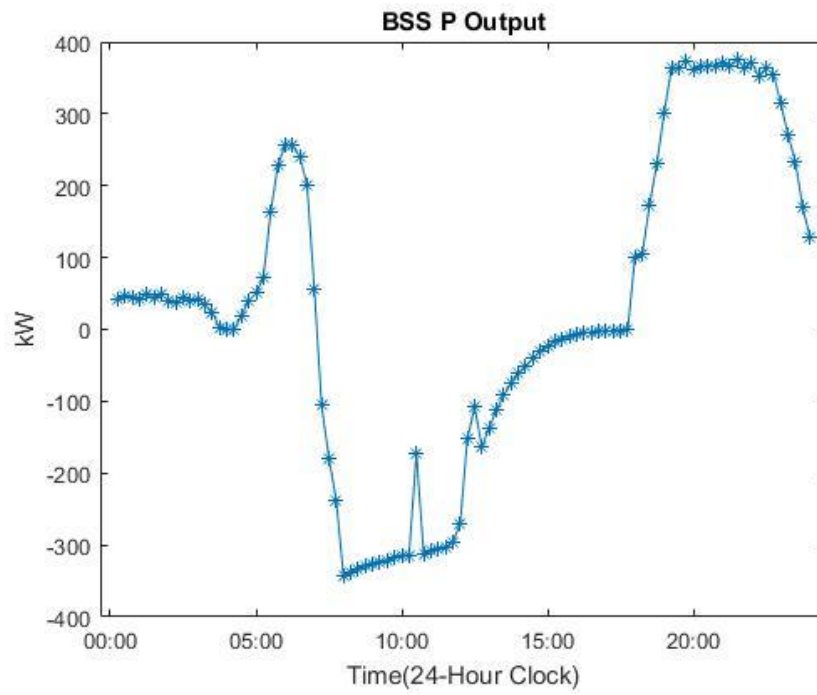
Figure 32: BSS power output/input in each time step (Case #5).

57
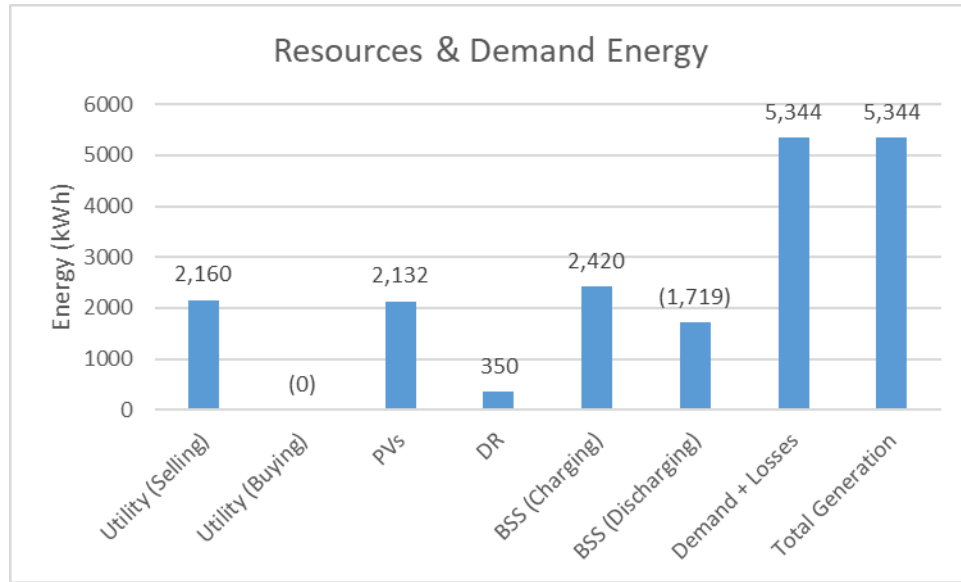
Figure 33: Resources and Demand Energy (Case #5).

On this simulation, even with a cloudy day, the algorithm was capable to find an efficient resource allocation to achieve a 99.99% load factor. However, even with optimization, a lower load factor could be obtained due to solar irradiation variances and less resources deployed (cases 8 and 9 show a scenario with less resources and case 14 show a scenario with a different storage technology). Nevertheless, this particular simulation showed the potential of the MOPF algorithm because it was able to achieve a very high load factor for a sunny and a cloudy day with a high integration of DERs; the algorithm managed to control the energy variances produced by the PVs using the BSS and DR resources. The graphs of those resources on cases 4 and 5 may look similar but are not exactly the same; their shape is different for each case. For example, at point 42 in the BSS graphs for cases 4 and 5, the BSS graph in case 5 shows and energy variance that is not present in case 4; the storage devices responded to a significant energy variance produced by a cloudy day to maintain a constant power demand from the utility. This high load factor means the utility will

58

not notice significant energy variances produced by DERs and it does not have to worry about the DERs capacity installed and their interaction with the grid. Having said that, even with 100% of renewables installed in a MG, the utility will not notice significant variances because they are being managed and controlled within the MG by applying optimization techniques.

6.6 Case #6: All DERs (Sunny day and Islanded) with optimization

This was a case with DERs available, no power supplied by the utility (or islanded operation), a sunny day and applying optimization. The sunny day irradiance curve is the same as the one presented in case 2. The Slack in this simulation is presented to study power unbalances, i.e., when the resources available are not capable to supply the demand. If the Slack delivers power, the MG had to interconnect with the utility (or to a backup generator) to cover the power mismatch. If there is no support from the utility or a backup generator, other solutions are required because the generation and demand will not be balanced and there would be failures in the MG. This particular scenario could serve as a tool to determine if the DERs available can supply all of the MG's demand, and also to determine the reliability of islanded MGs. The following graphs were obtained after simulating case 6.

Figure 34: Utility/Slack real power (P) injection in each time step (Case #6).

Figure 35: Utility/Slack reactive power (Q) injection in each time step (Case #6).

60
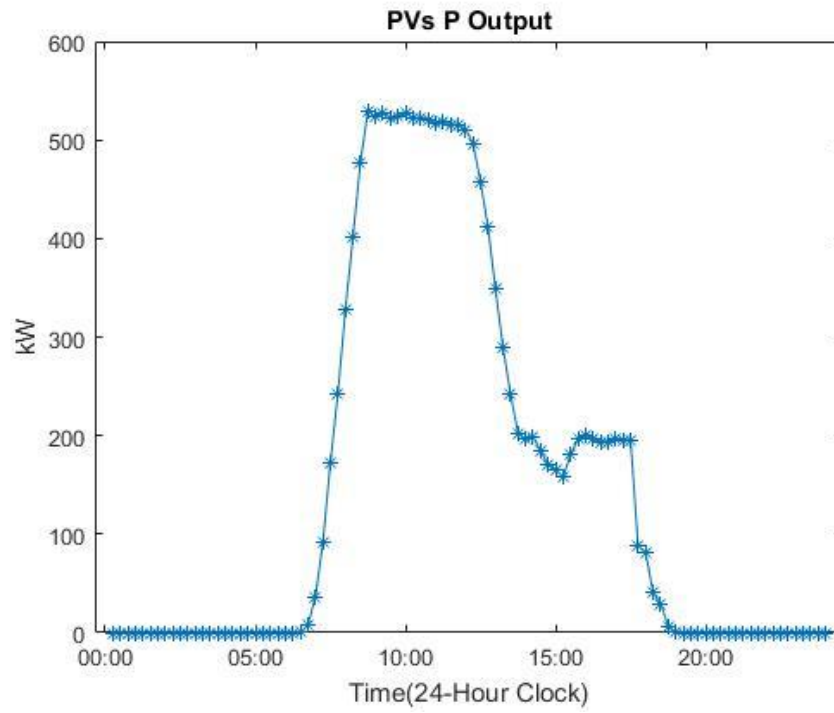
*Figure 36: PVs real power output in each time step (Case #6).*
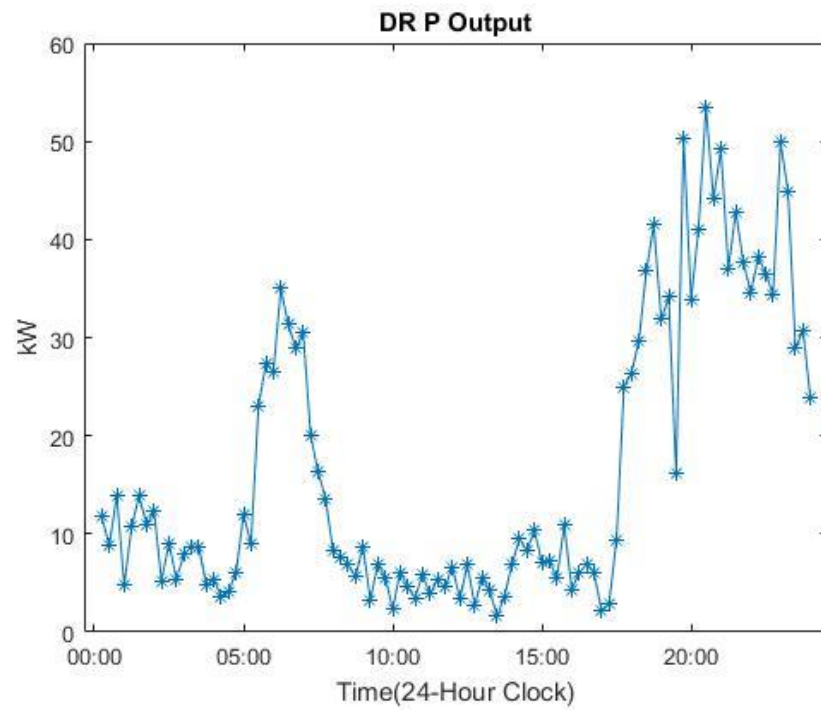
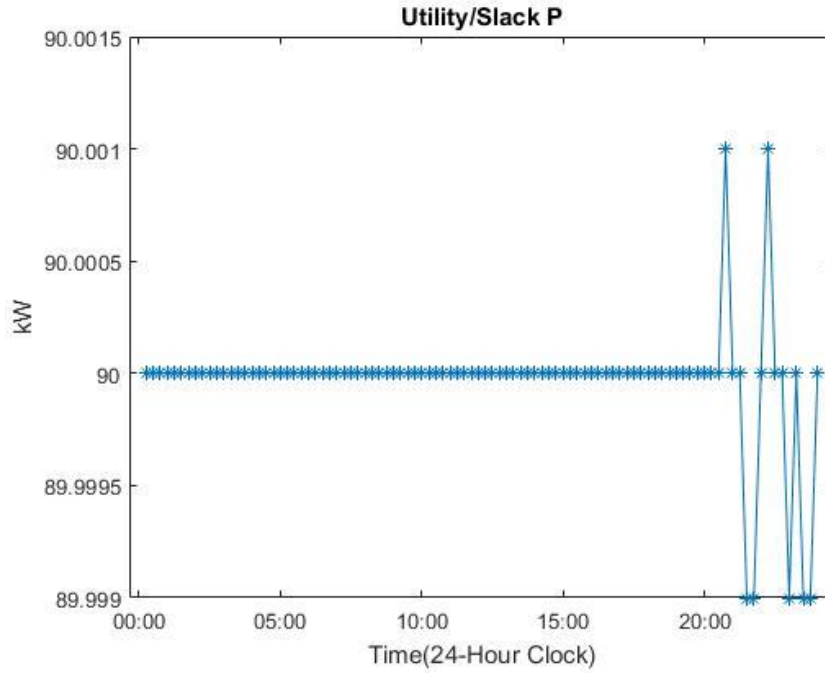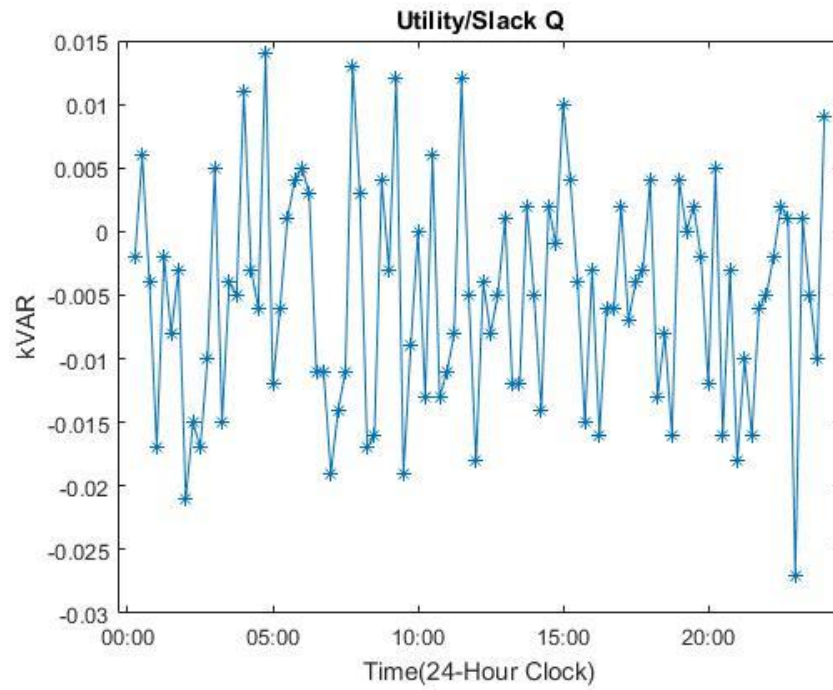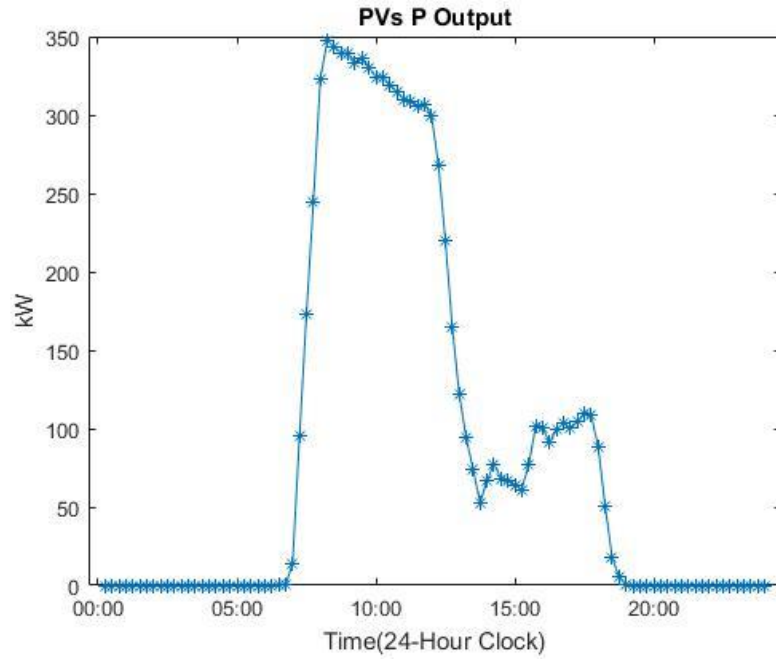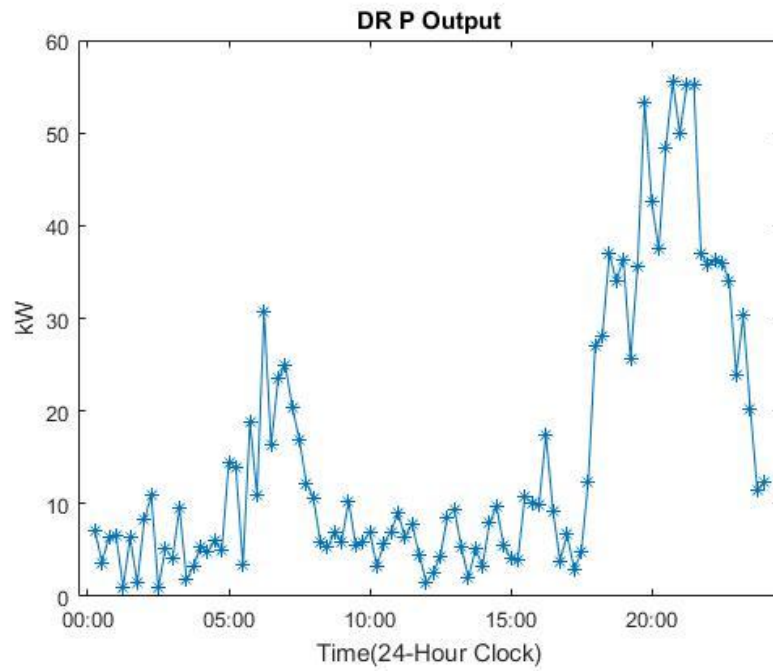*Figure 37: Demand response applied in each time step (Case #6).*

61
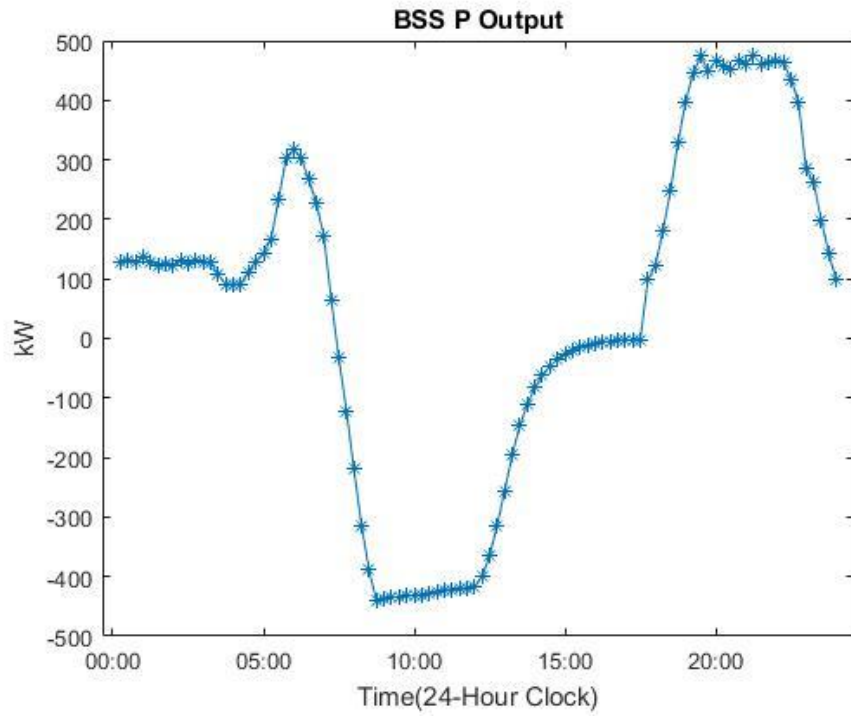
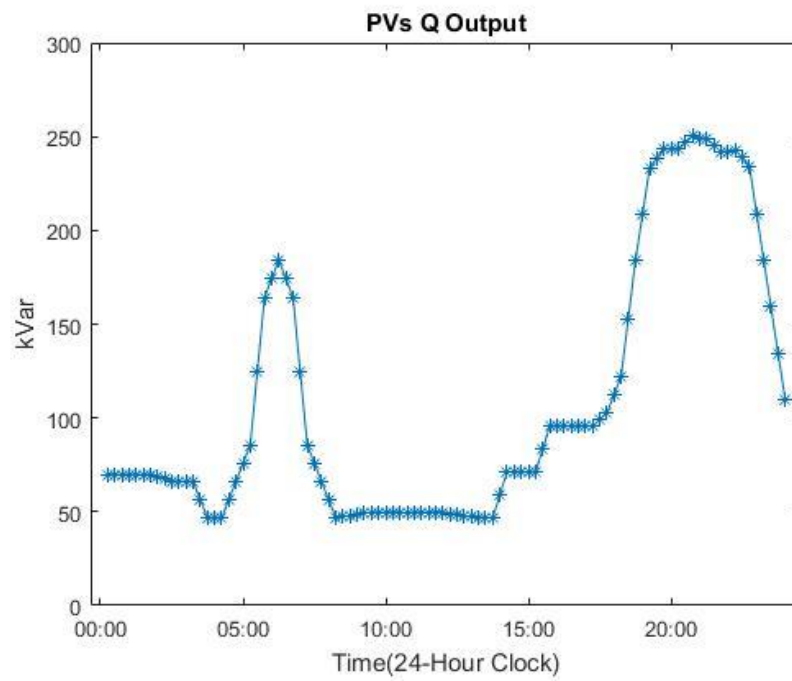*Figure 38: BSS power output/input in each time step (Case #6).*
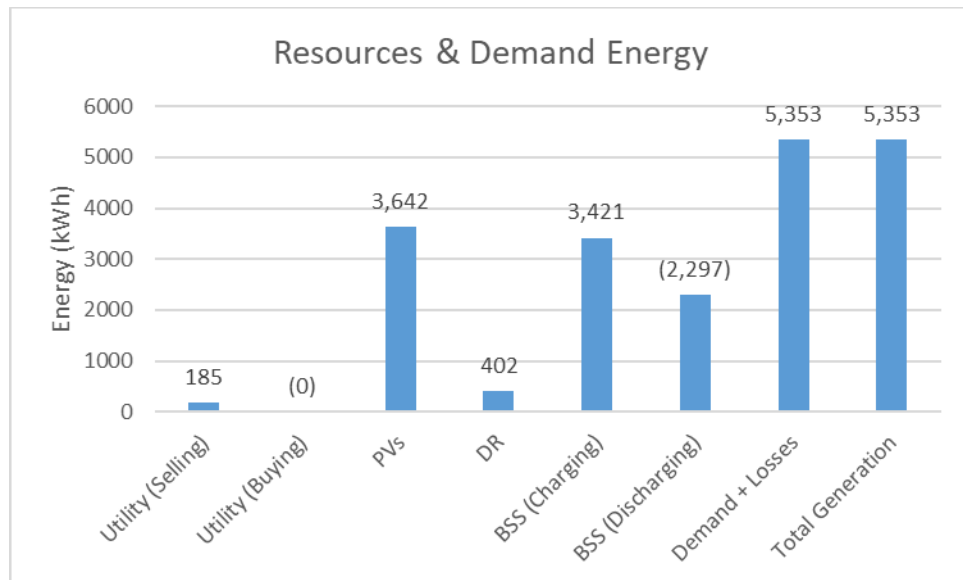
Figure 39: Resources and Demand Energy (Case #6).

62

On this simulation, the Slack was not always disabled (delivering zero-power). All values in this curve are very close to 0-kW except on the demand peaks. Based on the resource allocation report (generated in MATLAB), almost all BSS resources have been depleted (reached the minimum SOC value) when the energy demand was reaching the first peak (morning peak); therefore, the BSS contribution was less. The PVs were not injecting power at that time because the solar irradiation was zero; the same happened when the demand was reaching the second peak (afternoon peak). The only resource available at that time was DR and it could not supply the whole demand by itself; thus, the Slack had to supply the power mismatch. It is important to notice that the highest power demanded from the utility was around 105-kW, (approximately 46% of the total demand at that time). For this scenario, the MG was able to supply the energy demand except on the demand peaks when the Slack was used. If the utility or a backup generator are not available, or the ramp rates limit their contribution, a possible solution to solve this could be to set a lower value to the minimum SOC on the storage devices to allow them to deliver more energy and cover the demand on those times. Another option could be to set higher DR percentages and prioritize the use of this resource. By doing this, the energy in the storage devices will last longer and could contribute to the demand peaks. Another option could be to install a BSS with a higher capacity (case 10 show a scenario with a higher capacity). The Slack's reactive power curve have very low values (thus, they can be neglected and considered as zero), therefore, the PVs could supply the reactive power demanded in the 24-hour period. The results show the power of the analysis framework developed in this thesis. Further simulations could be done to test each of the options described to ensure stand-alone operation.

6.7 Case #7: All DERs (Cloudy day and Islanded) with optimization

This case is the same as the previous one, the only difference is the solar irradiation curve (a sunny day for case 6 and a cloudy day for case 7). The following graphs were obtained after simulating case 7.
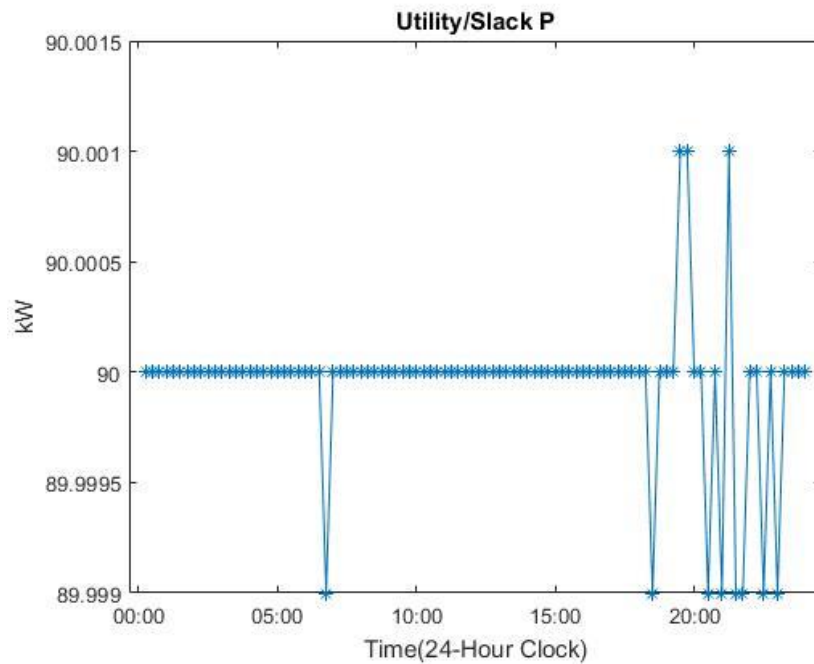

Figure 40: Utility/Slack real power (P) injection in each time step (Case #7).

Figure 41: Utility/Slack reactive power (Q) injection in each time step (Case #7).
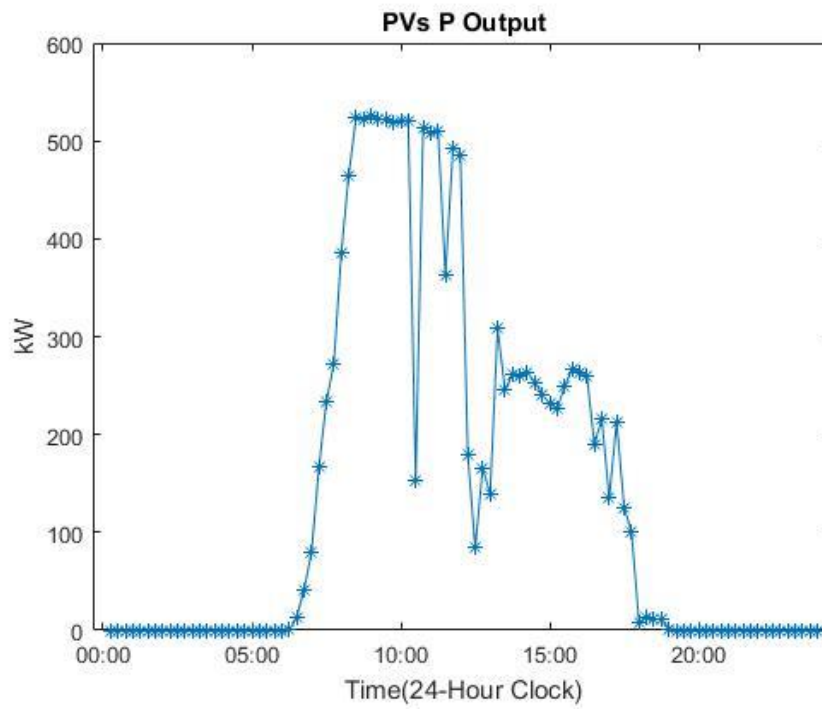
Figure 42: PVs real power output in each time step (Case #7).

65

Figure 43: Demand response applied in each time step (Case #7).
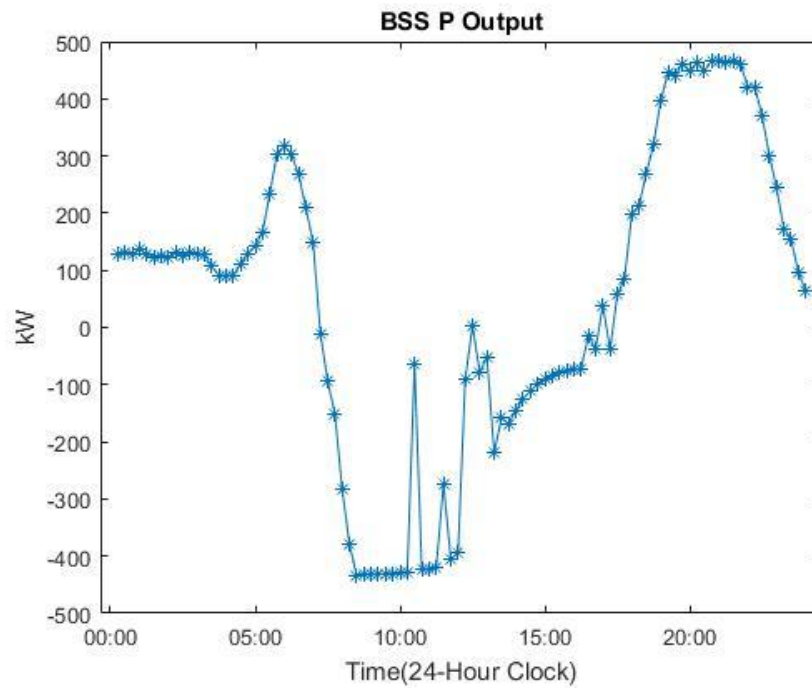
Figure 44: Storage power output/input in each time step (Case #7).
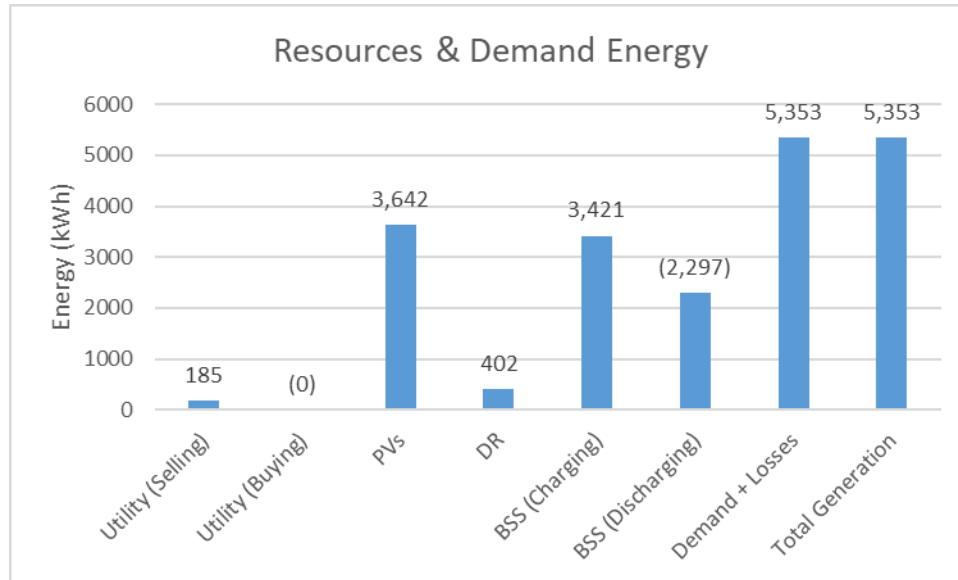
Figure 45: Resources and Demand Energy (Case #7).

The results obtained in this case are very similar as the ones obtained in the previous case, but, with the variations caused by the cloudy day, the power demanded from the Slack was a little bit higher. The maximum power delivered by the Slack was around 165-kW (approximately 44% of the energy demanded at that time). Again, if the utility cannot cover the mismatch or the ramp does not allow it, and backup generator is not available, other actions (similar to the ones mentioned on case 6) are required to balance the generation with the electric energy demand.

6.8 Case #8: Less DERs (Sunny day and Islanded) with optimization

This case is similar as case 4 but with less resources; not all customers have a PV system and a storage device. The percentage of customers with PVs and storage was chosen randomly using a MATLAB script (e.g., 70% of PVs and 40% of BSS for busbar #4, 50% of PVs and 10% of BSS for busbar #5, etc.). This scenario shows how the optimization results change by having less resources available in the MG. The following graphs were obtained after simulating case 8:

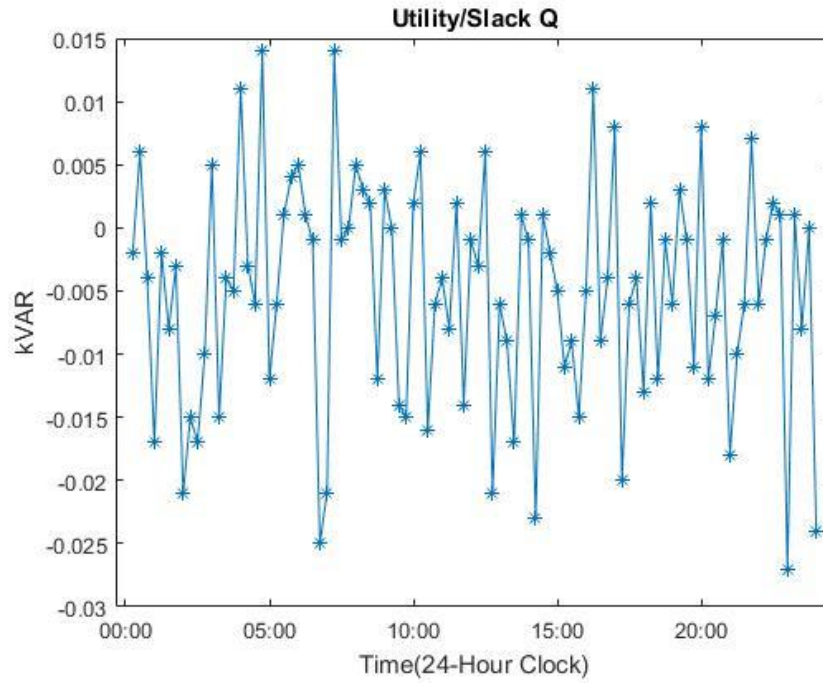*Figure 46: Utility/Slack real power (P) injection in each time step (Case #8).*

*Figure 47: Utility/Slack reactive power (Q) injection in each time step (Case #8).*
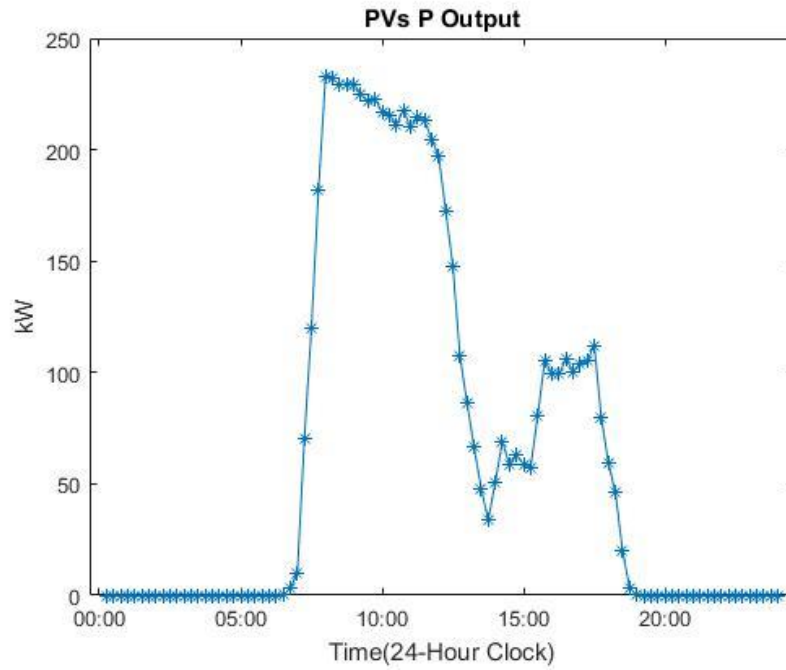
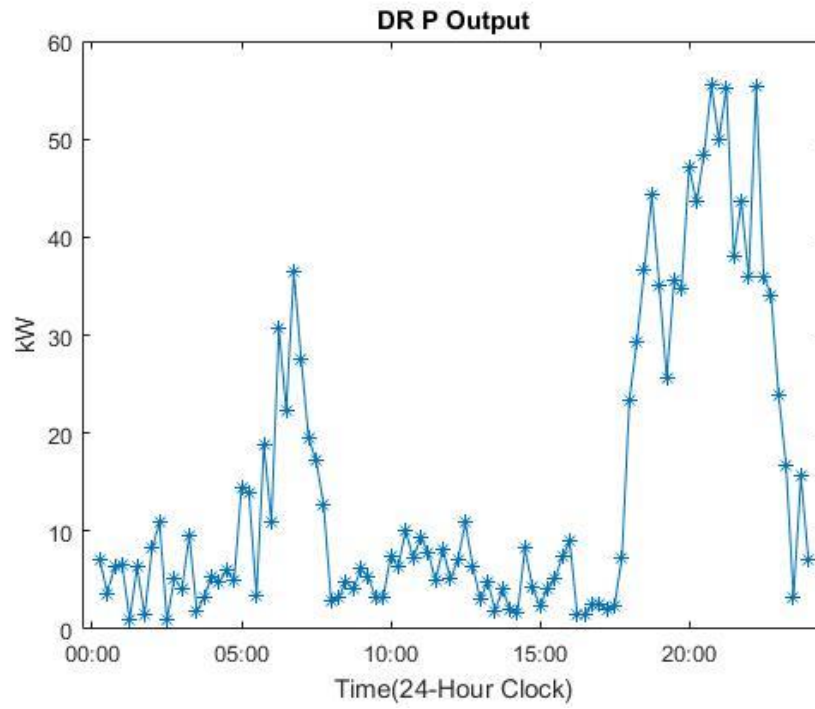*Figure 48: PVs real power output in each time step (Case #8).*

*Figure 49: Demand response applied in each time step (Case #8).*

69
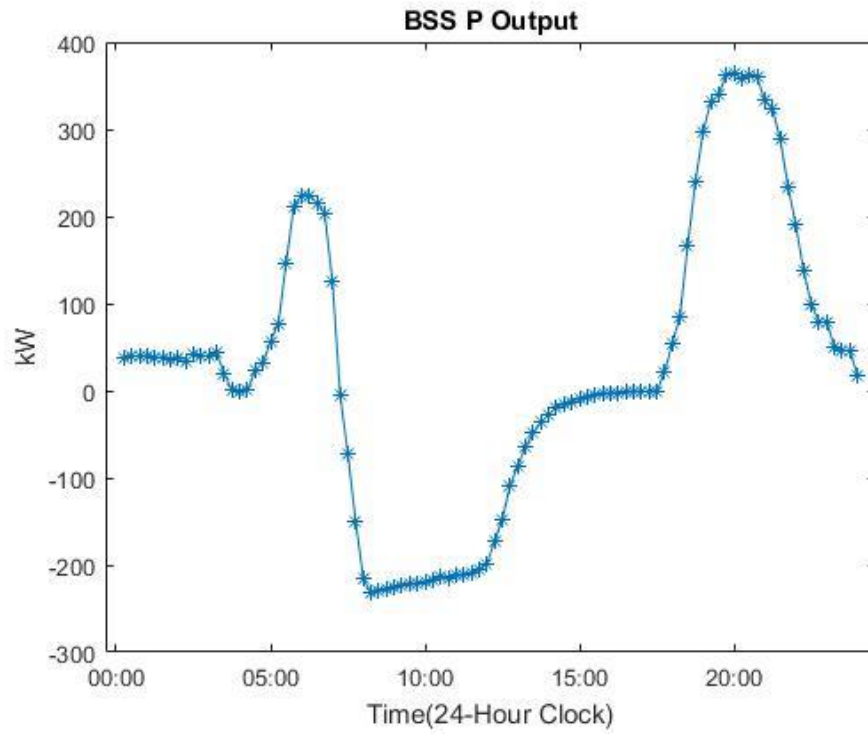
*Figure 50: Storage power output/input in each time step (Case #8).*
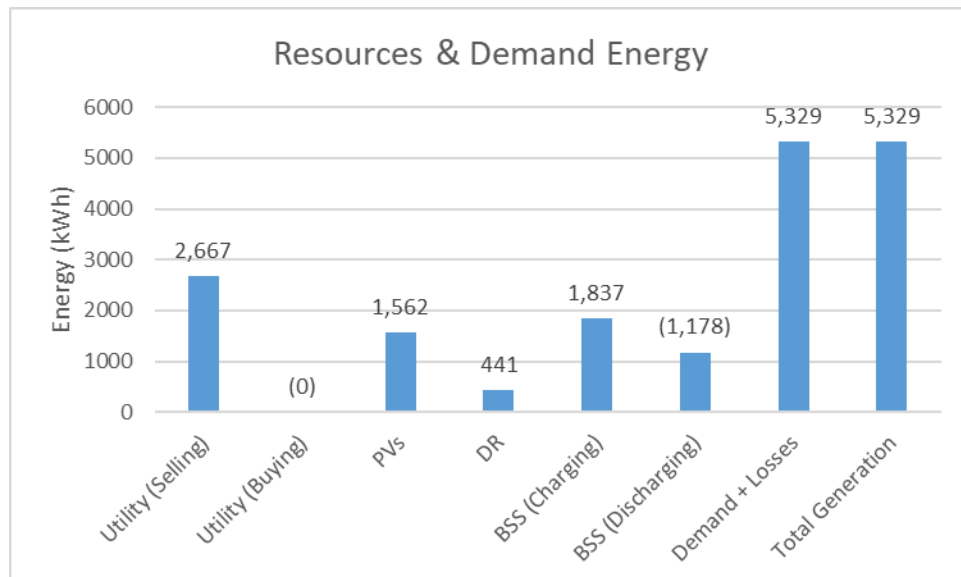
Figure 51: Resources and Demand Energy (Case #8).

70

On this simulation, the utility's real power injection is close to 90-kW except on the demand peaks were the injection was greater than 90-kW. The storage devices were not depleted all the time, but since there are less resources deployed, their contribution was less (less installed capacity). Therefore, the Slack was used to cover the mismatch. This happens because the MG does not have enough local energy resources. Even with optimization, a low load factor could be obtained if there are not enough resources. For this particular scenario the load factor was 39.97%, lower than the value obtained in case 4 (same scenario but with more energy resources). The highest power demanded from the utility/slack was around 350-kW (approximately 72% of the energy demand at that time); a significant amount of power. If the utility cannot supply this power, or the ramp rate does not allow it, other actions are required (as the ones mentioned in case 6) to balance the generation with the energy demand. Another solution is to deploy more resources or increase the power contracted with the utility.

6.9 Case #9: Less DERs (Cloudy day and Islanded) with optimization

This case is the same as the previous one, the only difference is the solar irradiance curve (a sunny day for case 8 and a cloudy day for case 9). The following graphs were obtained after simulating case 9.
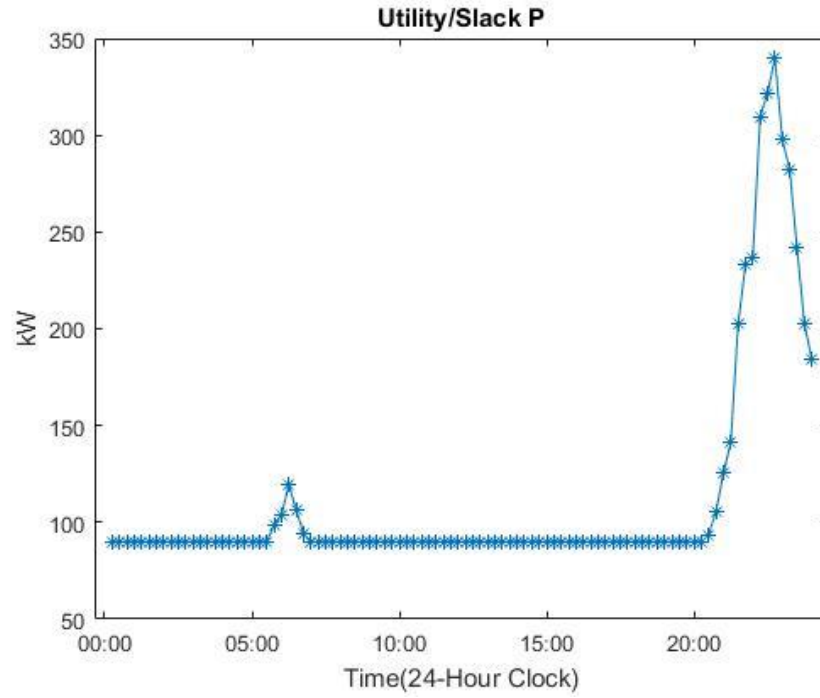
Figure 52: Utility/Slack real power (P) injection in each time step (Case #9).
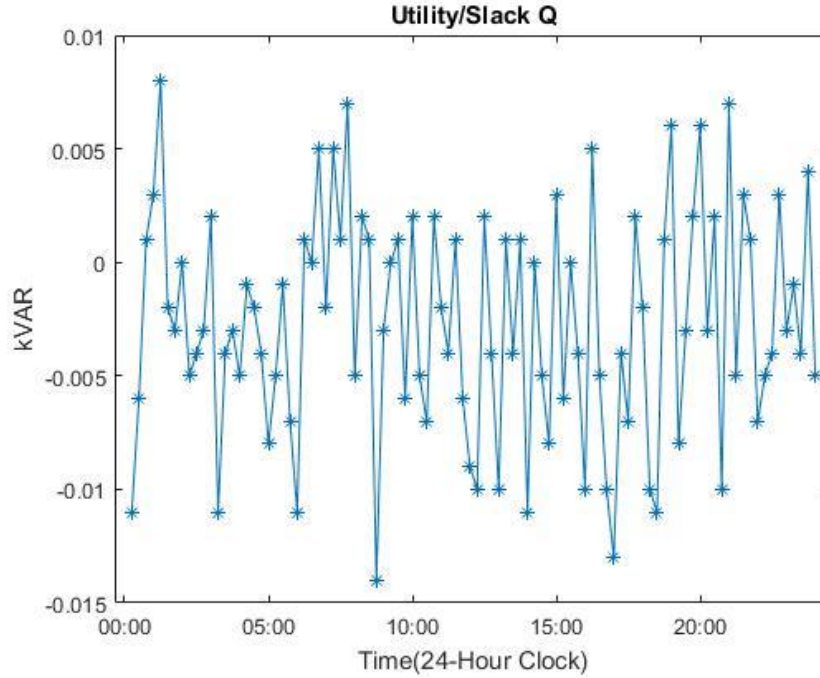
Figure 53: Utility/Slack reactive power (Q) injection in each time step (Case #9).

72
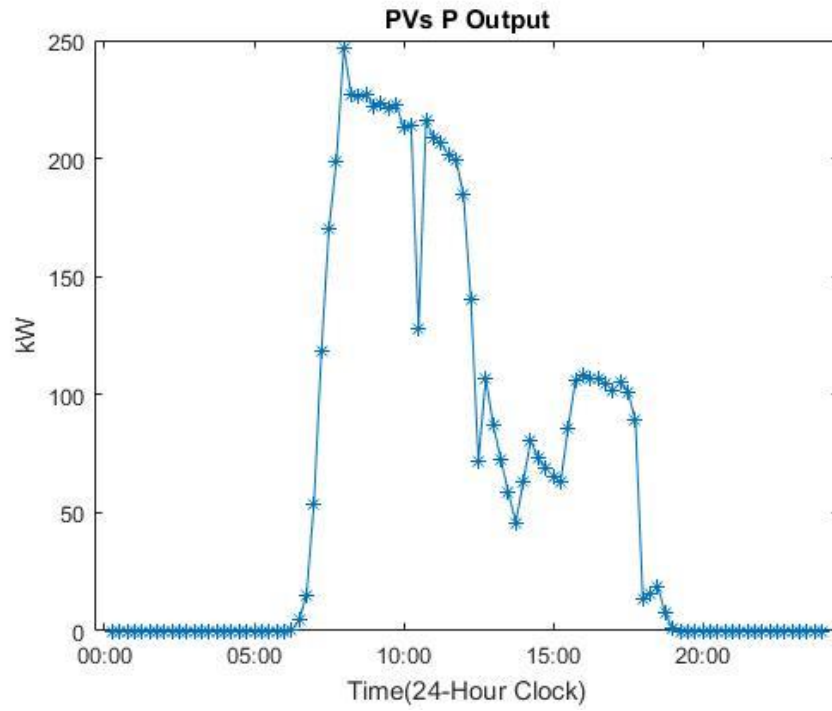
Figure 54: PVs real power output in each time step (Case #9).
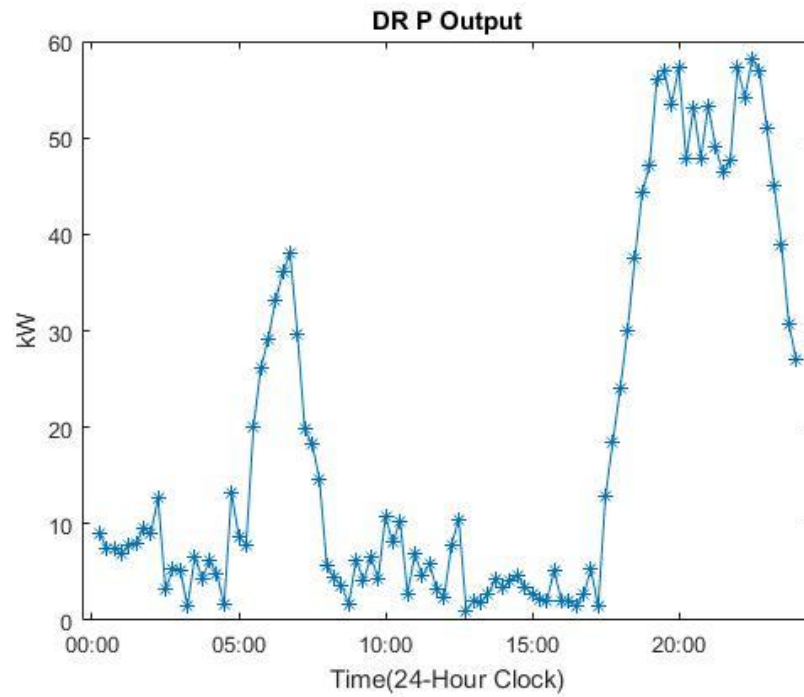
Figure 55: Demand response applied in each time step (Case #9).

73
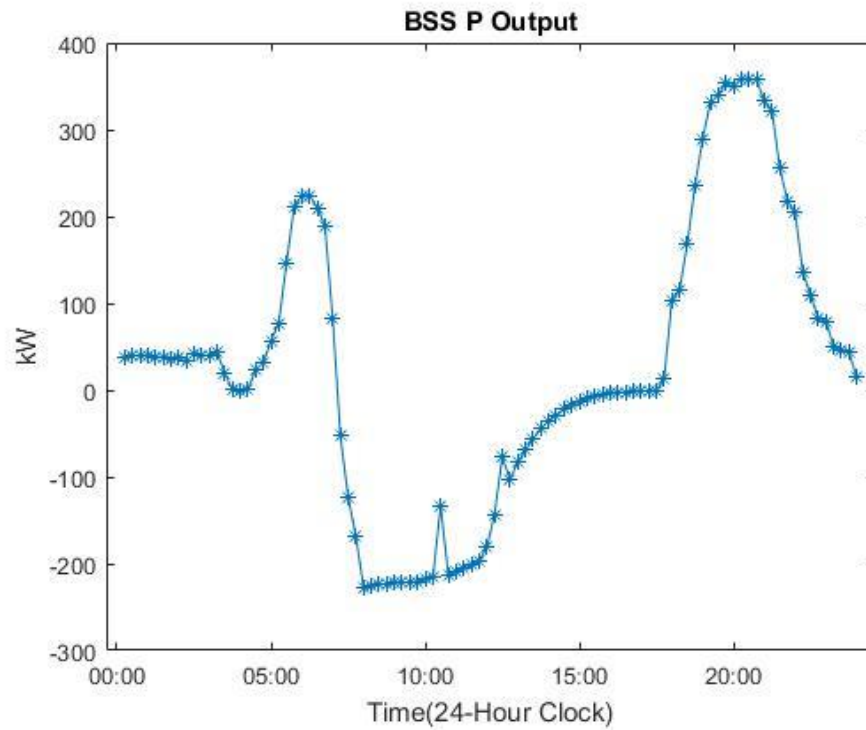
Figure 56: Storage power output/input in each time step (Case #9).
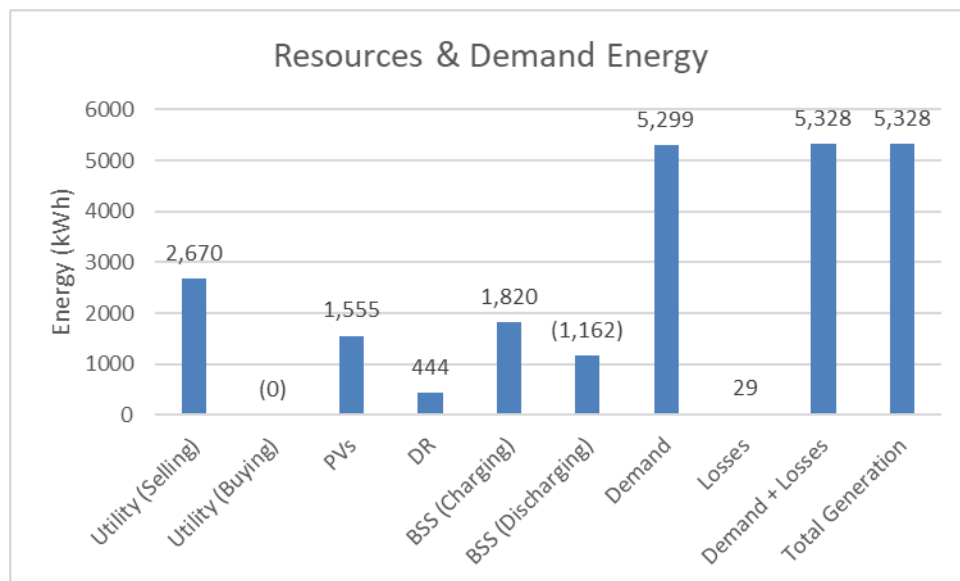
Figure 57: Resources and Demand Energy (Case #9).

74

The results obtained in this simulation were similar as the ones obtained in case 8; the graphs differences are minimal. Again, even with optimization the DERs cannot cover the demand peaks. On this case, the maximum power demanded from the utility was around 340-kW (approximately 72% of the demand at that time); a significant amount of power, similar to case 8.

6.10 Case #10: All DERs (Sunny day, PIKA battery) with optimization

This case is the same as case 4, but with a higher storage capacity. For this simulation, all customers have a PIKA Harbor Plus battery (Li-ion Technology), which has a 20.28-kWh (15.90-kWh usable) capacity and a 6.7-kW of charge/discharge rate [47]. The following graphs were obtained after simulating case 10:
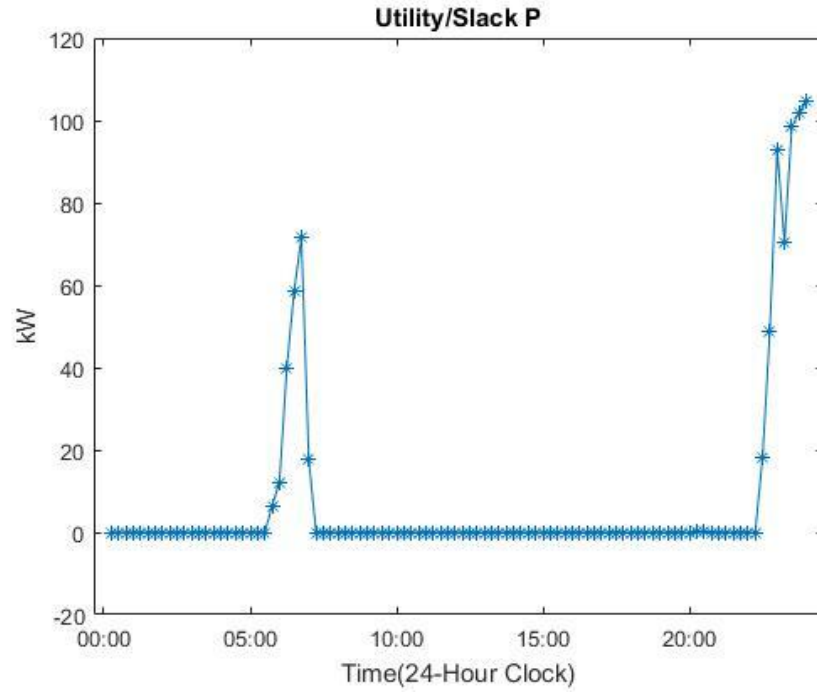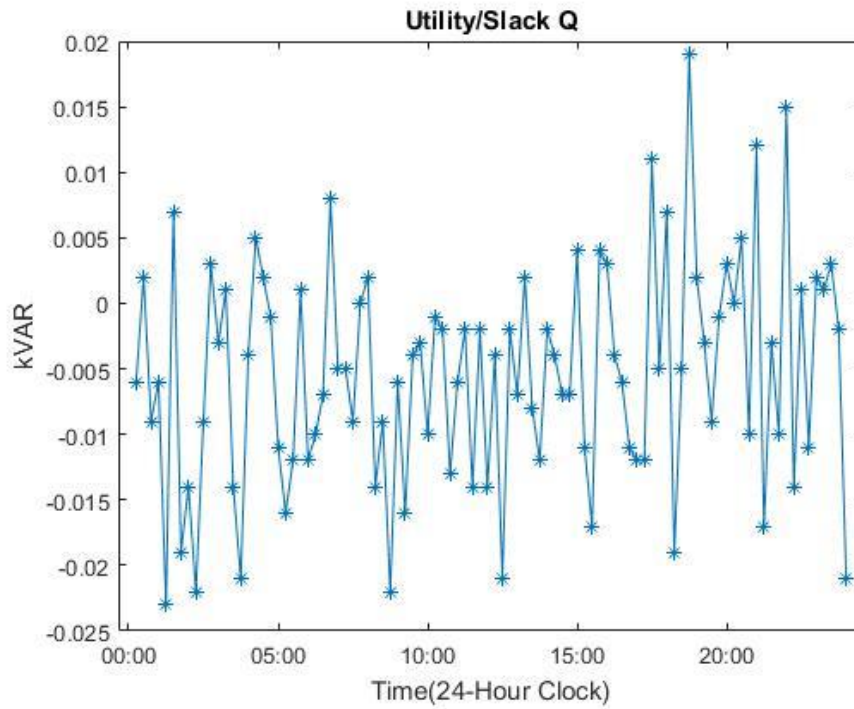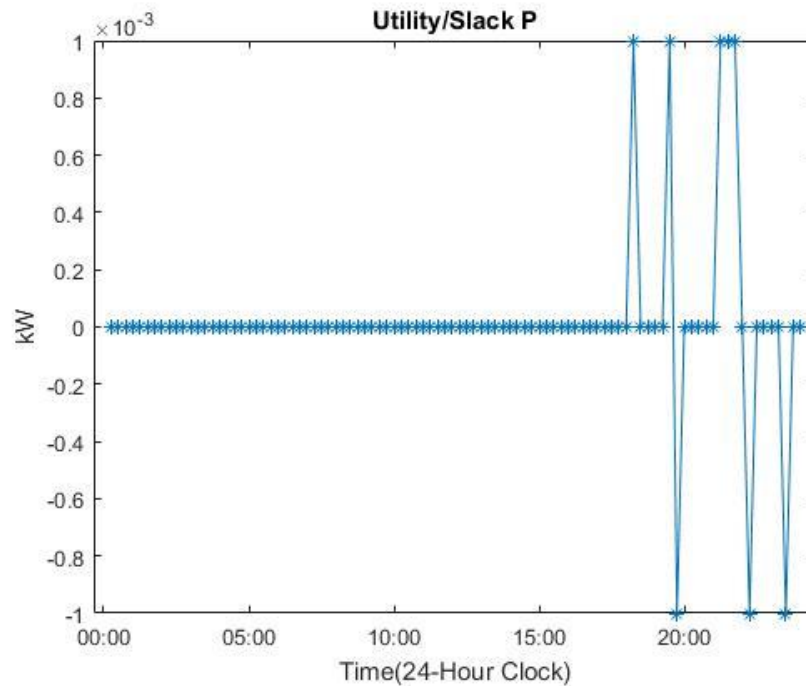

Figure 58: Utility/Slack real power (P) injection in each time step (Case #10).

75
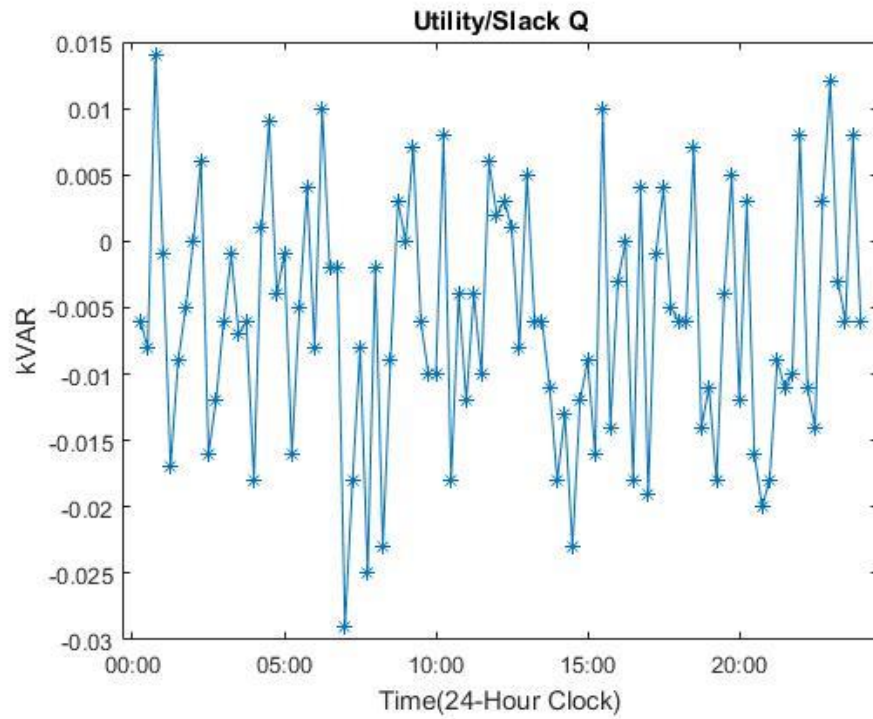
*Figure 59: Utility/Slack reactive power (Q) injection in each time step (Case #10).*
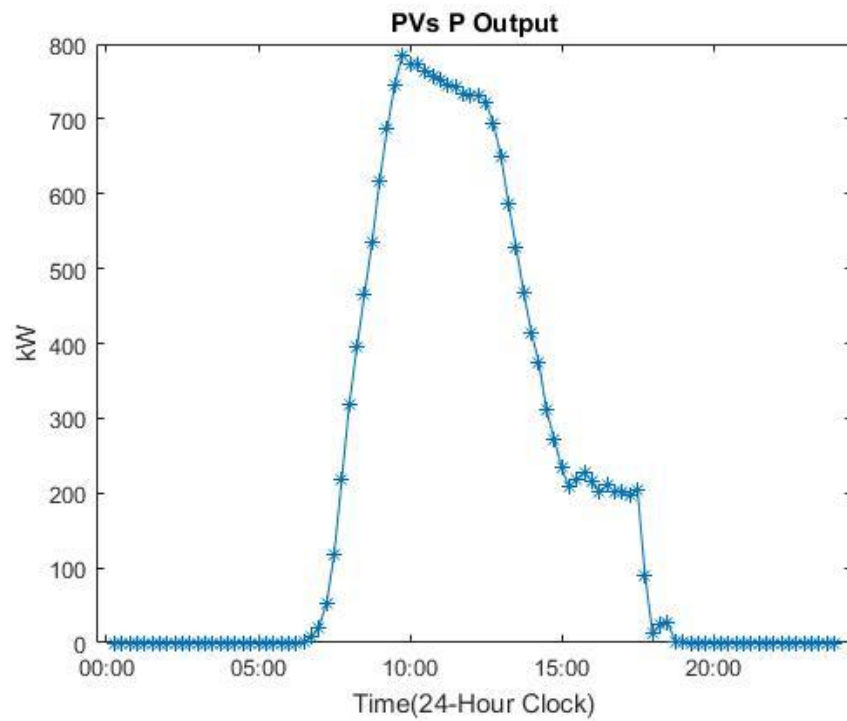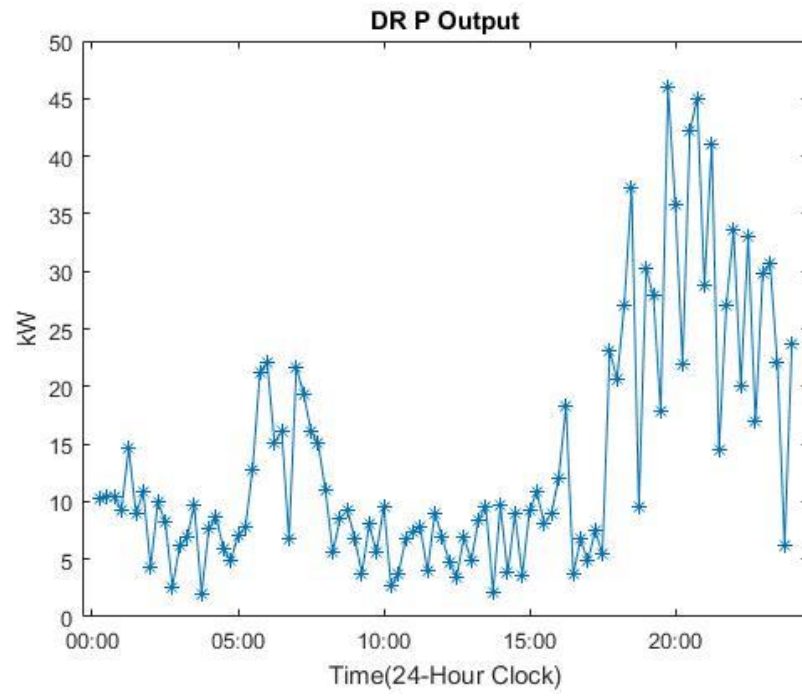
Figure 61: Demand response applied in each time step (Case #10).
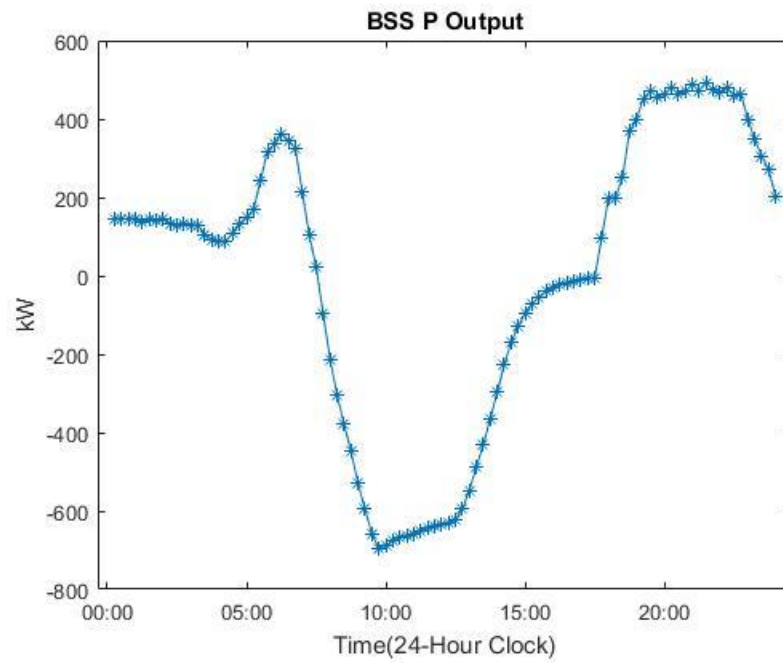
Figure 62: Storage power output/input in each time step (Case #10).
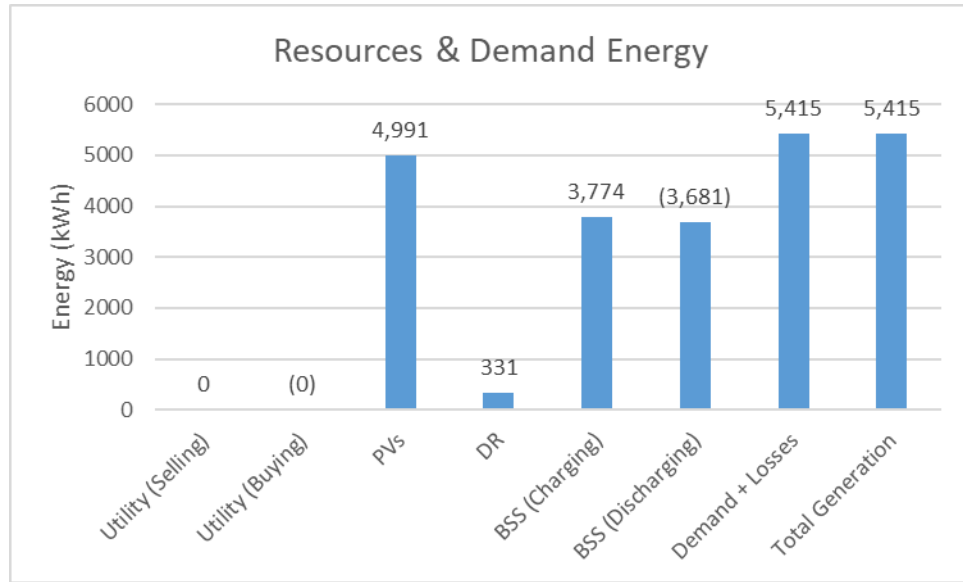
Figure 63: Resources and Demand Energy (Case #10).

This case yielded different results. Since there is a high integration of DERs and a vast storage capacity, the Slack's real power curve is practically zero all the time. Thus, for this particular scenario, the DERs could supply the whole demand without relying on the utility due to the vast storage capacity in the MG. Of course, there is an additional cost for this case.

6.11 Case #11: All DERs (Cloudy day, PIKA battery) with optimization

This case is the same as the previous one, the only difference is the solar irradiance curve (a sunny day for case 10 and a cloudy day for case 11). The following graphs were obtained after simulating case 11.
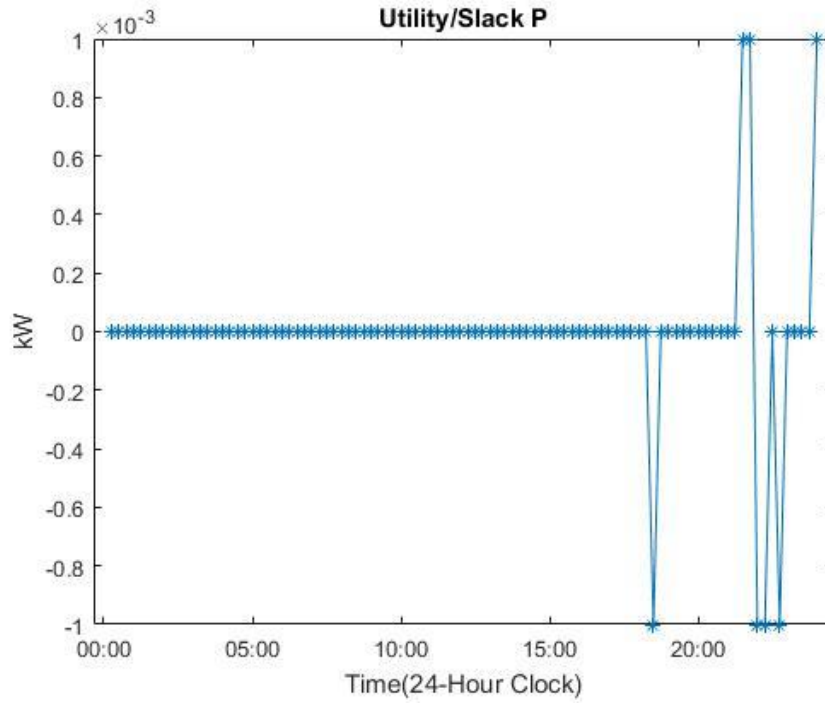
Figure 64: Utility/Slack real power (P) injection in each time step (Case #11).
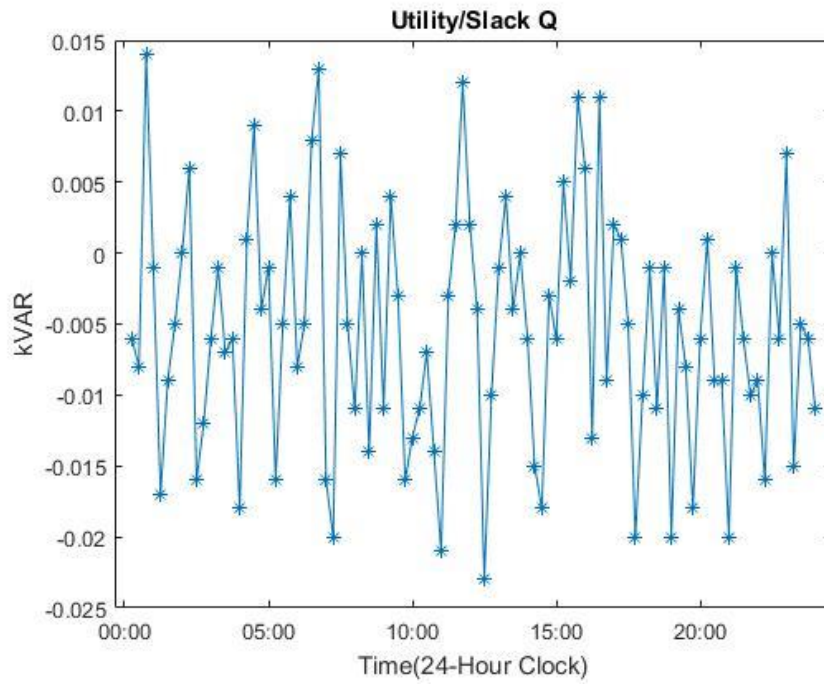
Figure 65: Utility/Slack reactive power (Q) injection in each time step (Case #11).

79
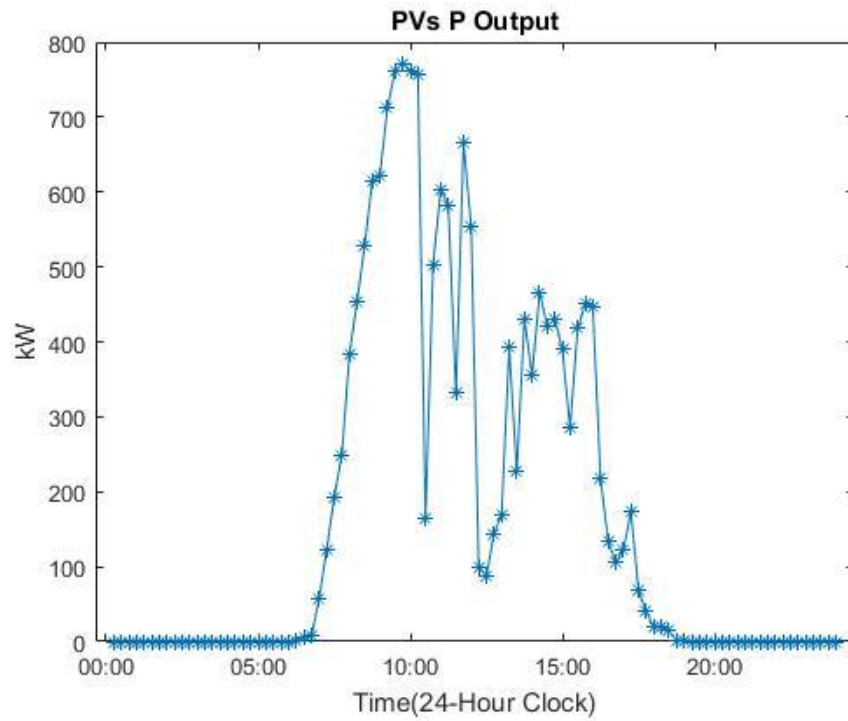
Figure 66: PVs real power output in each time step (Case #11).
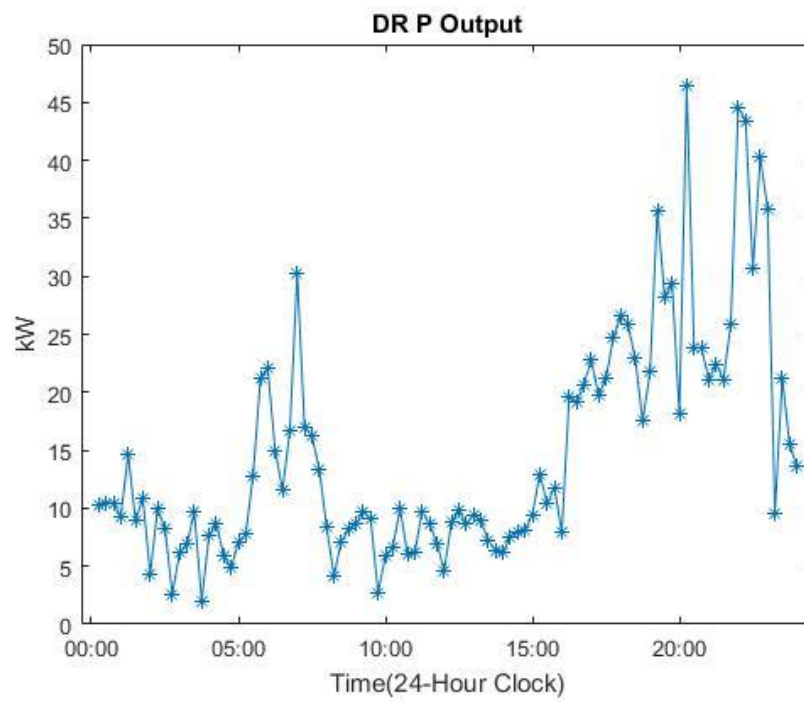
Figure 67: Demand response applied in each time step (Case #11).
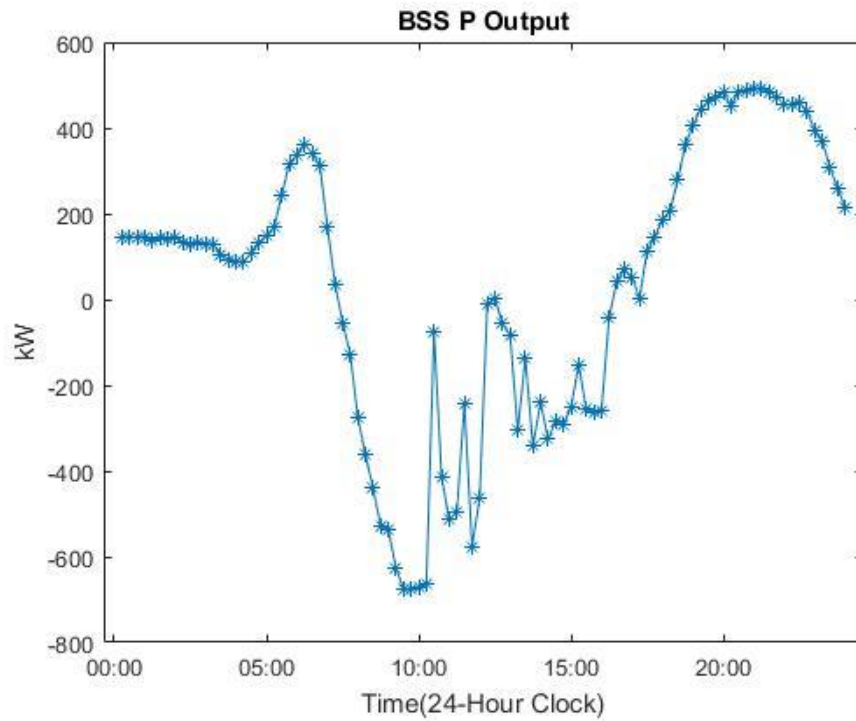
Figure 68: Storage power output/input in each time step (Case #11).
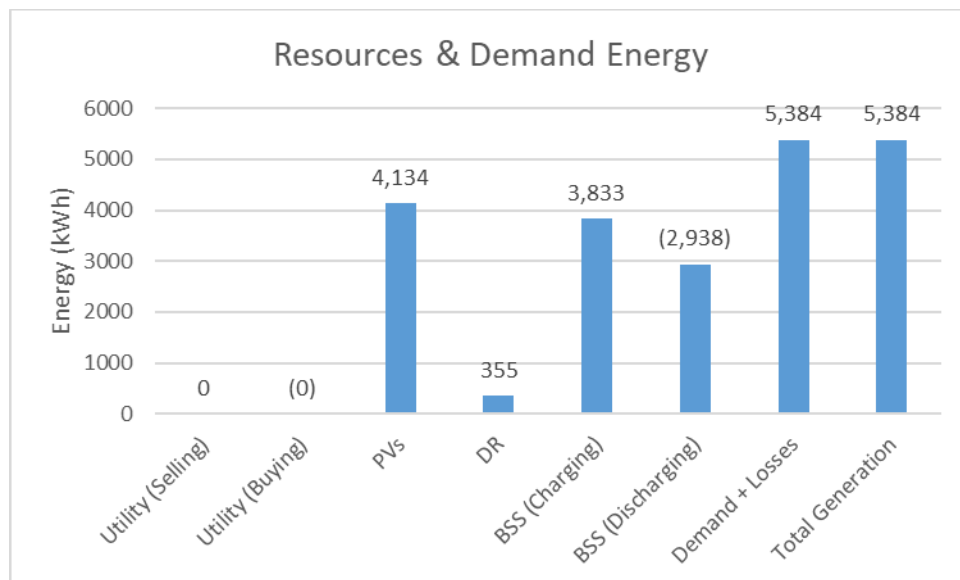
Figure 69: Resources and Demand Energy (Case #11).

81

On this simulation, even with a cloudy day, the MG could supply the demand without relying on the utility due to a high the integration of DERs and the vast storage capacity; all values from the Slack's real power curve are practically zero. These results can only be obtained with a high integration of DERs, a vast storage capacity, flexible DR and applying optimization techniques; those are key features needed to achieve a sustainable MG. Again, this could be achieved only if additional cost is incurred to buy more storage capacity.

6.12 Case #12: All DERs (Sunny day, PIKA battery, selling energy) with optimization

This case is the same as case 10 (a sunny day with a higher storage capacity), but selling 90-kW to the utility on each time step. The goal in this scenario was to see if the MG was able to sell power to the utility and supply the energy demand. The following graphs were obtained after simulating case 12.
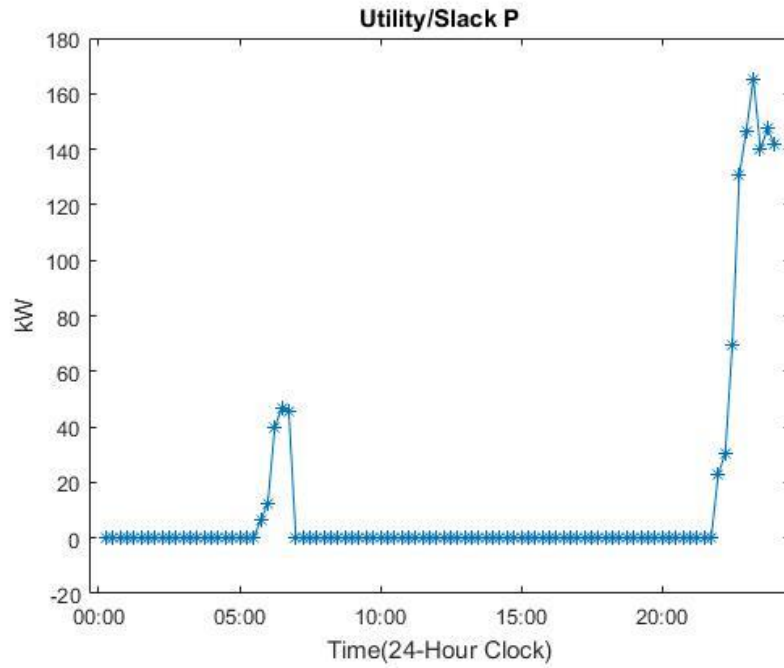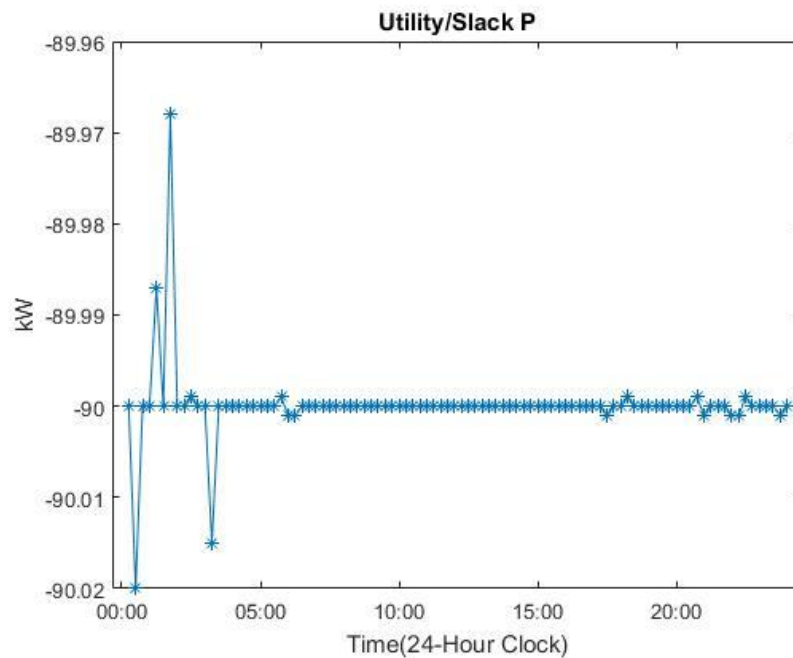

Figure 70: Utility/Slack k real power (P) injection in each time step (Case #12).
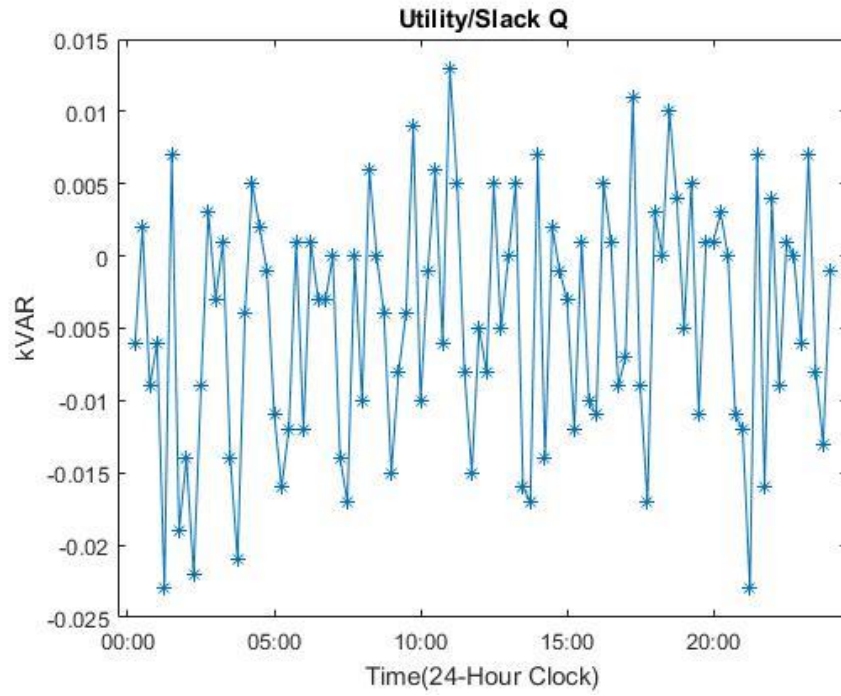
82
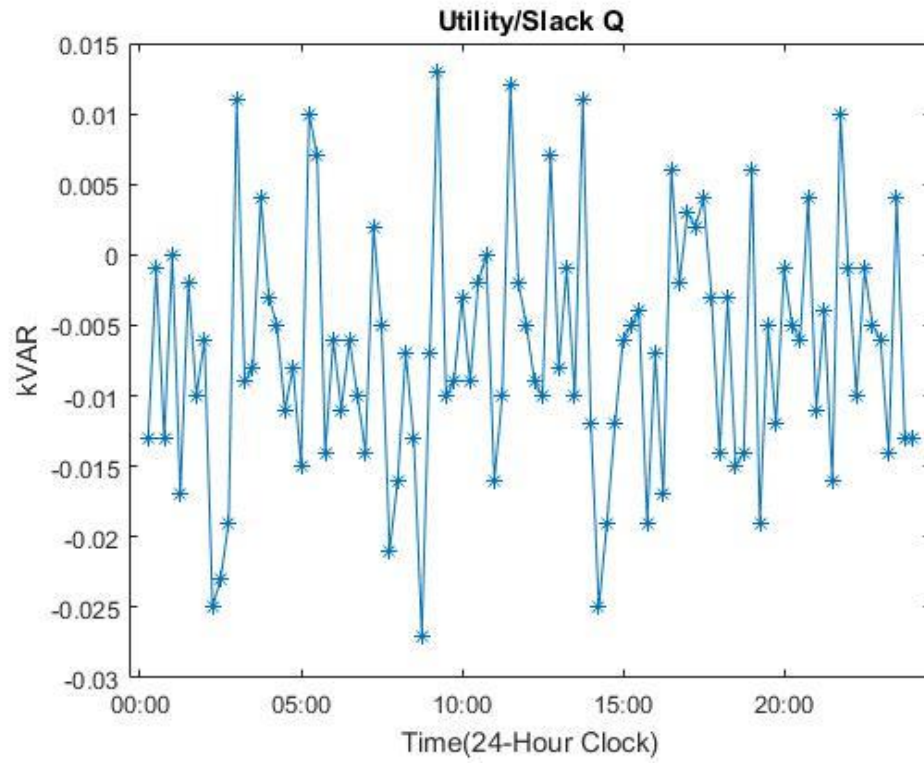
*Figure 71: Utility/Slack reactive power (Q) injection in each time step (Case #12).*
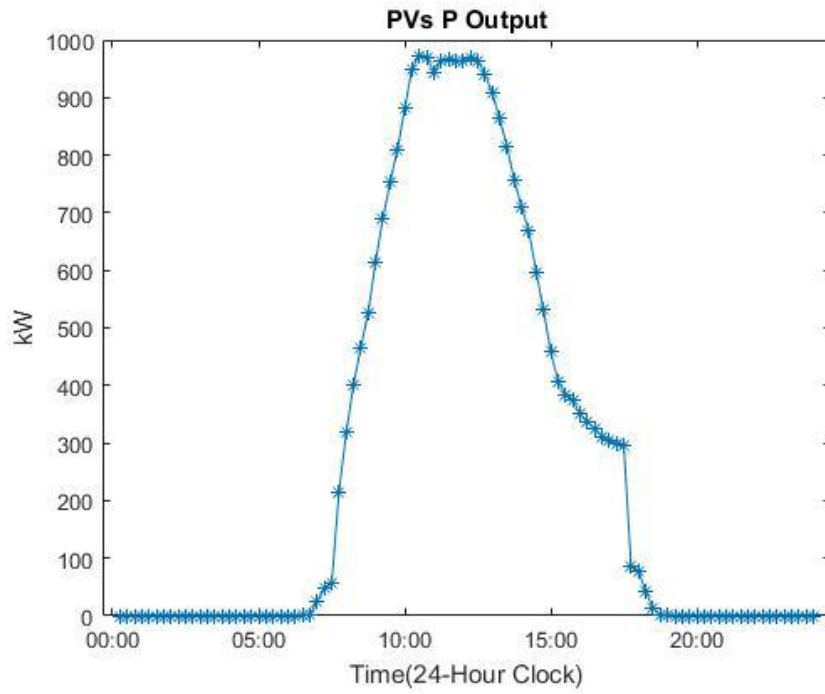
Figure 72: PVs real power output in each time step (Case #12).
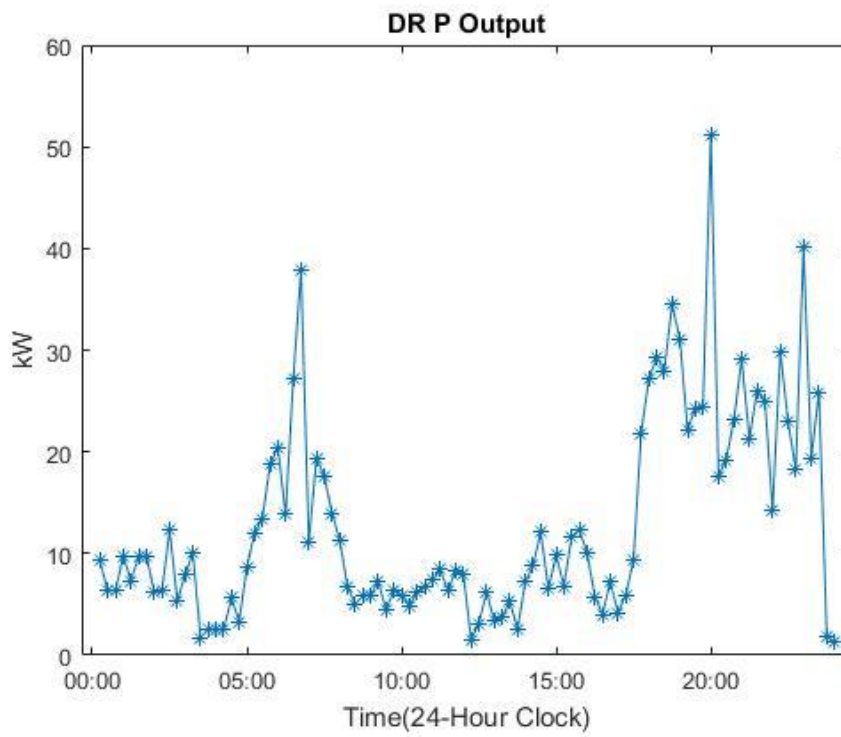
Figure 73: Demand response applied in each time step (Case #12).

84
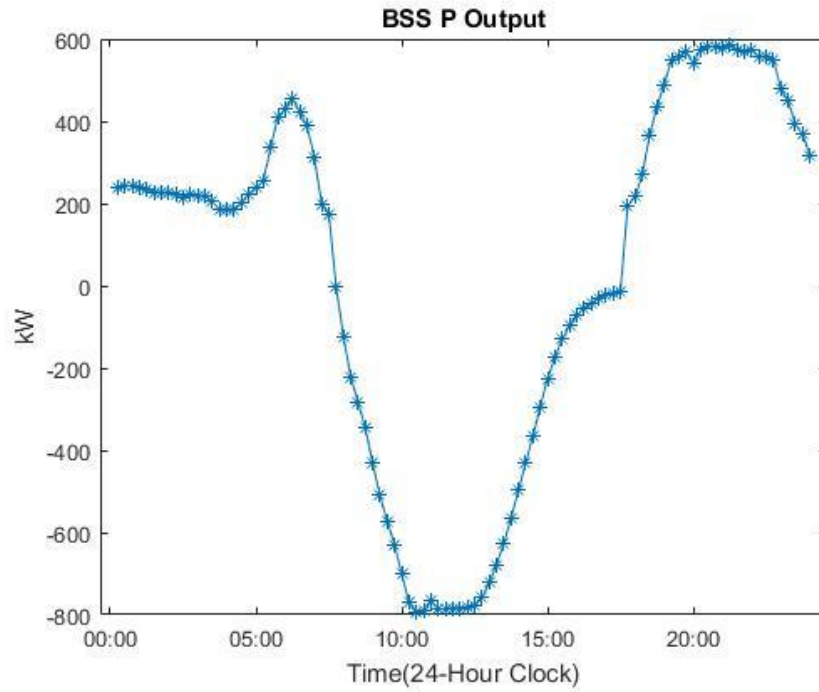
Figure 74: Storage power output/input in each time step (Case #12).
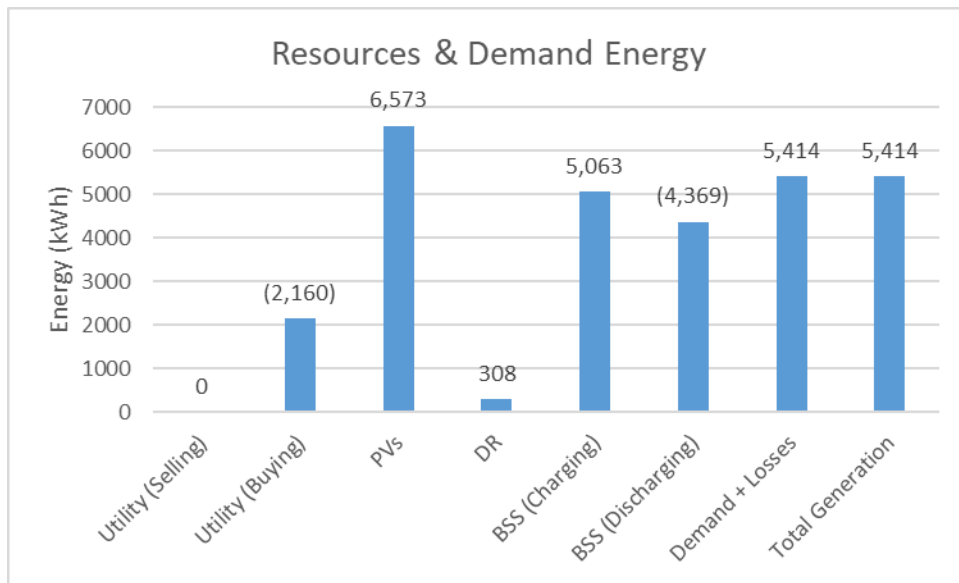
Figure 75: Resources and Demand Energy (Case #12).

This simulation showed that the MG can supply the energy demand while selling 90-kW

to the utility on each time step; all values from the utility/slack real power curve are practically -

90-kW every time (a negative value means a power flow in the utility's direction). The load factor obtained in this case was 99.98%; a very high value.

6.13 Case #13: All DERs (Cloudy day, PIKA battery, selling energy) with optimization

This case is the same as the previous one, the only difference is the solar irradiation curve (a sunny day for case 12 and a cloudy day for case 13). The following graphs were obtained after simulating case 13.
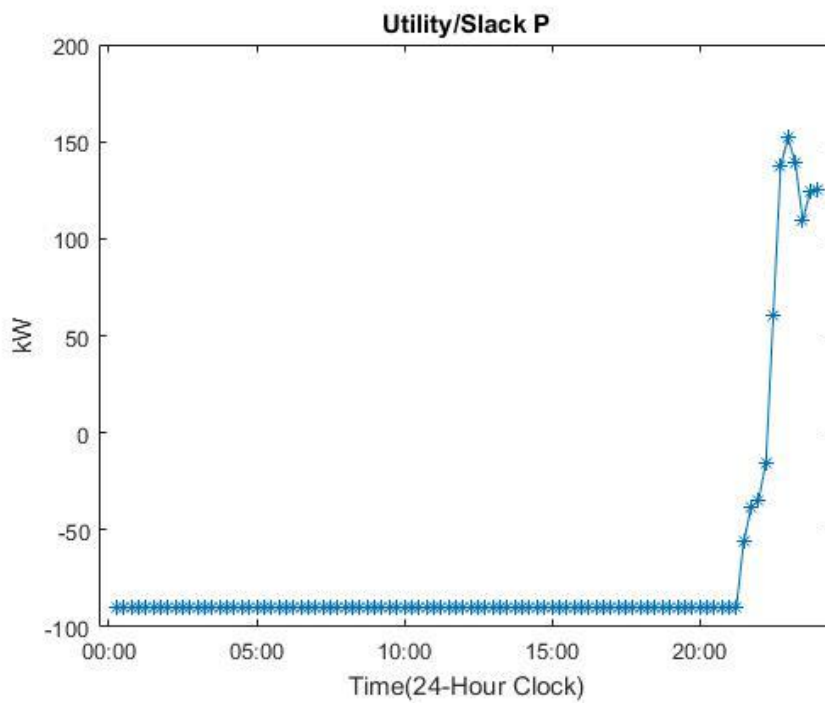
Figure 76: Utility/Slack real power (P) injection in each time step (Case #13).
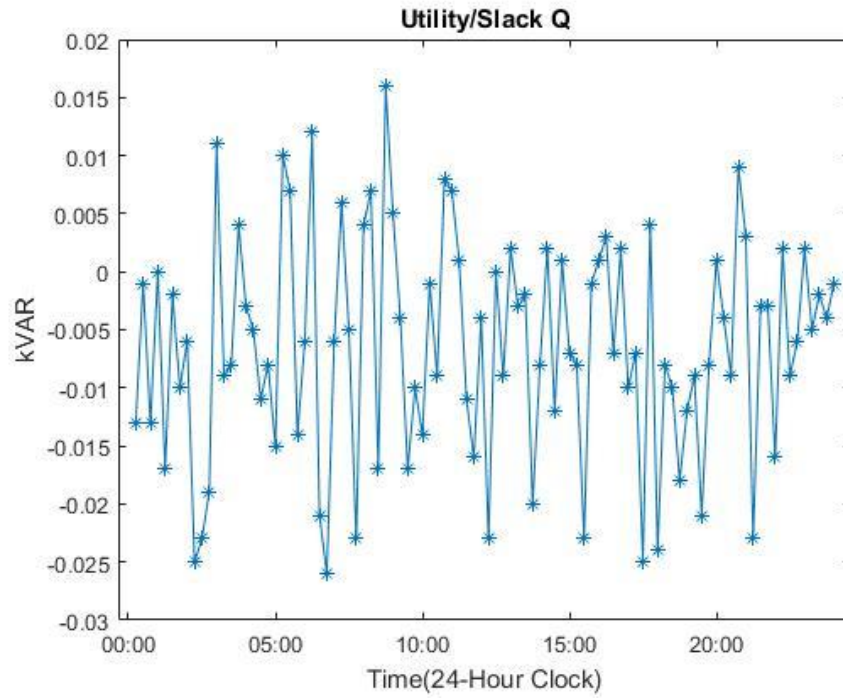
Figure 77: Utility/Slack reactive power (Q) injection in each time step (Case #13).
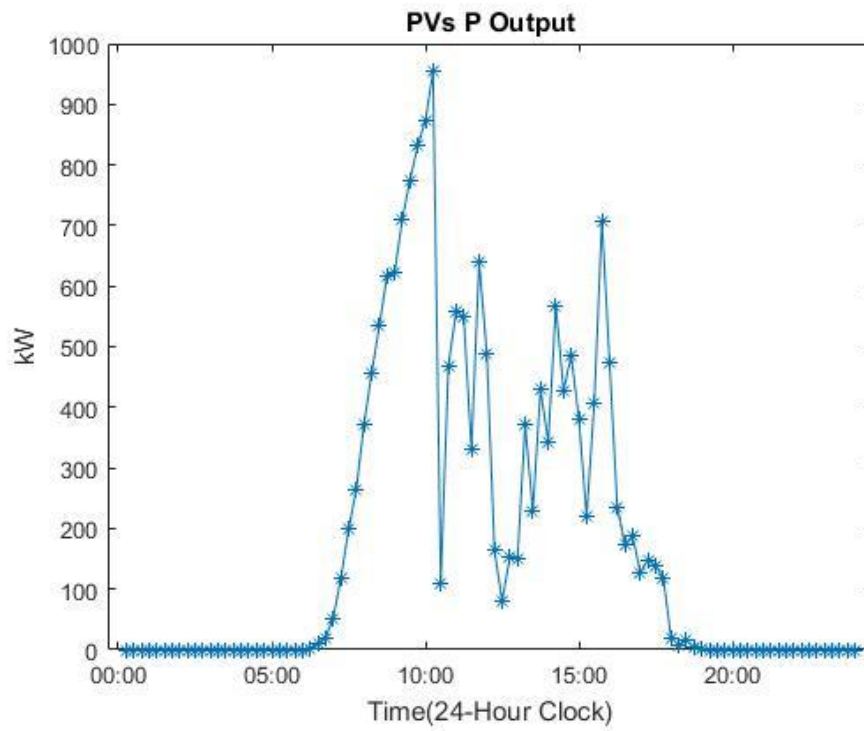
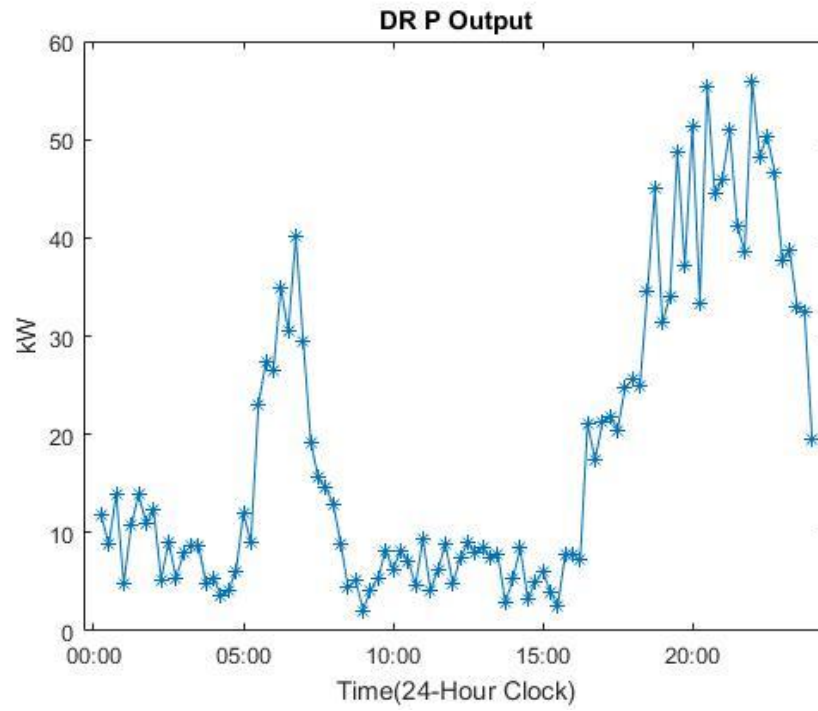*Figure 78: PVs real power output in each time step (Case #13).*

87
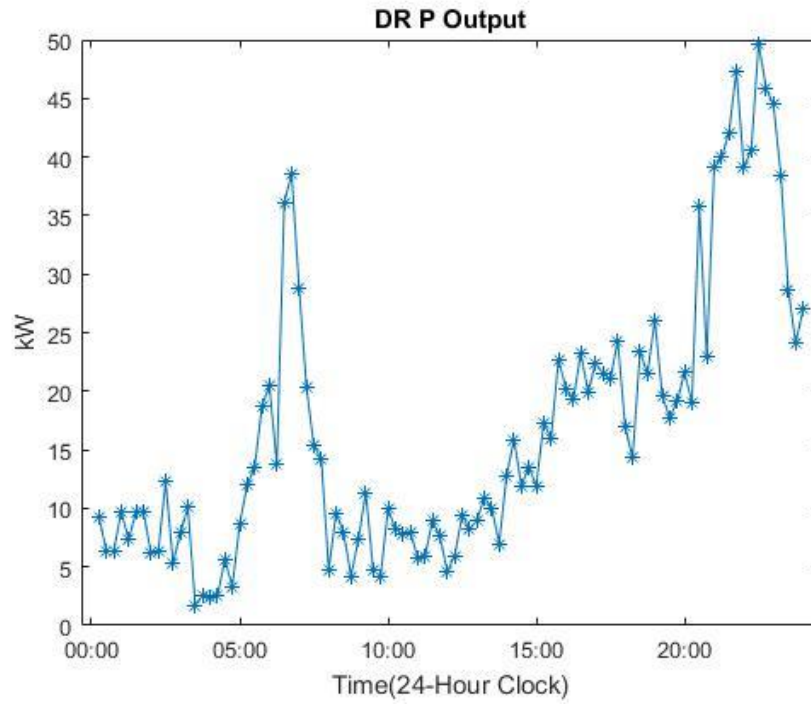
*Figure 79: Demand response applied in each time step (Case #13).*
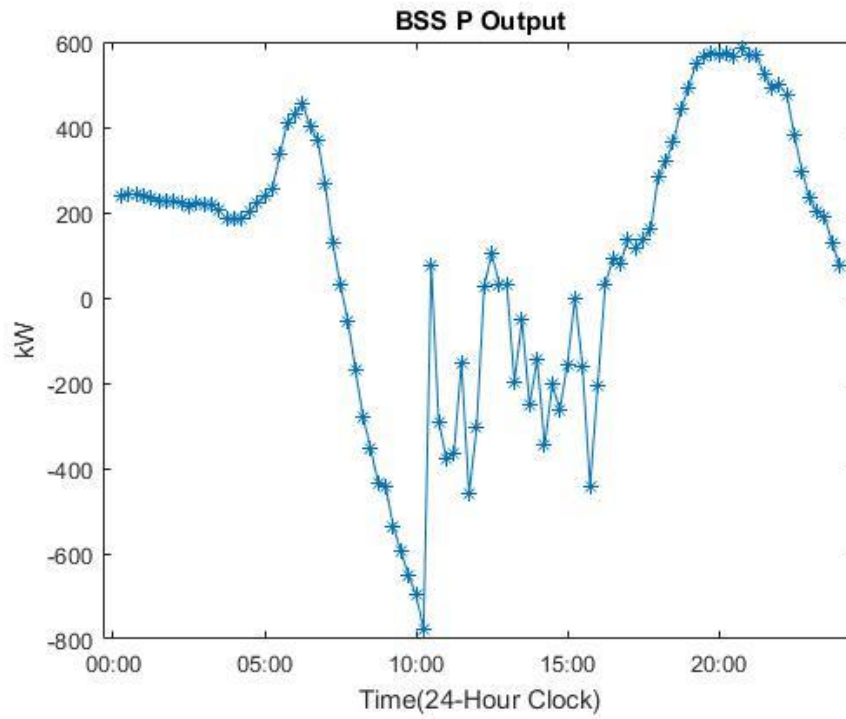
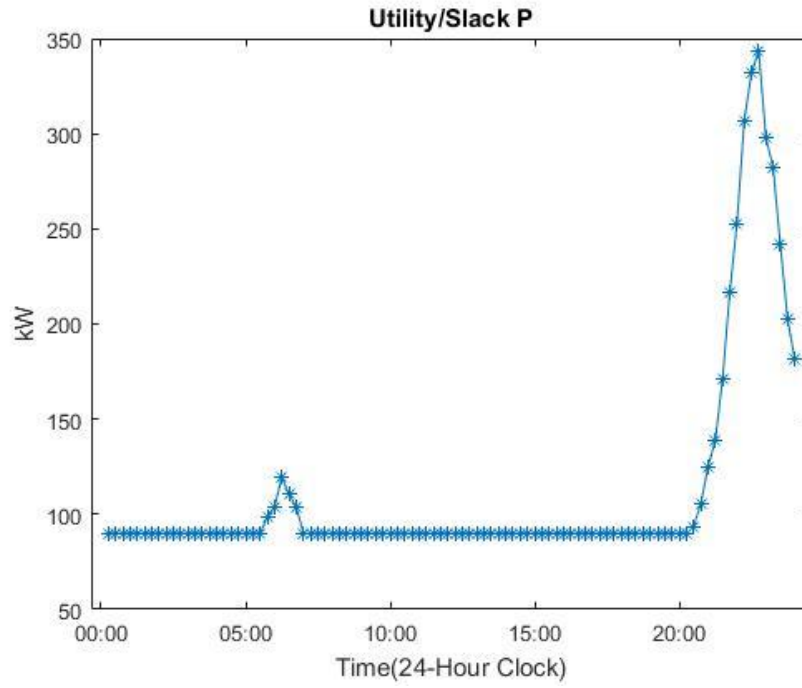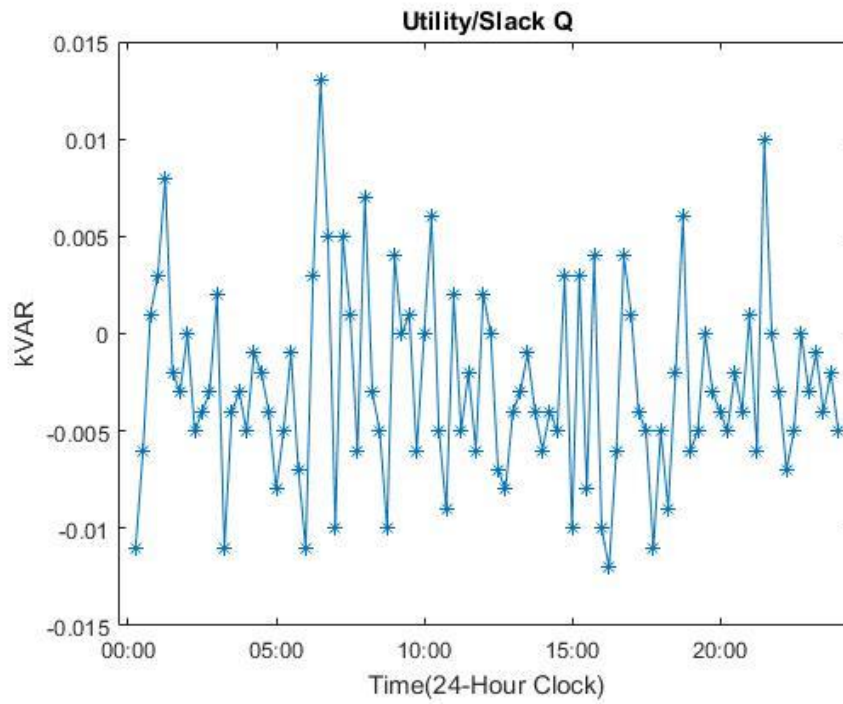*Figure 80: Storage power output/input in each time step (Case #13).*

88
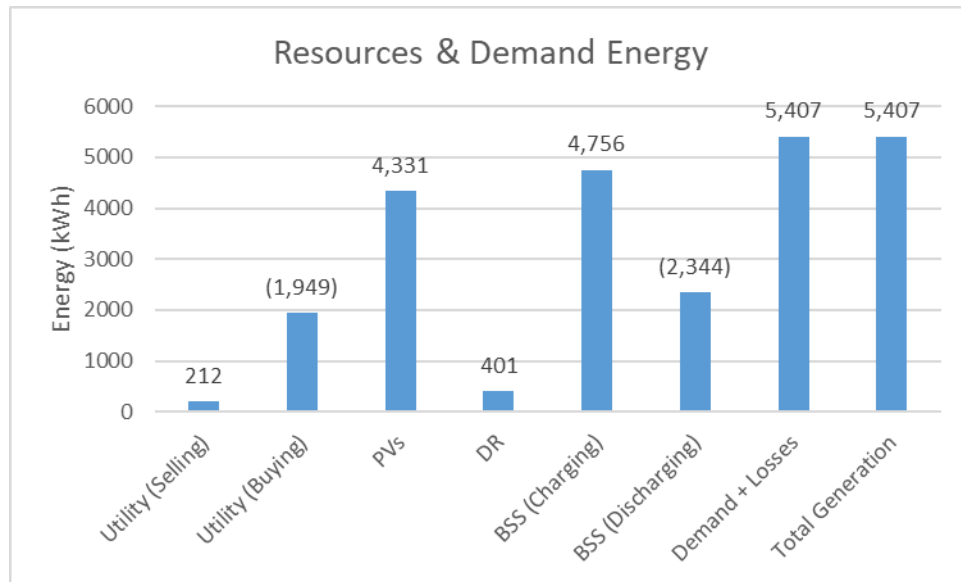
Figure 81: Resources and Demand Energy (Case #13).

This simulation showed that the MG cannot supply the energy demand and sell 90-kW to the utility all the time with a cloudy day. There are times (close to the afternoon peak) where MG fell short of resources (most storage devices were depleted) and the utility had to supply energy instead of buying it from the MG. This was due to the cloudy day because not all BSS resources could charge to 100% (PVs produced less energy in this scenario). That means, the MG needs to supply a lower amount of power to the utility in cloudy days given that it will not have sufficient energy to satisfy the demand and supplying energy to the utility in the 24-hour period.

6.14 Case #14: All DERs (Sunny day, EnergyCell battery) with optimization

This was a case to compare the behavior and results obtained by using a different storage technology; same as case 6, but using the EnergyCell 200NC (Lead-acid) instead of the LG RESU10H (Li-ion). This battery has maximum capacity of 2.136-kWh and a maximum charge

rate of 0.7632-kW. For this scenario, each customer has 4 batteries, thus, the BSS has a maximum capacity of 8.54-kWh with a charge rate of 3.05-kW. The batteries have a depth of discharge (DoD) of 50%, (equivalent to 4.27-kW), a minimum SOC of 40% (equivalent to 3.42-kWh of reserved energy) and an initial SOC of 70%, equivalent to 5.98-kWh. The following graphs were obtained after simulating case 14.
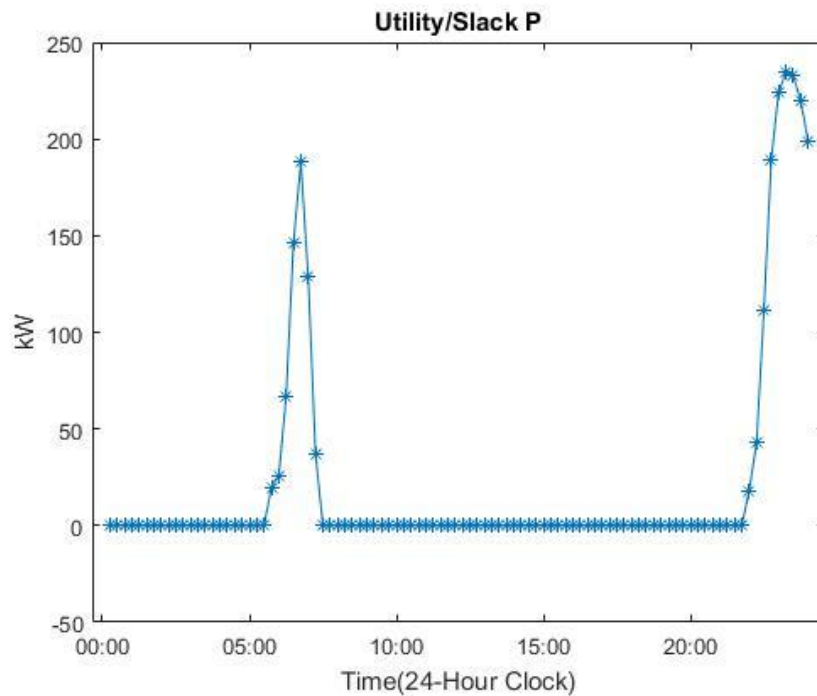
Figure 82: Utility/Slack real power (P) injection in each time step (Case #14).
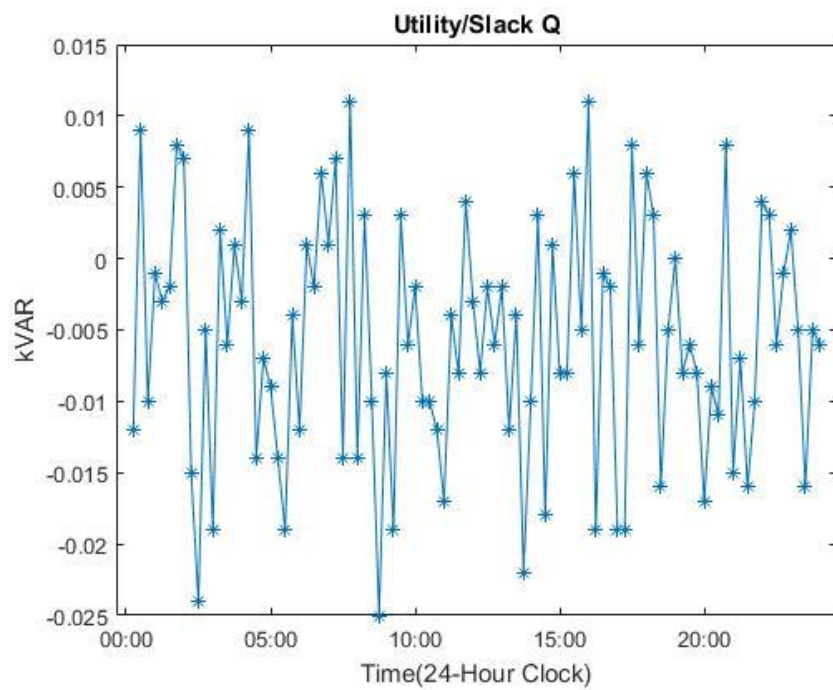
*Figure 83: Utility/Slack reactive power (Q) injection in each time step (Case #14).*
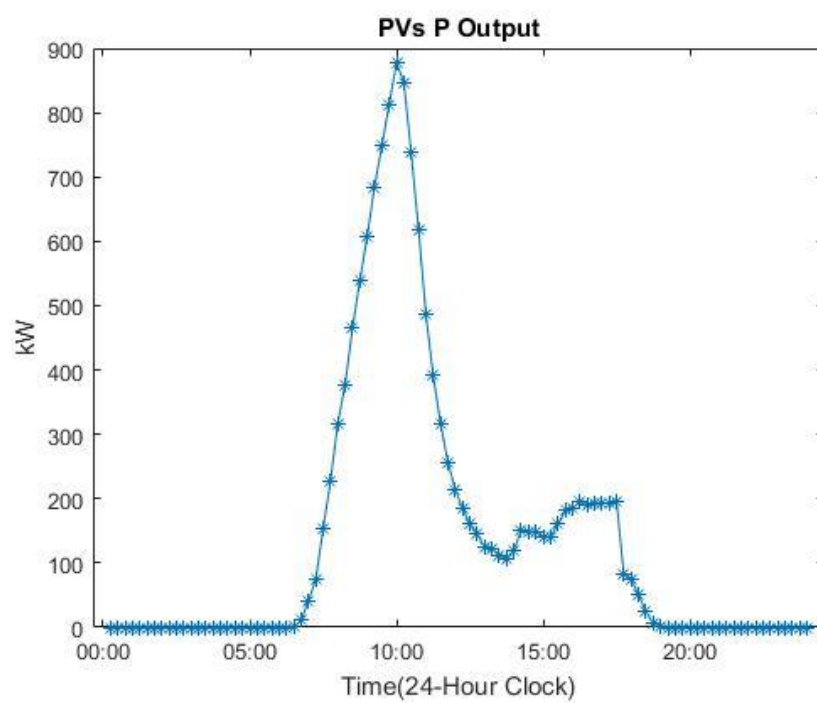
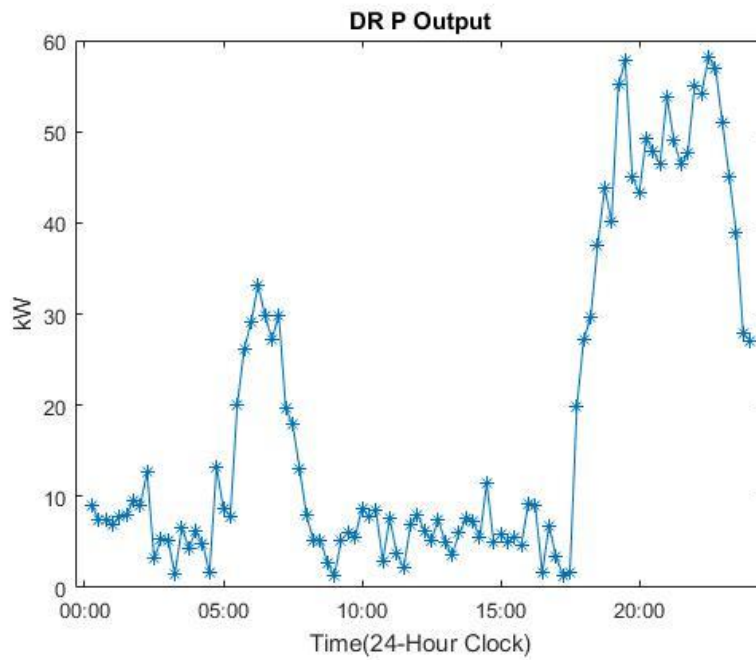*Figure 84: PVs real power output in each time step (Case #14).*

91
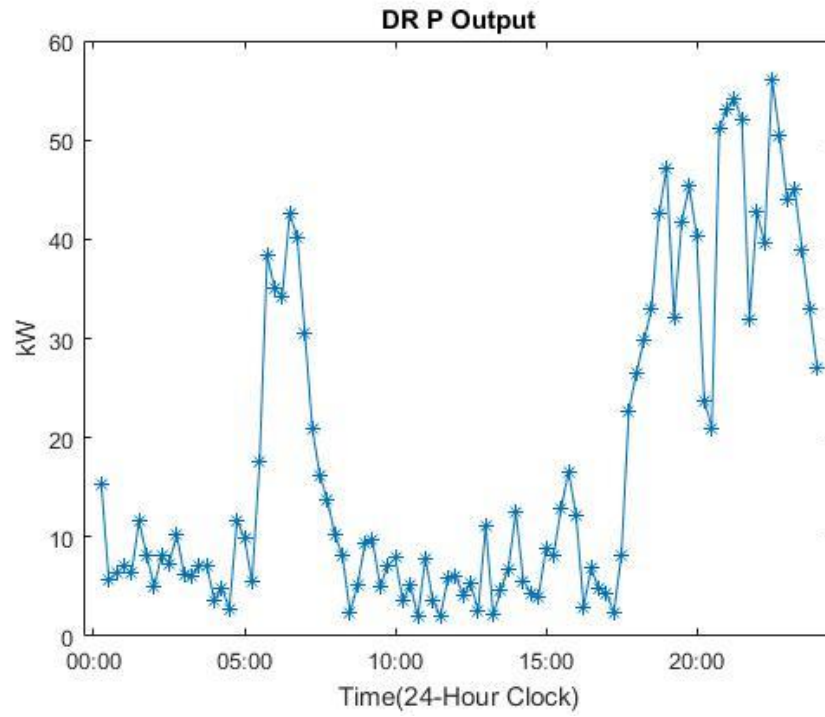
*Figure 85: Demand response applied in each time step (Case #14).*
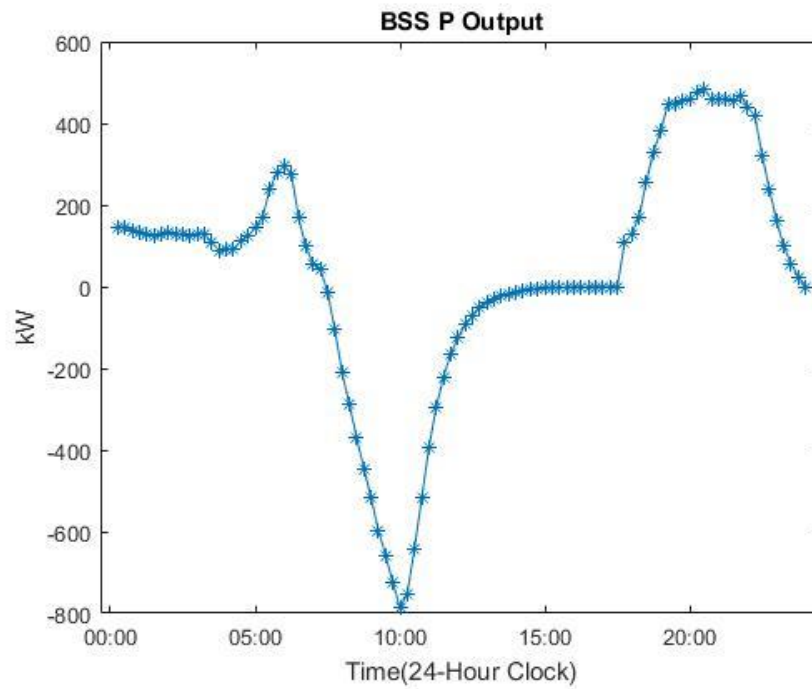
*Figure 86: Storage power output/input in each time step (Case #14).*

92
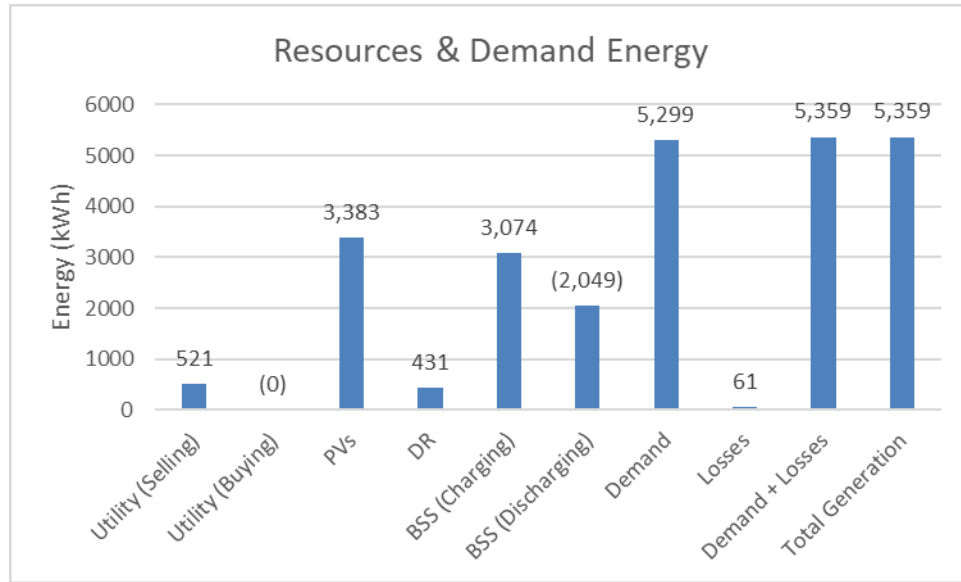
Figure 87: Resources and Demand Energy (Case #14).

The results obtained in this simulation are very similar as the ones obtained in case 6 (with the LG RESU10H). Based on the results, the technology being used (Li-ion or Lead-acid) was not a determining factor; on the other hand, the storage's capacity, charge and discharge rates are. A BSS with a large capacity will allow a higher amount of energy to be stored. Thus, it will allow a higher contribution during those times where the PVs are not providing power. With a higher charge and discharge rates, the BSS can control better energy variances in the system; but, on the other hand, setting high charge/discharge rates can decrease the BSS life expectancy [48], [49]. From [50], Li-ion technologies have a better performance than Lead-acid technologies. Both will serve the purpose and can help to achieve a high load factor in a MG. Nevertheless, their performance and technology characteristics will determine their life expectancy and long-term contribution as an energy resource in a MG, but this analysis was out of the scope of this thesis.

6.15 Analysis of results

The results showed that a high integration of DERs, with sufficient storage, customers that are willing to be flexible in their energy use (i.e., contribute DR), and applying optimization techniques, a MG could supply his energy demand, could also work islanded from the utility, or can sell energy to the utility while satisfying its own energy demand. The MOPF algorithm is able to find the best use of resources, but this depends on the MG's conditions, topology and available resources. If there are not enough local resources the DERs are not enough to cover the energy demand. An important aspect the optimization was able to achieve was a reduction in the emissions produced by the utility. The following figure shows the total utility/slack emissions for each case.
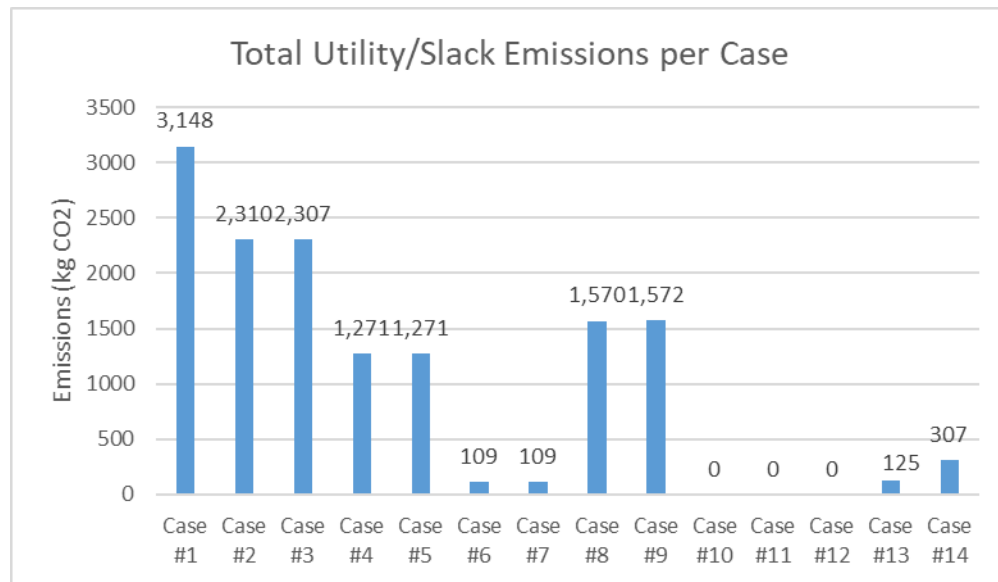
Figure 88: Total kg CO2 Emissions per Case

Based on the previous figure, the lowest emissions were obtained on the cases were optimization was applied (cases with optimization were 4 to 14). The only cases where the

emissions were zero happened in cases 10, 11 and 12 because they did not rely on the utility or any fossil-fuel generator. Those cases represent a MG with 100% of renewable resources and zero-emissions to the environment during operation achieved through optimization. This assumes appropriate disposition of equipment once their useful life is reached.

DR was another important energy resource in this optimization that helped to balance the energy generation with the demand. This is why it is important to consider social aspects such as customers with different demand elasticities (different levels of willingness to reduce their energy demand) because this will determine the amount of DR available in the system. If social considerations are not taken into account, DR could not be used properly as an energy resource. Fixing a determined DR percentage for the whole demand, as done in [44], will not be a very realistic or even feasible scenario, because its being assumed that every end-customer will contribute with the same amount of DR, which is not necessarily true. From the DR graphs obtained on each case, it can be seen that this resource was used when needed to balance the energy generation with the demand and it was mostly used on the demand peaks.

This thesis has resulted in a framework to study and design sustainable microgrids, since sustainability considerations are included in the optimization to find the best allocation of resources: economic aspects (different resources have different rates of kWh, prioritized as: PVs=1st priority, DR=2nd priority, BSS=3rd priority and Slack=last priority), social aspects (four customer categories with different demand elasticities and thus different DR contribution) and environmental aspects (the utility/slack is composed of several fossil-fuel generator resources and is used only when needed). The three pillars of sustainability are being considered in the optimization, thus, a sustainable MG could also be achieved through the MOPF optimization.

The simulations showed that a MG could operate in Islanded mode, thus, they could be used in case of natural disasters. Hurricane Maria destroyed or severely damaged almost half of Puerto Rico's transmission infrastructure, while destroying or severely damaging over 75% of the distribution infrastructure. The damages were so severe that only 65.4% of the power had been restored after 90 days [51]. Many customers are in remote places and/or places with limited access. If MGs were available in those places, those customers would have had minimal access to electricity. Even if the MGs receive damage during a hurricane, the repairs could have lasted days or weeks, not months. Those MGs could also have been used to supply energy to nearby neighborhoods or communities, while the bulk system was being repaired; this could have been a valuable service provided by a MGs and DERs.

Costs were calculated for each case, and the following figure shows the total cost of energy generation for the 24-hour period for each case.
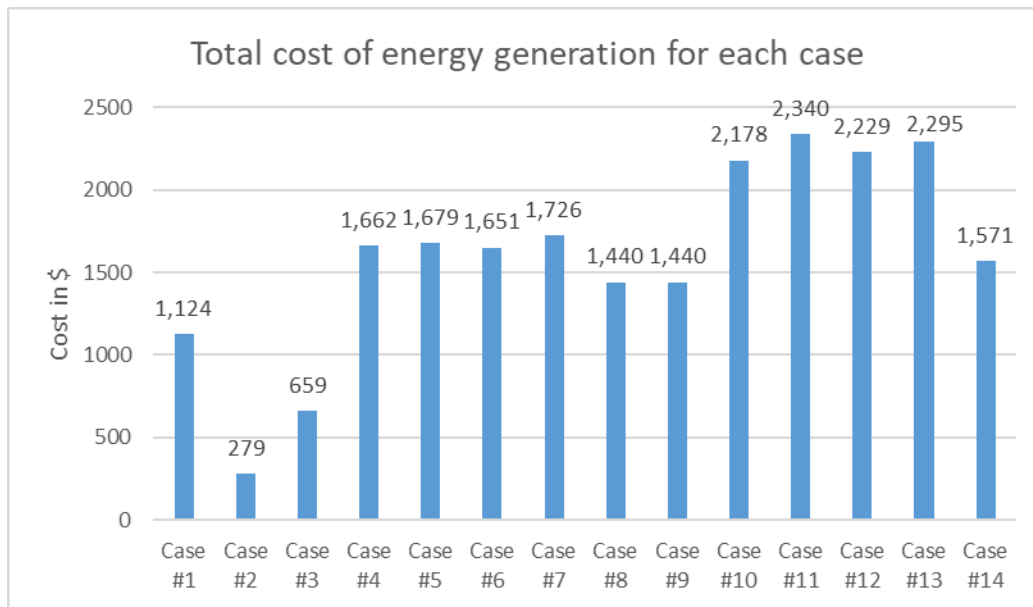
Figure 89: Total cost of energy generation for each case

On case 1, the utility was delivering all the energy demand, thus, will be used as the base case to make cost comparison. The lower costs were obtained on cases 2 and 3. On those cases, the PVs were injecting their maximum power available and they sold very high amounts of energy to the utility. They reduced the total costs significantly, but they also yielded the lowest load factor values (higher energy variations on the system.

The total costs on the cases with optimization and all DERs available (cases 4-14) were higher. This makes sense because the energy contracted from the utility was fixed and the energy demand was being supplied by resources that were costlier that the utility (some resources such as storage devices have higher rates than the utility). Thus, it can be seen a direct proportion between the load factor and the costs of energy production in a MG (at least for these particular cases simulated). To achieve a high load factor, by optimizing the use of the resources in a MG, there is a price to pay if conventional economic measures are used. For example, if costs were assigned to environmental emissions, to resilience capability and to social benefits, the cost comparison would show higher values for utility power, and lower for renewable-based MG. A MG life cycle assessment and emission costs analysis that supports the previous statement is presented in Appendix G.

In a MG, there might be some resource limitations, because not every customer can afford to pay/invest in distributed resources such as a PV system and BSS. As presented in [52], the average cost for residential PV system is around $3.22 (per Watt, AC); this cost includes the overall costs of buying, installing and maintaining the system. In Puerto Rico that cost has been found to be around $3 per Watt. For the BSS, the range is between $5,000-$7000 for the storage device; or $400-$750 per kWh of storage [53]. Thus, a customer who wishes to install a 3-kW PV system must pay/invest around $ 9,000, and if he/her wishes to add storage of 9.8-kWh, another $7,350

must be paid, thus, the whole system will cost around $16,350. This is a considerable investment and not every customer can afford this. This is one of the reasons some end-customers sign a PPA contract with a third-party company who can provide them a PV system without any initial investment [11].

6.16 Enhanced Optimization Architecture for a MG

In order to develop a robust and more reliable Energy Management System Platform, considering even more aspects that might affect the system, more realistic data, and also considering the possible existence of an energy market, the following architecture was developed after the test and analyses made with MOPF algorithm.
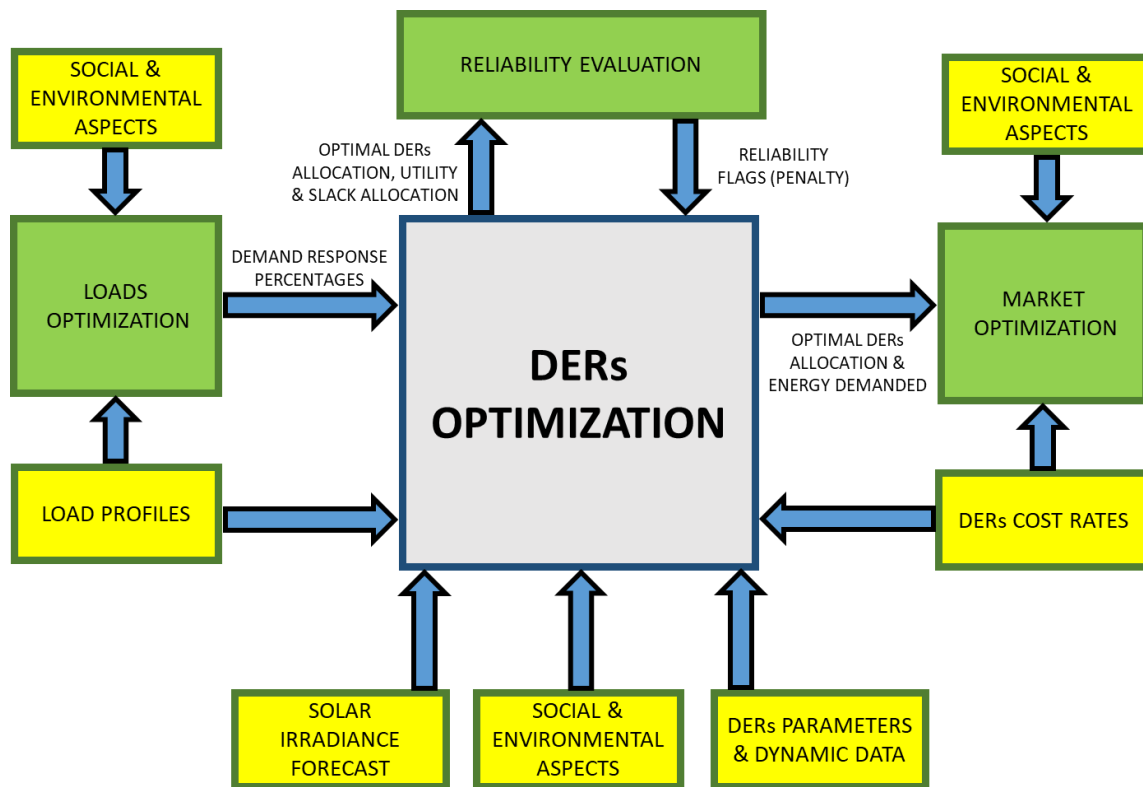
Figure 90: Optimization architecture for a MG.

This architecture has three optimization blocks. The first one is for load optimization where the application of evolutionary algorithms for load forecasting can be applied [54]. The output of this optimization block will be the maximum DR percentage that an end-user is willing to contribute with in each time step; social and environmental aspects could be considered in this block. This data will be one of the inputs for the DERs optimization block since DR is considered as an energy resource. The second block is for DERs optimization and its details, tests and results were already discussed and presented on the previous chapters of this thesis. The third one is for market optimization where an auction energy system and a brokerage system can be implemented to support a market at the distribution level [55]. Social and environmental aspects could also be considered in this block. The efficient allocation of the resources and the energy demanded by each end-customer will be the inputs used of this block since these are the energy bids issued by producers and consumers.

Furthermore, on this architecture there is also a reliability block, where the output obtained in the DERs optimization block can be used to evaluate reliability indices [56]. If there is a reliability violation to the system, this block can raise a flag or sent a penalty signal to the DERs optimization block to let it know there is a reliability concern in the system and it needs to find another solution to the problem. In addition, there are other blocks with dynamic data for the optimization blocks, such as the solar irradiance forecast, as well as other data of these customers that might affect the load forecast optimization, DERs optimization and the market optimization.

To show the algorithm's flexibility, it was modified and tested to optimize an energy market scenario (presented in Appendix I). It can also be extended to address other concerning topics in the MG's field such as resiliency and faults.

MOPF is a tool that can be used to optimize a system for more extended periods, rather than a 24-hour period, in long-term simulations. For example, if long-term forecasted data of the system's demand and solar irradiation were available, future energy contracts with the utility could be analyzed. If the objective function is modified, it could be used to determine the minimum storage and PVs capacity necessary in the system under a worst-case scenario. In addition, another resource such as demand response with negative values could be considered to increase the energy demand, rather than decrease it, when there is energy excess in the system. This tool can be modified and adapted to solve and analyze any particular problem or scenario desired by the user with different topologies, resource integration, different time periods and different resolutions (with different time steps). The MOPF has the flexibility to change the search method as well: the GPS algorithm, which is being used to find the decision variables vector, could be changed if a more efficient method is identified for the MOPF.

Chapter 7:   Conclusions and Future Work

7.1 Conclusions

One of the key contributions of this thesis is the development of a new MOPF algorithm to address and optimize problems related to microgrids. The breadth of elements or objectives that this new algorithm includes sets it apart from other MG optimization methods found in literature. This algorithm represents a sustainable microgrid analysis and design framework that includes social, economic and environmental objectives using a multi-objective optimization approach. The GPS algorithm used as the foundation for the MOPF was able to efficiently prune unstable or unfeasible solutions out from the search space and arrive to good values in the process of balancing supply and demand in the MG. This thesis is the first instance of the use of the GPS algorithm in this MG context.

The MOPF was used to develop and study energy allocation scenarios for the achievement of sustainability and self-reliance of microgrids. Resources optimized included the amount of non-renewable energy (from the utility), distributed storage, consumption reduction strategies (demand response) and PV systems. There is no available algorithm found in technical literature that considers all the elements and aspects considered in MOPF at once, thus, it's a novel algorithm with several considerations to optimize MGs, and an algorithm that has the flexibility to be modified and enhanced to better address the user desires and future problems to be studied. For example, the framework could be extended to study the interaction of groups of microgrids with sub-transmission and transmission systems as well.

The architecture presented on section 6.16 is another contribution that will provide even more realistic scenarios to make analyses in the MG's field (it will probably require implementation with a different programming languages and heavy computational resources).

The application of this algorithm and the results presented in this thesis answered the questions posed in Section 1.2, which are also contributions of this work:

- MOPF determined the best use the resources in each time step. Its output is the efficient allocation of the available resources complying with the system's constraints, taking into consideration social and environmental aspects, and with the best objective function value found in the search space (either local or global solution). It provided a feasible and stable configuration from this search space as long as the system's constraints, conditions and topology allow it. It also balanced the generation with the energy demand plus losses.

- To maximize the benefits provided by DERs, the best use of the resources in each time step needs to be found; MOPF achieved this. With MOPF, other objectives to maximize benefits from DERs desired by the user could be added to analyze other scenarios desired by the user. MOPF is a flexible tool that can be modified and enhanced to better address the user desires and objectives to solve a particular problem. Thus, it is a tool to maximize the benefits provided by a MG with DERs.

- Each DER behaves differently because their dynamics and models are different from each one. With MOPF, the disturbances, variances or intermittencies from DERs were managed and controlled by compensating energy shortages with other resources. This coordination and management of resources can only be achieved though optimization or an advanced and controlled energy management system; as achieved with MOPF.

- Based on [44] and the results obtained with MOPF a zero or low net energy MG can be achieved. As presented on cases 4 and 5, the utility was delivering a constant amount of power and the resources were optimized to supply the rest of the demand while trying to achieve the highest load factor possible as possible. Comparing these results with the base cases, it can be seen that without MOPF a zero or low net energy MG could not be achieved; the load factor was low on those cases. As well, if the resources in a MG are limited or scarce, it will be very difficult to achieve a high load factor as well. A high integration of DERs is needed to obtain better results and, to manage and coordinate those resources, MOPF was necessary.

- The injection of reactive power from PVs, and optimized DERs can affect the system positively since those energy resources are contributing to supply the reactive power demand in the system; relying less on the utility. MOPF balanced the resources available with the energy demand, thus, maintain the frequency within its nominal value and also ensuring that voltages are within the defined bounds (As defined by ANSI C84.1-1995 standard [57]); an example of the voltages obtained in the optimization is presented in Appendix B. Without MOPF, a high integration of DERs not being optimized could violate a constraint, such as the voltage bounds, in the system because their interaction with the MG is not being managed and controlled properly. As presented in [58], if the PV's energy injection is very high, voltages could exceed their bounds and cause harms to the system or the loads connected to it. Therefore, MOPF helped to control and manage the interaction of DERs in the system and how they affect the system's constraints.

- If the optimization results comply with the constraints and the limitations presented on the tree pillars of sustainability figure, a sustainable MG can be achieved. Since MOPF

considers economic, social and environmental aspects, the efficient allocation will guarantee a sustainable MG. Without optimization and a high integration of DERs, a sustainable MG cannot be achieved; or it can be very difficult.

- The algorithm's output is the efficient allocation of resources in each time step and thus can be used to emulate energy bids of a distribution level market. Therefore, those bids already consider the MG's constraints and sustainability considerations. If those bids are not optimized, a system constraint could be violated and cause harm to the system or the loads connected to it; an unfeasible configuration could also occur. Therefore, without optimization of bids (users with DERs) the market could fail. Thus, MOPF support the creation of an energy market at the distribution level.

7.2 Future Work

The following topics and recommendations could be considered as extensions of this thesis:

- Modify and adapt MOPF algorithm to optimize an energy market; using market objectives and constraints.

- Creation of other scenarios, with different topologies, different resources, different conditions and with a smaller time step to obtain an output with a higher resolution. Simulations with a lower step size will require better computational resources (hardware).

- Enhance the algorithm with different routines to see if it can be used for real-time optimization. For example, test of linearized models and method approximations in the optimization.

- Complete and test the Enhanced Optimization Architecture for a MG structure.

- Use MOPF as a tool to make fault analyses and also use it to analyze how a MG can help the bulk system in case of a fault.

- Use MOPF as a tool to measure and evaluate the reliability of MGs.

References

[1]   J. Mossoba, M. Kromer, P. Faill, S. Katz, B. Borowy, S. Nichols, and L. Casey, "Analysis of Solar Irradiance Intermittency Mitigation Using Constant DC Voltage PV and EV Battery Storage," *IEEE Transp. Electrif. Conf. Expo*, 2012.

[2]   N. Modi, "Low Inertia Power Systems : Frequency Response Challenges and a Possible Solution," *Australas. Univ. Power Eng. Conf.*, 2016.

[3]   Energy Sentry., "Load Factor Calculations." [Online]. Available: http://energysentry.com/newsletters/load-factor-calculations.php.

[4]   "What Your Electrical Load Factor is Telling You," 2014. [Online]. Available: https://efficiencyinnovascotia.wordpress.com/2014/02/14/what-your-electrical-load-factor-is-telling-you/.

[5]   "Austin Energy, 'Customer care understanding load factor how to calculate load factor load factor.'" [Online]. Available: https://austinenergy.com/wps/wcm/connect/8fe76160-0f73-4c44-a735-529e5c7bee61/understandingLoadFactor.pdf?MOD=AJPERES.

[6]   P. K. Nag, "Power Plant Engineering," 2014.

[7]   P. Planet., "Electrical Load Factor." [Online]. Available: http://www.demandcharge.com/Web_Pages/Articles/Electrical_Load_Factor.html.

[8]   R. Weisenmiller, "WHAT IS A MICROGRID?" [Online]. Available: https://energycenter.org/self-generation-incentive-program/business/technologies/microgrid.

[9]   J. Blanc, B. Duretz, and A. De Selle, "The Benefits of Demand Response for Utilities," 2014. [Online]. Available: https://www.schneider-

electric.com/solutions/ie/en/med/679448846/application/pdf/2398_998-2095-08-22-14ar0_en.pdf.

[10] U.S. Department of Energy, "The Potential Benefits of Distributed Generation and the Rate- Related Issues That May Impede Its Expansion." [Online]. Available: http://energy.gov/sites/prod/files/oeprod/DocumentsandMedia/1817_Report_-final.pdf.

[11] "SUNNOVA'S PPA Plan." [Online]. Available: http://www.sunnova.com/service/solar-as-a-service/our-plans/ppa/.

[12] J. Lazar and W. Gonzalez, "Smart Rate Design For a Smart Future," 2015. [Online]. Available: http://www.raponline.org/featured-work/smart-rate-design.

[13] S. Corneli, S. Kihm, L. Schwartz, and L. Berkeley, "Electric Industry Structure and Regulatory Responses in a High Distributed Energy Resources Future," 2015. [Online]. Available: https://emp.lbl.gov/sites/all/files/lbnl-1003823.pdf.

[14] J. Nocedal, S. J. Wright, and S. M. Robinson, "Numerical Optimization," 2006.

[15] W. Lin, C. Tu, and M. Tsai, "Energy Management Strategy for Microgrids by Using Enhanced Bee Colony Optimization," *energies*, vol. 9, no. 1, 2016.

[16] P. De Martini and J. D. Taft, "A Tale of Two Visions," *IEEE power energy Mag.*, vol. 14, no. 3, pp. 63–69, 2016.

[17] M. N. Akter, S. Member, M. A. Mahmud, and A. M. T. Oo, "A Hierarchical Transactive Energy Management System for Microgrids," *Power Energy Soc. Gen. Meet.*, 2016.

[18] A. Rojas and T. Rousan, "Microgrid control strategy: Derived from stakeholder requirements analysis," *IEEE Power Energy Mag.*, vol. 15, no. 4, pp. 72–79, 2017.

[19] S. Shokoohi and H. Bevrani, "An Intelligent Droop Control for Simultaneous Voltage and Frequency Regulation in Islanded Microgrids," *IEEE Trans. Smart Grid*, vol. 4, no. 3, pp.

1505–1513, 2013.

[20] P. De Martini, R. Ambrosio, and E. Gunther, "Transactive Energy: GridWise Architecture Council Foundational Session," 2012.

[21] D. Sciano, "Distributed Resource Integration." [Online]. Available: http://www.nyiso.com/public/webdocs/markets_operations/committees/environmental_a%09dvisory_council/meeting_materials/2016-05-06/Con_Ed_EAC_May_6_2016.pdf.

[22] S. M. Sajjadi, P. Mandal, B. Tseng, and M. Velez-reyes, "Transactive Energy Market in Distribution Systems : A Case Study of Energy Trading Between Transactive Nodes," *North Am. Power Symp.*, 2016.

[23] P. Lilienthal, "Microgrid Value Propositions," 2012. [Online]. Available: http://microgridnews.com/microgrid-value-propositions/.

[24] NYSERDA, "Microgrids: An Assessment Of The Value, Opportunities And Barriers To Deployment In New York State," 2010.

[25] Environmental Protection Agency (EPA), "Learn About Sustainability." [Online]. Available: https://www.epa.gov/sustainability/learn-about-sustainability#what.

[26] R. Sharma, "Sustainable Microgrids - Increasing Access to Energy (Markets)," *Power Syst. Conf. Clemson Univ.*

[27] Rinkesh, "What is Sustainable Energy?" [Online]. Available: https://www.conserve-energy-future.com/sustainableenergy.php.

[28] S. Annala, "Households Willingness To Engage in Demand Response in the Finnish Retail Electricity Market : an Empirical Study," 2015.

[29] THEMA Consulting Group, "Demand response in the Nordic electricity market: Input to strategy on demand flexibility," 2014.

[30]   M. E. Club, "How to Measure Demand Elasticity?" [Online]. Available:

https://www.managerial-economics-club.com/demand-elasticity.html.

[31]   "Price Elasticity Of Demand." [Online]. Available:

https://www.investopedia.com/terms/p/priceelasticity.asp.

[32]   Campbell R. McConnell, S. L. Brue, and S. M. Flynn, "Microeconomics, 19e," 2011.

[33]   C. R. Malavika, "Environmental Effects Associated with Battery Disposal," 2004.

[Online]. Available: http://www.frost.com/sublib/display-market-insight-

top.do?id=20759887.

[34]   K. Kattenburg, "What Do Batteries Do to the Environment If Not Properly Recycled?"

[Online]. Available: http://education.seattlepi.com/batteries-environment-not-properly-

recycled-3916.html.

[35]   U.S. Department of Energy, "Environment Baseline , Volume 1 : Greenhouse Gas

Emissions from the U . S . Power Sector," 2016.

[36]   E. De Santis, A. Rizzi, A. Sadeghian, F. Massimo, and F. Mascioli, "Genetic Optimization

of a Fuzzy Control System for Energy Flow Management in Micro-Grids," *Jt. IFSA World

Congr. NAFIPS Annu. Meet.*, 2013.

[37]   W. Shi, S. Member, X. Xie, C. Chu, and R. Gadh, "Distributed Optimal Energy

Management in Microgrids," *IEEE Trans. Smart Grid*, vol. 6, no. 3, pp. 1137–1146, 2015.

[38]   R. D. Zimmerman and C. E. Murillo-Sánchez, "MATPOWER 6.0." [Online]. Available:

http://www.pserc.cornell.edu/matpower/.

[39]   MathWorks, "Global Optimization Toolbox User ' s Guide." [Online]. Available:

https://www.mathworks.com/products/global-optimization.html.

[40]   MathWorks, "Pattern Search Terminology." [Online]. Available:

https://www.mathworks.com/help/gads/pattern-search-terminology.html?searchHighlight=pattern search&s_tid=doc_srchtitle.

[41]   Mathworks, "How Pattern Search Polling Works." [Online]. Available: https://www.mathworks.com/help/gads/how-pattern-search-polling-works.html.

[42]   A. Garces, "A Linear Three-Phase Load Flow for Power Distribution Systems," *IEEE Trans. Power Syst.*, vol. 31, no. 1, pp. 827–828, 2016.

[43]   J. A. M. Rupa and S. Ganesh, "Power Flow Analysis for Radial Distribution System Using Backward / Forward Sweep Method," *Int. J. Electr. Comput. Eng.*, vol. 8, no. 10, pp. 1628–1632, 2014.

[44]   I. Jordan, "Towards a Zero Net Energy Community Microgrid," 2017.

[45]   "LG RESU10H datasheet." [Online]. Available: https://d3g1qce46u5dao.cloudfront.net/data_sheet/resu10h_datasheet_rev1_3.pdf.

[46]   AEE, "Estructura Tarifaria Autoridad de Energía Eléctrica." [Online]. Available: https://www.aeepr.com/Documentos/Ley57/Presentacion Tarifas para Pagina AEE Internet - 05-19-2015.pdf.

[47]   "PIKA ENERGY Harbor Plus datasheet." [Online]. Available: https://www.pika-energy.com/files/datasheets/pika_harbor_plus_datasheet.pdf.

[48]   Ultralife, "Li-Ion vs . Lead Acid," 2007. [Online]. Available: http://www.beck-elektronik.de/uploads/media/lithium-ion-vs-lead-acid.pdf.

[49]   G. Albright, J. Edie, and S. Al-Hallaj, "A Comparison of Lead Acid to Lithium-ion in Stationary Storage Applications," 2012.

[50]   H. Ullah, S. Chalise, and R. Tonkoski, "Feasibility Study of Energy Storage Technologies for Remote Microgrid 's Energy Management Systems," *Int. Symp. Power Electron.*

Electr. Drives, Autom. Motion, 2016.

[51]   FEMA, "Statistics Progress in Puerto Rico." [Online]. Available:

https://www.fema.gov/hurricane-maria.

[52]   R. Fu, D. Feldman, R. Margolis, M. Woodhouse, K. Ardani, R. Fu, D. Feldman, R.

Margolis, M. Woodhouse, and K. Ardani, "U.S. Solar Photovoltaic System Cost

Benchmark," 2017.

[53]   E. Sage, "How much does solar storage cost ? Understanding solar battery prices.," 2018.

[Online]. Available: https://www.energysage.com/solar/solar-energy-storage/what-do-

solar-batteries-cost/.

[54]   D. Rosa and W. Rivera, "Application of Evolutionary Algorithms for Load Forecasting in

Smart Grids," 2018.

[55]   H. M. Meza and M. Rodriguez-martinez, "Cloud-based and Big data-enabled Brokerage

System for Smart Grids," *IEEE Int. Congr. Big Data*, 2017.

[56]   J. Jiménez, I. J. Forty, A. Irizarry-rivera, C. Lebrón, and F. Andrade, "Reliability of a PV

and Batteries Microgrid and Social Aspects- A Case Study," 2018.

[57]   "ANSI C84.1 ELECTRIC POWER SYSTEMS AND EQUIPMENT - VOLTAGE

RANGES." [Online]. Available: http://www.powerqualityworld.com/2011/04/ansi-c84-1-

voltage-ratings-60-hertz.html.

[58]   N. Lopez, "Voltage Regulation and Reactive Power Services from Rooftop Photovoltaic

Systems for Distributed Generation Rates," 2017.

[59]   "45 Busbar Community Distribution System." [Online]. Available:

https://drive.google.com/open?id=1E-Nwfa-s6W7EexhOs6FzD6XiUEVyPBwJ.

[60]   R. K. Khadanga and A. Kumar, "Hybrid adaptive 'gbest'-guided gravitational search and

pattern search algorithm for automatic generation control of multi-area power system,"
IET Gener. Transm. Distrib., vol. 11, no. 13, pp. 3257–3267, 2017.

[61]   S. Alimohammadi, "Multi-Stage Algorithm For Uncertainty Analysis of Solar Power
Forecasting," *IEEE PES Gen. Meet.*, 2016.

[62]   N. Soni, "Optimal LFC System of Interconnected Thermal Power Plants using Hybrid
Particle Swarm Optimization-Pattern Search Algorithm (h PSO-PS)," *2nd Int. Conf.
Commun. Control Intell. Syst.*, 2016.

[63]   V. Vermeulen, J. M. Strauss, and H. J. Vermeulen, "Optimisation of solar PV plant
locations for grid support using genetic algorithm and pattern search," *IEEE 6th Int. Conf.
Power Energy*, 2016.

[64]   B. Lacosere, "A hybrid whale algorithm and pattern search technique for optimal power
flow problem," *8th Int. Conf. Model. Identif. Control*, 2016.

[65]   A. B. F. Amini, "Flowchart of optimization using the pattern search method." [Online].
Available: https://www.researchgate.net/figure/Flowchart-of-optimization-using-the-
pattern-search-method_fig6_258338656.

[66]   C. Wu and X. Lv, "Analysis on Power Flow of Distribution Network with DGs," *China
Int. Conf. Electr. Distrib.*, 2012.

[67]   D. Wu, G. Li, J. Yang, and J. Wu, "Calculation of Load Supply Capability for Distribution
Networks with Distributed Generations," *IEEE PES Asia-Pacific Power Energy Eng.
Conf.*, 2013.

[68]   G. Diaz, J. Gomez-Aleixandre, and J. Coto, "Direct Backward/Forward Sweep Algorithm
for Solving Load Power Flows in AC Droop-Regulated Microgrids," *IEEE Trans. Smart
Grid*, vol. 7, no. 5, pp. 2208–2217, 2016.

[69]   J. Fengli, P. Zailin, W. Shihong, H. Rui, and Z. Yunan, "Power flow calculation for radial distribution systems with distributed generation," *IEEE Int. Conf. Mechatronics Autom.*, 2012.

[70]   X. Tang and G. Tang, "Power Flow for Distribution Network with Distributed Generation," *Asia-Pacific Power Energy Eng. Conf.*, 2010.

[71]   L. Zhang, W. Tang, and H. Guan, "The back/forward sweep-based power flow method for distribution networks with DGs," *2nd Conf. Power Electron. Intell. Transp. Syst.*, 2009.

[72]   D. Ming and G. Xue-feng, "Three-phase power flow for the weakly meshed distribution network with the distributed generation," *Asia-Pacific Power Energy Eng. Conf.*, 2009.

[73]   H. Liu, S. Cheng, C. Huang, and Y. Hou, "Unbalanced power flow calculation for low-voltage distribution systems including DGs," *IEEE Innov. Smart Grid Technol. - Asia*, 2012.

[74]   Frontline, "Optimization Problem Types: Convex Optimization." [Online]. Available: https://www.solver.com/convex-optimization.

[75]   I. Laradji, "Non-convex optimization." [Online]. Available: https://www.cs.ubc.ca/labs/lci/mlrg/slides/non_convex_optimization.pdf.

[76]   A. A. Bilich, L. Goyal, J. Hansen, A. Krishnan, and K. Langham, "Assessing the Life Cycle Environmental Impacts and Benefits of PV-Microgrid Systems in Off-Grid Communities," 2016. .

[77]   E. Wygonik and A. Goodchild, "Evaluating CO_2 emissions, cost, and service quality trade-offs in an urban delivery system case study," *IATSS Res.*, vol. 35, no. 1, pp. 7–15, 2011.

[78]   J. D. Rhodes, "When Will Rooftop Solar Be Cheaper Than the Grid?," 2016. [Online].

Available: https://www.usnews.com/news/articles/2016-03-31/when-will-rooftop-solar-be-cheaper-than-the-grid.

[79]   Solar Central, "Solar Electricity Costs." [Online]. Available:

http://solarcellcentral.com/cost_page.html.

[80]   NREL, "Energy Snapshot: Puerto Rico," 2015. [Online]. Available:

http://www.nrel.gov/docs/fy15osti/62708.pdf.

[81]   E. O'Neill-Carrillo, A. L. Figueroa-Acevedo, and A. Irizarry-Rivera, "Improved

Permitting and Interconnection Processes for Rooftop PV Systems in Puerto Rico.," 2013.

[82]   S. Hench, "How is the cost for batteries per kWh calculated?" [Online]. Available:

https://www.quora.com/How-is-the-cost-for-batteries-per-kWh-calculated-Energy-storage-battery-companies-get-prices-of-800-per-kWh-for-their-cells-and-Tesla-says-their-Powerwall-costs-about-350-per-kWh-How-are-these-figures-calculated-with-grid-electricity.

[83]   W. W. Hogan, "Providing Incentives for Efficient Demand Response," 2009. [Online].

Available:

https://sites.hks.harvard.edu/fs/whogan/Hogan_Demand_Response_102909.pdf.

Appendixes

Appendix A: Algorithm Scripts

The main script to run the algorithm is: MAIN_MOPF.m. This script calls other 26 scripts, 28 data files and reads data from an excel file with the system's topology. The pattern search algorithm uses as function the OPF_unbalanced.m script. On this appendix, only the mentioned scripts (main scripts) are presented, the remaining scripts are available at [59].

MAIN_MOPF Script:

```matlab
% Title: 45 Bus Microgrid Optimization with Distributed Energy Resources
% Description: Algorithm to find the optimal DERs allocation in a Microgrid, taking into
account physical and operational constrains of the system and resources
% Algorithm Name: Microgrids Optimal Power Flow (MOPF)
% Autor: Ramón A. Reyes Colón, MSEE Graduate Student
% Advisor: Dr. Efraín O'neill Carillo
% Email: ramon.reyes7@upr.edu, efrain.oneill@upr.edu
% University of Puero Rico, Mayaguez Campus
% Variables selection is done using the Matlab routine patternsearch(GPSPositiveBasis2N)
with a defined flatstart point
% Unbalanced Load Flow is done using the Back-Forward Sweep Algorith written by Dr
Alejandro Garcés, Universidad Tecnológica de Pereira
% Last Revision: Febuary 4, 2018
%-----------------------------------------------------------------------
%-----------------------------------------------------------------------
%-----------------------------------------------------------------------
clear all;close all; clc % Clean and close all i the workspace
%_____ Declaration of global variables_____
global Pn Pd Pgen Feeder
global Pgmax Pgmin Qgmax Qgmin Drmax Drmin Stomax Stomin
global ratesP ratesQ ratesDr ratesSt
global costP costQ costDr costSto
global Pvar Qvar Drvar Stovar Pgenc Qgenc
global f penalty Res  var viol lftol optiter Ploss Qloss ub lb  maxiter Vmin Vmax sf
global xxP1 xxP2 xxP3 xxQ1 xxQ2 xxQ3 xxDr1 xxDr2 xxDr3 xxSto1 xxSto2 xxSto3
global  varcount  q_enable p_enable dr_enable sto_enable
global SOC SOCmin SOCmax SOCvar delta_t weight

%_____Load data_____
load('SOCmax.mat');load('SOCmin.mat');load('SOC.mat'); % Current State of charge and its
limits before the optimization. Loads once, at the beginning of the optimization. This
value is actulized in each time step. Battery model has a dynamic equation
load('sunny96');load('cloudy96'); % Solar Irradiation curves
%_____Start clock_____
tic
%-----------------------------------------------------------------------
%-----------------------------------------------------------------------
%-----------------------------------------------------------------------

%_____Case Study(User Input)_____
case_study='45 Bus Microgrid'; % Define case study (excel file)
Feeder = LoadFeeder(case_study); %Load Case Study data and topology (Load data from excel
file)
solar_case=sunny96; %Define solar irradiation curve to be used. Curves: sunny96(Sunny
day), cloudy96 (Cloudy day)

%_____Optimization Step_____
delta_t=0.25; % Optimization step in hours

for t=1:24*(1/delta_t)
    t % Shows optimization step time
```

116

```
%_____Load Data_____
load('Pgmax.mat');load('Pgmin.mat'); % PVs P data
load('Qgmin.mat');load('Qgmax.mat'); % PVs Q data
load('Stomax.mat');load('Stomin.mat');% BSS data
load('ratesP.mat');load('ratesQ.mat');load('ratesDr.mat');load('ratesSt.mat'); % rates↙
Data
load('Pna.mat');load('Pnb.mat');load('Pnc.mat');% Demand P data
load('Qna.mat');load('Qnb.mat');load('Qnc.mat'); % Demand Q data
load('Drmaxa.mat');load('Drmaxb.mat');load('Drmaxc.mat');% DR data


%_____User Input Data_____

%_____Rate's Weight_____
weight=[1 1E1 1E2]; %DERs Priority. 1st=PV 2nd=DR 3rd=Storage
ratesP=ratesP*weight(1);ratesQ=ratesQ*weight(1);ratesDr=ratesDr*weight(2)↙
ratesSt=ratesSt*weight(3); % Apply priority

%_____Voltage Boundaries_____
Vmin=0.95;% Maximum p.u voltage
Vmax=1.05;% Maximum p.u voltage

%_____Iterations & Tolerances_____
maxiter=1E3;% maximum iterations for load flow.
optiter=1E3;% maximum iterations for optimization routine.
lftol=1E-3;% tolerance for the load flow.
opttol=1E-3;%tolerance for the optimization routine

%_____Enables, Activate/Deactivate Resources_____
p_enable=1;%Enable/Disable PVs P injection
q_enable=1;%Enable/Disable PVs Q injection
dr_enable=1;%Enable/Disable Demand Response
sto_enable=1;%Enable/Disable Storage
pv_at_max=0; % 1=PVs inject maximum of energy available

%_____Utility Power Contract (kW & kVar) per phase_____
Pna(2,:)=0; % Phase A
Pnb(2,:)=0; % Phase B
Pnc(2,:)=0; % Phase C

Qna(2,:)=0; % Phase A
Qnb(2,:)=0; % Phase B
Qnc(2,:)=0; % Phase C


%_____Dynamic Data & Models (Changes as a function of time)_____
loads_data; % demand profiles data
dr_model; %Demand Response Model
pv_model; %PV model
```

```matlab
%_____Enables, # of variables, bounds and indexes_____
enables; %define active or inactive DERs
var=sum(sum(Pgmax~=0))+sum(sum(Qgmax~=0))+sum(sum(Drmax~=0))+sum(sum(Stomax~=0))%↙
Determine # of decision variables
lb(1,1:var)=0; % lower bounds
ub(1,1:var)=1; % upper bounds
indexes; % DERs Indexes, find where the resources are located in each busbar


%_____Problem's Limiting conditions_____
storage_conditions; %Storage charge/discharge rate limits

%_____ Inital Point, Flatstart_____
flat_start;

%_____Optimization Routine_____
algorithm='GPSPositiveBasis2N';
options = optimoptions(@patternsearch,'PollMethod',algorithm,'SearchMethod',↙
algorithm,'StepTolerance',1E-3,'FunctionTolerance',opttol);
[x,F,flag,out] = patternsearch(@(x) OPF_unbalanced(x),x0,[],[],[],[],lb,ub,[],options);

%_____Actualize New SOC value for Storage resources. This new value will be used in↙
the next t+1 optimization.
SOC=SOCvar; % Actualize State of Charge

%_____Show results_____
optresults; % Display optimization results,
toc %Return elapsed time
store_data; %Store data in matrices

end
```

118

OPF_unbalanced Script:

```matlab
% Title: 45 Bus Microgrid Optimization with Distributed Energy Resources
% Description: Algorithm to find the optimal DERs allocation in a Microgrid, taking into
account physical and operational constrains of the system and resources
% Algorithm Name: Microgrids Optimal Power Flow (MOPF)
% Autor: Ramón A. Reyes Colón, MSEE Graduate Student
% Advisor: Dr. Efraín O'neill Carillo
% Email: ramon.reyes7@upr.edu, efrain.oneill@upr.edu
% University of Puero Rico, Mayaguez Campus
% Variables selection is done using the Matlab routine patternsearch(GPSPositiveBasis2N)
with a defined flatstart point
% Unbalanced Load Flow is done using the Back-Forward Sweep Algorith written by Dr.
Alejandro Garcés, Universidad Tecnológica de Pereira
% Last Revision: February 4, 2018

function F = OPF_unbalanced(x)
global Pn Pd Pgen Feeder
global Pgmax Pgmin Qgmax Qgmin Drmax Drmin Stomax Stomin
global ratesP ratesQ ratesDr ratesSt
global costP costQ costDr costSto
global Pvar Qvar Drvar Stovar Pgenc Qgenc
global f penalty Res  var viol lftol optiter Ploss Qloss ub lb  maxiter Vmin Vmax sf
global xxP1 xxP2 xxP3 xxQ1 xxQ2 xxQ3 xxDr1 xxDr2 xxDr3 xxSto1 xxSto2 xxSto3
global  varcount  q_enable p_enable dr_enable sto_enable
global SOC SOCmin SOCmax SOCvar delta_t weight
%_____Random Variables Selection_____
var_rand_selection;

%_____New Storage SOC_____
storage_model; %BSS SOC with limits

%_____Sum of ramdom Selections_____
sum_random_selections;

%_____Unbalanced Load Flow_____
unbalanced_load_flow;

%_____Costs_____
cost_calc;

%_____Objective Function with sign and weight_____
objective_functions;
objectives_sign_and_weight;

%_____Penalties & Violations_____
penalty_functions;

%_____Sum of weigthed objective functions and penalties_____
F=sum(f.*sf)+sum(penalty)+sum(viol);
```

Appendix B: Scripts Output

The information in this appendix is part of the output obtained in report generated in MATLAB. The whole output for each case consists of a 533-page document; 7,462 pages for the 14 cases output. This data includes the load flow data in each time step, a summary of the total costs, DERs generation, system losses, violations and penalty values. It also includes detailed information of the allocation of each resource [59]. For example: The matrix "Pvar" has the PV allocation for a specific time. "Pvar" has 3 columns and 45 rows; columns are phase A, phase B and phase C, respectively; rows are busbar 1, busbar 2..., busbar 45, respectively.

```
    10
```

Optimization terminated: mesh size less than options.MeshTolerance.
-------------------------------Optimization Results-------------------------------

--------PHASE VOLTAGES --

NODE	VAn(pu)	VAn(deg)	VBn(pu)	VBn(deg)	VCn(pu)	VCn(deg)
N1	1.0000 <	0.0000	1.0000 <	-120.0000	1.0000 <	120.0000
N2	1.0000 <	0.0000	1.0000 <	-120.0000	1.0000 <	120.0000
N3	0.9996 <	-0.2571	0.9996 <	-120.2571	0.9996 <	119.7429
N4	1.0036 <	-0.1461	1.0040 <	-120.1365	.	
N5	1.0038 <	-0.1368	1.0041 <	-120.1275	.	
N6	1.0038 <	-0.1295	1.0041 <	-120.1199	.	
N7	1.0036 <	-0.1461	.		1.0038 <	119.8645
N8	1.0038 <	-0.1367	.		1.0039 <	119.8737
N9	1.0039 <	-0.1273	.		1.0040 <	119.8828
N10	.		1.0040 <	-120.1365	1.0038 <	119.8645
N11	.		1.0041 <	-120.1275	1.0039 <	119.8737
N12	.		1.0042 <	-120.1185	1.0040 <	119.8819
N13	.		1.0043 <	-120.1098	1.0041 <	119.8898
N14	0.9924 <	-0.5224	0.9921 <	-120.5322	.	
N15	0.9921 <	-0.5342	0.9917 <	-120.5451	.	
N16	0.9918 <	-0.5460	0.9914 <	-120.5573	.	
N17	0.9915 <	-0.5569	0.9911 <	-120.5693	.	
N18	0.9924 <	-0.5224	.		0.9923 <	119.4668
N19	0.9921 <	-0.5345	.		0.9919 <	119.4540
N20	0.9918 <	-0.5462	.		0.9916 <	119.4417
N21	.		0.9921 <	-120.5322	0.9923 <	119.4668
N22	.		0.9918 <	-120.5441	0.9920 <	119.4549
N23	.		0.9915 <	-120.5560	0.9916 <	119.4422
N24	1.0036 <	-0.1461	1.0040 <	-120.1365	1.0038 <	119.8645
N25	1.0038 <	-0.1368	1.0041 <	-120.1275	1.0038 <	119.8645
N26	1.0038 <	-0.1295	1.0041 <	-120.1199	1.0038 <	119.8645
N27	1.0036 <	-0.1461	.		1.0038 <	119.8645
N28	1.0038 <	-0.1367	.		1.0039 <	119.8737
N29	1.0039 <	-0.1273	.		1.0040 <	119.8828
N30	.		1.0040 <	-120.1365	1.0038 <	119.8645
N31	.		1.0041 <	-120.1275	1.0039 <	119.8737
N32	.		1.0042 <	-120.1185	1.0040 <	119.8819
N33	.		1.0043 <	-120.1098	1.0041 <	119.8898
N34	0.9924 <	-0.5224	0.9921 <	-120.5322	0.9923 <	119.4668
N35	0.9921 <	-0.5342	0.9917 <	-120.5451	0.9923 <	119.4668
N36	0.9918 <	-0.5460	0.9914 <	-120.5573	0.9923 <	119.4668
N37	0.9915 <	-0.5569	0.9911 <	-120.5693	0.9923 <	119.4668
N38	0.9924 <	-0.5224	.		0.9923 <	119.4668
N39	0.9921 <	-0.5345	.		0.9919 <	119.4540
N40	0.9918 <	-0.5462	.		0.9916 <	119.4417
N41	.		0.9921 <	-120.5322	0.9923 <	119.4668
N42	.		0.9918 <	-120.5441	0.9920 <	119.4549
N43	.		0.9915 <	-120.5560	0.9916 <	119.4422
N44	1.0036 <	-0.1461	1.0040 <	-120.1365	1.0038 <	119.8645

N45   0.9924 < -0.5224   0.9921 < -120.5322   0.9923 < 119.4668

Total Cost: $ 62.016000

Total Utility/Slack P Injection: 90.000000 kW

Total Utility/Slack Q Injection: 0.000000 kVar

Total PVs P Injection: 373.720000 kW

Total PVs Q Injection: 46.031000 kVar

Total DR: 4.445000 kW

Total BSS: -375.200000 kW

Total P Demand: 91.190947 kW

Total Q Demand: 44.165791 kVar

Total System Losses: 1.775000 kW

Voltage Violations: 0

Penalty value: 4.011666e-05

PVs Optimal Allocation

Pvar =

         0   0   0
         0   0   0
         0   0   0
   18.0378   18.0378   0
   18.0378   18.0378   0
   18.0378   18.0378   0
   18.0378   0   18.0378
   18.0378   0   18.0378
   18.0378   0   18.0378
         0   18.0378   18.0378
         0   18.0378   18.0378
         0   18.0378   18.0378
         0   18.0378   18.0378
    4.5094   8.4552   0
         0   0   0
         0   0   0
         0   0   0
         0   0   0
         0   0   0

```
           0            0            0
           0            0            0
           0            0            0
           0            0            0
           0            0            0
           0            0            0
           0            0            0
           0            0            0
           0            0            0
           0            0            0
           0            0            0
           0            0            0
           0            0            0
           0            0            0
           0            0            0
           0            0            0
           0            0            0
           0            0            0
           0            0            0
           0            0            0
           0            0            0
           0            0            0
           0            0            0
           0            0            0
           0            0            0
           0            0            0
           0            0            0
```

DR Optimal Allocation

Drvar =

```
           0            0            0
           0            0            0
           0            0            0
      0.1340       0.0887            0
           0            0            0
           0            0            0
      0.3457            0       0.4671
      0.1199            0       0.1699
      0.2232            0       0.3222
           0            0       0.4490
           0            0       0.2232
           0       0.0515       0.0047
           0            0            0
      0.2840            0            0
      0.2407            0            0
      0.1272            0            0
      0.2370            0            0
      0.3958            0            0
      0.2487            0            0
      0.3131            0            0
```

123

```
        0           0           0
        0           0           0
        0           0           0
        0           0           0
        0           0           0
        0           0           0
        0           0           0
        0           0           0
        0           0           0
        0           0           0
        0           0           0
        0           0           0
        0           0           0
        0           0           0
        0           0           0
        0           0           0
        0           0           0
        0           0           0
        0           0           0
        0           0           0
        0           0           0
        0           0           0
        0           0           0
        0           0           0
        0           0           0
```

BSS Optimal Allocation

Stovar =

```
        0           0           0
        0           0           0
        0           0           0
 -11.0000    -11.0000           0
 -11.0000    -11.0000           0
 -11.0000    -11.0000           0
 -11.0000           0    -11.0000
 -11.0000           0    -11.0000
 -11.0000           0    -11.0000
        0    -11.0000    -11.0000
        0    -11.0000    -11.0000
        0    -11.0000    -11.0000
        0    -11.0000    -11.0000
  -7.4000    -11.0000           0
  -7.4000     -7.4000           0
  -7.4000     -7.4000           0
  -7.4000     -7.4000           0
  -7.4000           0    -11.0000
  -7.4000           0     -7.4000
  -7.4000           0     -7.4000
        0     -7.4000     -7.4000
```

124

```
        0    -7.4000    -7.4000
        0    -7.4000    -7.4000
        0          0          0
        0          0          0
        0          0          0
        0          0          0
        0          0          0
        0          0          0
        0          0          0
        0          0          0
        0          0          0
        0          0          0
        0          0          0
        0          0          0
        0          0          0
        0          0          0
        0          0          0
        0          0          0
        0          0          0
        0          0          0
        0          0          0
        0          0          0
        0          0          0
        0          0          0
```

BSS Energy Available

SOC =

```
        0          0          0
        0          0          0
        0          0          0
  58.4500    50.2000          0
  61.2000    61.2000          0
  61.2000    61.2000          0
  61.2000          0    50.2000
  61.2000          0    61.2000
  61.2000          0    61.2000
        0    61.2000    61.2000
        0    61.2000    61.2000
        0    61.2000    61.2000
        0    61.2000    61.2000
  98.0000    79.6000          0
  98.0000    98.0000          0
  98.0000    98.0000          0
  98.0000    98.0000          0
  98.0000          0    79.6000
  98.0000          0    98.0000
  98.0000          0    98.0000
        0    98.0000    98.0000
        0    98.0000    98.0000
```

```
       0    98.0000    98.0000
       0          0          0
       0          0          0
       0          0          0
       0          0          0
       0          0          0
       0          0          0
       0          0          0
       0          0          0
       0          0          0
       0          0          0
       0          0          0
       0          0          0
       0          0          0
       0          0          0
       0          0          0
       0          0          0
       0          0          0
       0          0          0
       0          0          0
       0          0          0
       0          0          0
       0          0          0

Elapsed time is 1704.022457 seconds.
```

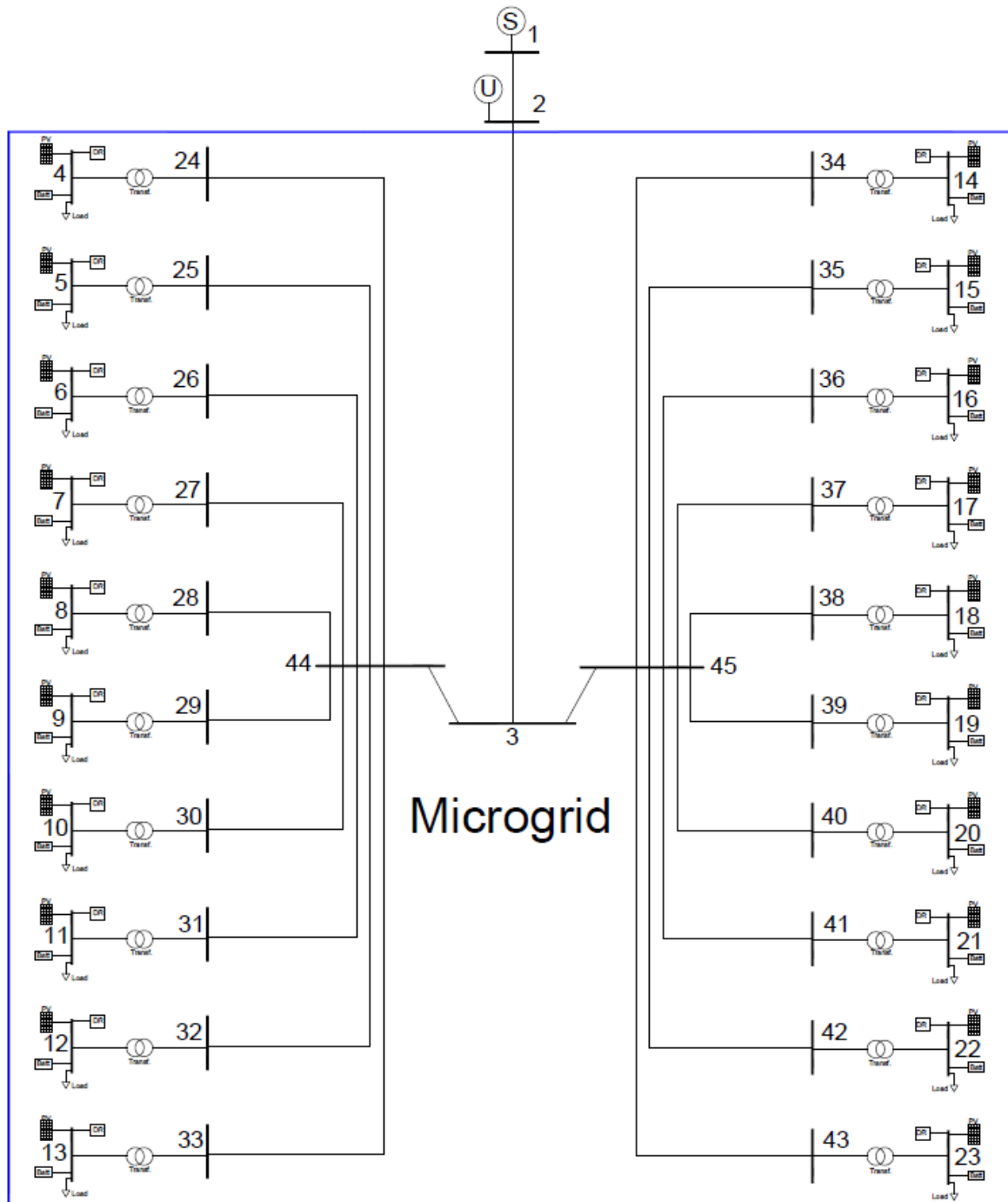**Appendix C: Case Study Topology**

Figure 91: 45-Bus Microgrid (Case study system; designed and drawn in AutoCAD)
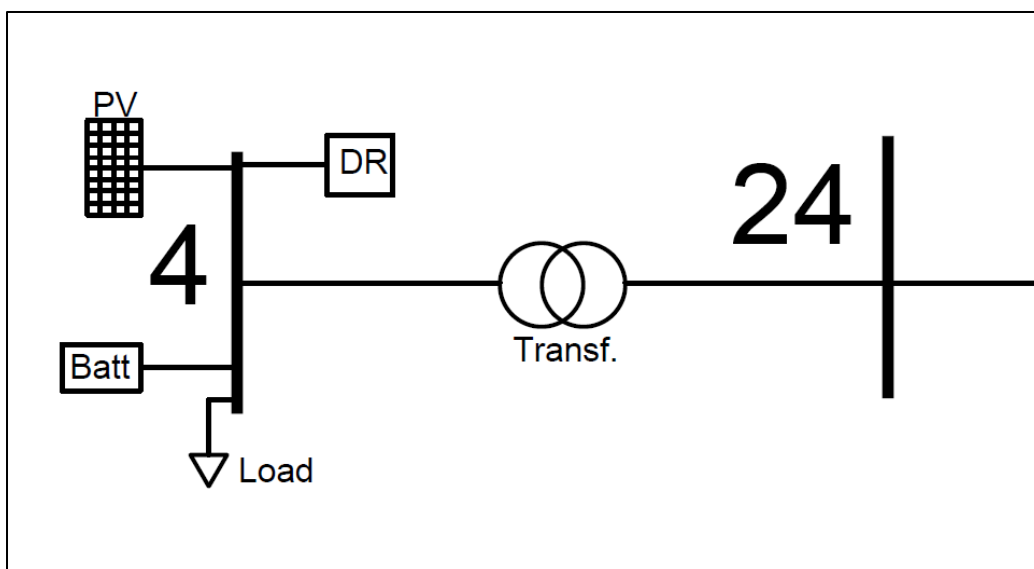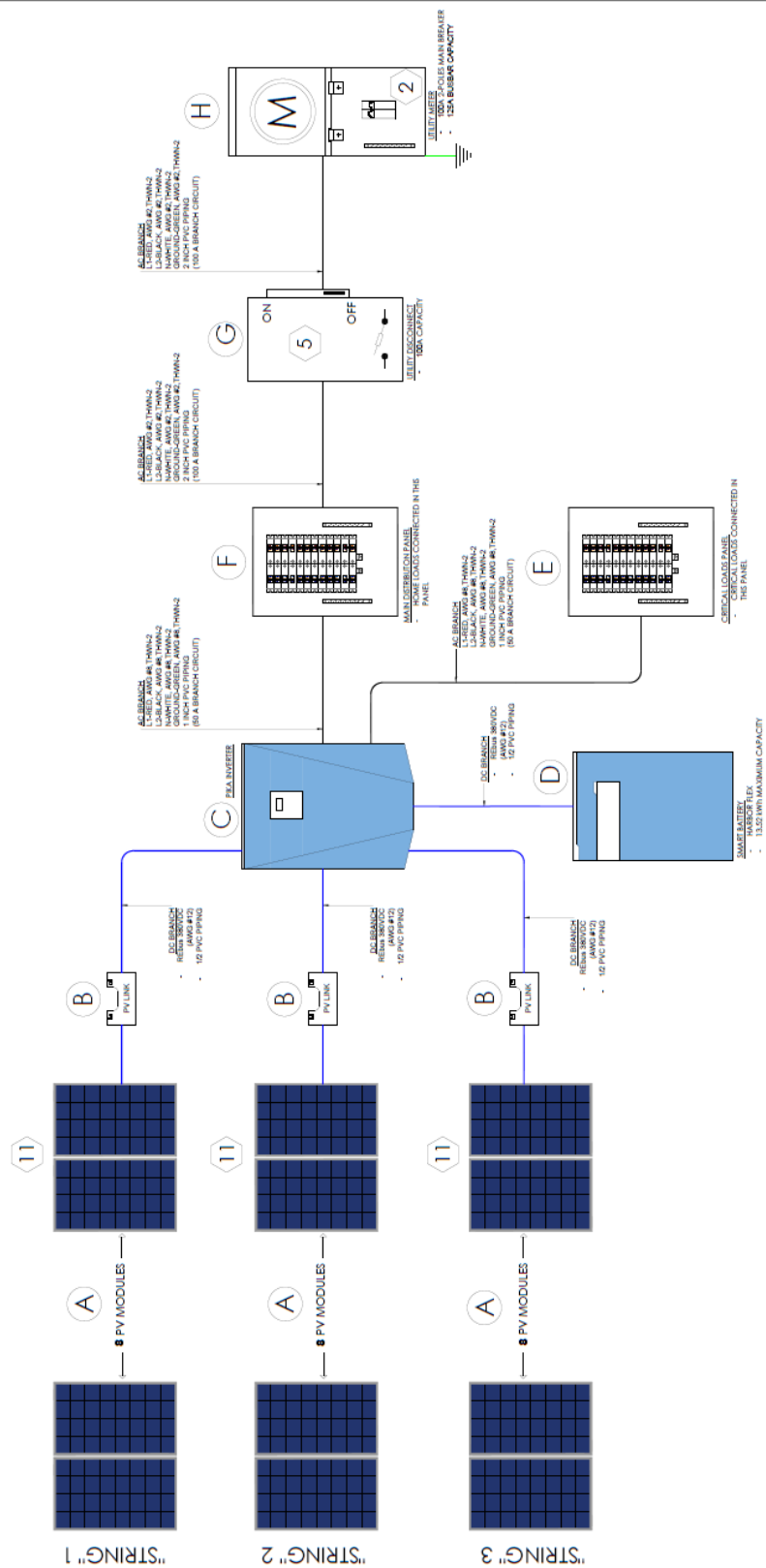
Figure 92: 45-Bus Microgrid close-up screenshot

Appendix D: Electrical Diagrams

In this appendix, the electrical diagrams for an enthusiastic and proactive customer system are

presented.

ELECTRIC DIAGRAM
ENTHUSIAST CUSTOMER'S SYSTEM

ELECTRIC DIAGRAM
ENTHUSIAST CUSTOMER'S SYSTEM

NOTES 1-11:

1. EQUIPMENTS SHALL BE INSTALLED IN ACCORDANCE WITH NEC ARTICLE 690.

2. PROVIDE WARNING SIGN PER NEC 690-7 READING: "WARNING-ELECTRIC SHOCK HAZARD- DO NOT TOUCH TERMINALS-TERMINALS ON BOTH THE LINE AND LOAD MAY BE ENERGIZED IN THE OFF POSITION".

3. LABEL BREAKER: "PHOTOVOLTAIC POWER SOURCE" PER NEC 705.10 . LABEL OUTPUT VOLTAGE AND MAX OPERATING CURRENT PER NEC 690.54

4. LABEL "PHOTOVOLTAIC SYSTEM DEDICATED KW-HR METER".

5. LABEL SWITCH AS "PHOTOVOLTAIC SYSTEM UTILITY DISCONNECT SWITCH" MARK DISCONNECT WITH AC OUTPUT OPERATING CURRENT AND VOLTAGE PER NEC 690.54.

6. MARK PHOTOVOLTAIC ARRAY DISCONNECT WITH PHOTOVOLTAIC POWER SOURCE RATINGS PER NEC 690.53.

7. CONDUCTORS ARE COPPER UNLESS OTHERWISE NOTED.

8. PV POWER SOURCE BREAKER TO BE LOCATED AT BOTTOM OF BUS PER NEC 690.64(B)(7) AND TO BE LABELED "WARNING, INVERTER OUTPUT CONNECTION. DO NOT RELOCATE THIS OVERCURRENT DEVICE".

9. ALL MODULE GROUND CONNECTIONS SHALL USE STAINLESS STEEL HARDWARE WITH AL/CU RATED LAY-IN LUGS (ILSCO GBL4-DBT) TO ALLOW MODULE CONNECTION

10. LABEL PANEL AS "INVERTER AC COMBINER PANEL". INCLUDE WARNING LABEL "WARNING-PHOTOVOLTAIC POWER SOURCE NO AC LOADS TO BE CONNECTED TO THIS PANEL".

11. LISTING AGENCY NAME AND NUMBER TO BE INDICATED ON POWER INVERTER AND SOLAR MODULES PER NEC 110.3(B).

12. CIRCUIT BREAKER TO BE SUITABLE FOR BACKFEED PER NEC 690.64 (B)(5).

ELECTRIC DIAGRAM
DESIGNED AND DRAWN BY:
RARC
787-200-1825
(rarc.eng@gmail.com)

NOTES A-H:

A. 24 HANWHA Q.PEAK-G4.1 300W
- PV MODULE OUTPUT MAX CURRENT = 9.77A. APPLYING FACTORS (AS PER NEC 2014):
  9.77 X 1.08 X 1.25 X 1.25 = 16.49 A DC
- 3 WIRES AWG #12 THWN-2 (1 POS, 1 NEUTRAL, 1 GROUND)
- 20A BREAKER PER PV STRING

B. PIKA S2500 SERIES SUBSTRING OPTIMIZER
- RATED POWER=2.5 kW
- UP TO 9 PV MODULES IN SERIES
- MAX STRING VOLTAGE =318.08 VDC APPLYING 1.25 FACTOR: 318.08 X 1.25 =397.60 VDC

C. PIKA X7600 INVERTER
- MAXIMUM INVERTER OUTPUT CURRENT= 31.67A APPLYING FACTORS (AS PER NEC 2014):
  31.67 X 1.25 = 39.59 A DC
- 4 WIRES AWG #8 THWN-2 (2 POS, 1 NEUTRAL, 1 GROUND)
- 1 INCH PVC CONDUIT
- 50A 2-POLES BREAKER

D. PIKA HARBOR FLEX SMART BATTERY
- BATTERY CAPACITY=13.52 kWh.
- DC VOLTAGE=350-420V
- MAX CONTINOUS POWER=4.5KW
- MAX PEAK POWER=10KW
- MAX PEAK CURRENT=10KW/360V=27.77A
- 30A BREAKER

E. CRITICAL LOADS PANEL
- RATINGS: 120/240V AC, 125A PANEL, NEMA 3R
- BACKUP LOADS CONNECTED IN THIS PANEL

F. MAIN DISTRIBUTION PANEL
- RATINGS: 120/240V AC, 125A PANEL, NEMA 3R
- HOME LOADS CONNECTED IN THIS PANEL
- MAIN BREAKER=100A
- MAIN BREAKER + INVERTER BREAKER = 100A + 50A =150A
- BUSBAR CAPACITY = 125A
- MAIN BREAKER + INVERTER BREAKER DOESN'T EXCEED 120% OF THE BUSBAR CAPACITY (COMPLY WITH NEC ARTICLE 705.12(D)(2)(3)(b))

G. PREPA DISCONNECT (REGULATION 7544)
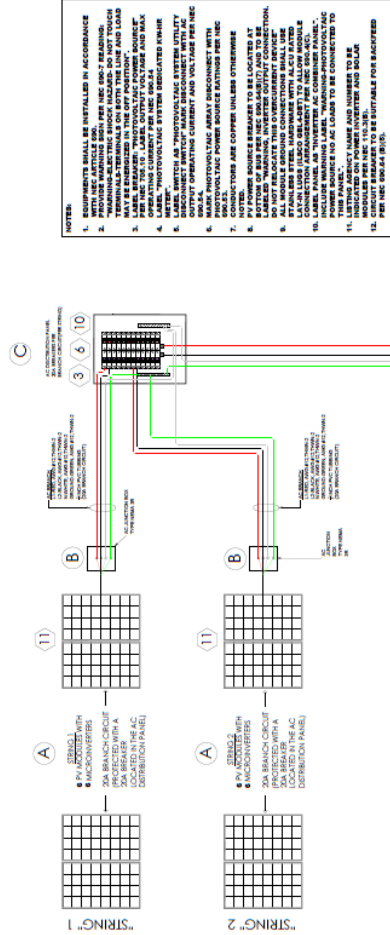- 240V AC, 100A AC, NEMA 3R

H. P.R.E.P.A METER WITH 100A MAIN BREAKER

131

ELECTRIC DIAGRAM
PROACTIVE CUSTOMER SYSTEM

INVERTER SPECS (FROM DATASHEET)

BRAND: ENPHASE ENERGY
MODEL: M250-60-2LL-S25
PEAK OUTPUT POWER = 250 WATTS
NOMINAL VOLTAGE/RANGE = 240 V / 211-264 V
NOMINAL OUTPUT CURRENT = 1 AMPS AC
MAXIMUM UNITS PER 20 A BRANCH CIRCUIT = 16 (SINGLE PHASE)

PV MODULE SPECS (FROM DATASHEET)

MODEL: BOVIET BVM6610-280
MAXIMUM POWER = 260 WATTS DC
MAXIMUM POWER VOLTAGE (VMP) = 30.7 VDC
MAXIMUM POWER CURRENT (IMP) = 8.42 ADC
OPEN CIRCUIT VOLTAGE (VOC) = 38.0 VDC
SHORT CIRCUIT CURRENT (ISC) = 9.01 ADC

AWG CABLES AMPACITY (THHN& THWN-2)(NEC 2014)

WIRE SIZE	AMPACITY
#12	30A
#10	40A
#8	55A
#6	75A
#4	95A
#2	130A
#1/0	170A
#2/0	195A
#3/0	225A
#4/0	260A

DESIGNED AND DRAWN BY:

NOTES:

A) 12 BOVIET BVM6610-280 260W AND
12 ENPHASE M250-60-2LL-S25 250W

PV MODULE OUTPUT MAX CURRENT = 9.01A.

APPLYING DERATE FACTORS (NEC 2014):
9.01 X 1.08 X 1.25 X 1.25 = 15.20 A DC
- 3 WIRES AWG #12 THWN-2 (1 POS,
1 NEUTRAL, 1 GROUND)

B) STRING 1 OUTPUT CURRENT = 6 X 1 = 6.00A
STRING 2 OUTPUT CURRENT = 6 X 1 = 6.00A

APPLYING DERATE FACTORS (NEC 2014):
STRING 1: 6.00 X 1.25 = 7.50 A AC
STRING 2: 6.00 X 1.25 = 7.50 A AC

- 4 WIRES AWG #12 THWN-2 (2 POS,
1 NEUTRAL, 1 GROUND)(PER STRING)
- 1/2 INCH PVC CONDUIT(PER STRING)

C) AC DISTRIBUTION PANEL
MAX CURRENT IN AC DISCONNECT = 15.00A
RATINGS: 120/240V AC, 125A PANEL, NEMA 3R
20A BREAKERS PER BRANCH CIRCUIT
(PER STRING)

D) SUNNOVA ITRON METER
RATINGS, 240V AC, 125A PANEL
20A BREAKER

E) P.R.E.P.A DISCONNECT (REGULATION 7544)
240V AC, 20A AC, NEMA 3R

F) P.R.E.P.A METER WITH 100A MAIN BREAKER
LOAD SIDE CONNECTION
MAIN BREAKER + GD BREAKER = 100A + 20A
=120A
BUSBAR CAPACITY = 125A
(MAIN BREAKER + GD BREAKER DOESN'T
EXCEED 120% OF THE BUSBAR CAPACITY)
(COMPLY WITH NEC ARTICLE 705.12(D)(2)(3)(b)

G) FACILITY MAIN DISTRIBUTION PANEL
MDP CAPACITY = 100A

H) KUP-L-Tap INSULATION PIERCING
CONNECTORS TO COMBINE THE WIRES FOR THE
LOAD SIDE CONNECTION

MAIN DISTRIBUTION PANEL

"STRING" 1

STRING
6 PV MODULES WITH
6 MICROINVERTERS
20A BRANCH CIRCUIT
PROTECTED WITH A
20A BREAKER
(LOCATED IN THE AC
DISTRIBUTION PANEL)

"STRING" 2

STRING 2
6 PV MODULES WITH
6 MICROINVERTERS
20A BRANCH CIRCUIT
PROTECTED WITH A
20A BREAKER
(LOCATED IN THE AC
DISTRIBUTION PANEL)

P.R.E.P.A. DISCONNECT
AMP CAPACITY = 20A
ON
OFF

SUNNOVA ITRON METER
20A 2-POLE BREAKER

P.R.E.P.A. METER
100A 2-POLE MAIN BREAKER
BUSBAR CAPACITY = 25A
LOAD SIDE CONNECTION

NOTES:

1. EQUIPMENTS SHALL BE INSTALLED IN ACCORDANCE WITH NEC ARTICLE 690.

2. PROVIDE WARNING SIGN PER NEC 690-7 READING: "WARNING-ELECTRIC SHOCK HAZARD-DO NOT TOUCH TERMINALS-TERMINALS ON BOTH THE LINE AND LOAD MAY BE ENERGIZED IN THE OFF POSITION".

3. LABEL BREAKER- "PHOTOVOLTAIC POWER SOURCE" PER NEC 705.10. LABEL OUTPUT VOLTAGE AND MAX.

4. LABEL "PHOTOVOLTAIC SYSTEM DEDICATED KWHR METER".

5. LABEL SWITCH AS "PHOTOVOLTAIC SYSTEM UTILITY DISCONNECT SWITCH" MARK DISCONNECT WITH AC OUTPUT OPERATING CURRENT AND VOLTAGE PER NEC 690.54.

6. MARK PHOTOVOLTAIC ARRAY DISCONNECT WITH PHOTOVOLTAIC POWER SOURCE RATINGS PER NEC 690.53.

7. CONDUCTORS ARE COPPER UNLESS OTHERWISE NOTED.

8. PV POWER SOURCE BREAKER TO BE LOCATED AT BOTTOM OF BUS PER NEC 690.64(B)(7) AND TO BE LABELED "WARNING, INVERTER OUTPUT CONNECTION, DO NOT RELOCATE THIS OVERCURRENT DEVICE".

9. ALL MODULE GROUND CONNECTIONS SHALL USE STAINLESS STEEL HARDWARE WITH ALCU RATED LAY-IN LUGS (ILSCO GBL-4DST) TO ALLOW MODULE CONNECTION ARRANGEMENT PER NEC 690.43.

10. LABEL PANEL AS "INVERTER AC COMBINER PANEL". INCLUDE WARNING LABEL "WARNING-PHOTOVOLTAIC POWER SOURCE NO AC LOADS TO BE CONNECTED TO THIS PANEL".

11. LISTING AGENCY NAME AND NUMBER TO BE INDICATED ON POWER INVERTER SOLAR MODULES PER NEC 110.3(B).

12. CIRCUIT BREAKER TO BE SUITABLE FOR BACKFEED PER NEC 690.64 (B)(5).

Appendix E: GPS and the Back/Forward Sweep algorithms

E.1 How the GPS algorithm works

The General Pattern Search (GPS) is a modern method of evolutionary programming. It has been used previously in the power systems field for automatic generation control (AGC) of a multi-area power system [60], for analysis of solar power forecasting [61], for the optimal load flow control (LFC) of interconnected thermal power plants [62], for the optimal PV plant location for grid support [63], for harmonics elimination on a DC source multilevel inverter, and to solve an optimal flow problem (OPF) in a power system (without DERs) [64], but it has not been used in the context of MGs with a very high integration of DERs such as PV systems, battery storage systems (BSS) and Demand Response; neither considering sustainability objectives (economic, social and environmental aspects at the same time). As well, it has not been used to optimize a dynamic system whose resources behave as a function of time (e.g., a day ahead optimization with forecasted data). Thus, it's a novel contribution since its being used to find efficient configurations of DERs in different time periods, considering the system's constraint's, sustainability objectives and management of energy variances to achieve a highest load factor in the system.

The GPS algorithm works by finding a sequence of points $x_0, x_1, x_{2,...} x_n$ that approaches to an optimal solution in the problem. In this process, the value of the objective function can either decrease or remain equal. The following example describe how the GPS algorithm works [40], [41]. For this example, *there are two decision variables with* initial point (flat start point) $x0 = [2.1, 1.7]$, and the ps_example.m function in MATLAB as the objective function.

```matlab
ps_example.m*  ✕  +
1        function f = ps_example(x)
2        %PS_EXAMPLE objective function for pattern search.
3
4        %   Copyright 2003-2004 The MathWorks, Inc.
5
6
7  -     for i = 1:size(x,1)
8  -         if  x(i,1) < -5
9  -             f(i) = (x(i,1)+5)^2 + abs(x(i,2));
10 -         elseif x(i,1) < -3
11 -             f(i) = -2*sin(x(i,1)) + abs(x(i,2));
12 -         elseif x(i,1) < 0
13 -             f(i) = 0.5*x(i,1) + 2 + abs(x(i,2));
14 -         elseif x(i,1) >= 0
15 -             f(i) = .3*sqrt(x(i,1)) + 5/2 +abs(x(i,2));
16 -         end
17 -     end
18
```

Figure 93: Objective function (ps_example.m function in MATLAB)

Iteration 1:

In the first iteration, the mesh size is 1 (default value in MATLAB; can be modified by the user) and the GPS algorithm adds the pattern vectors to the initial point $x0 = [2.1, 1.7]$ to compute the mesh points and evaluate the objective function in iteration 1:

$$[1, 0] + x0 = [3.1, 1.7]; \ f(3.1, 1.7) = 4.7820$$

$$[0, 1] + x0 = [2.1, 2.7]; \ f(2.1, 2.7) = 5.6347$$

$$[-1, 0] + x0 = [1.1, 1.7]; \ f(3.1, 1.7) = 4.5146$$

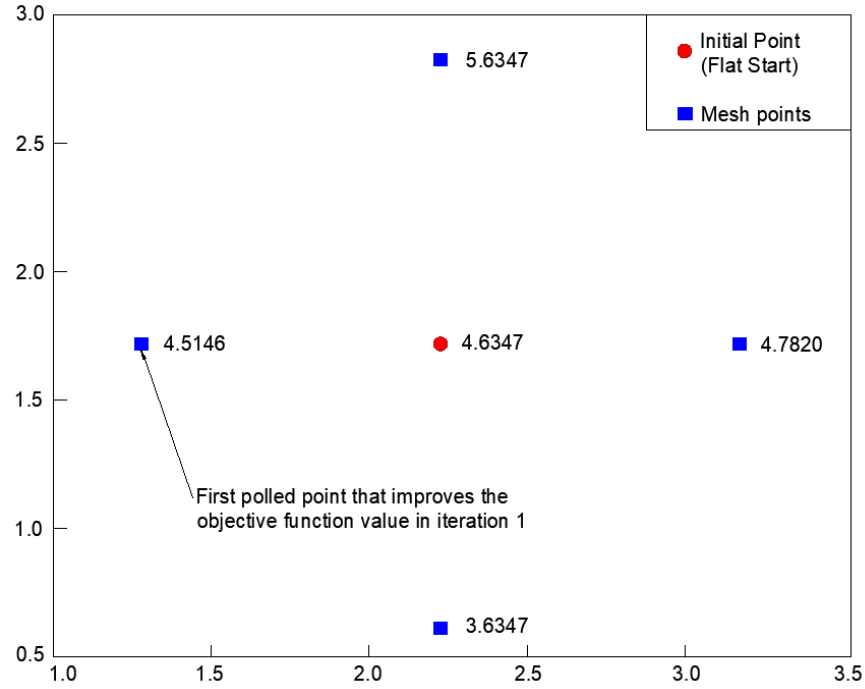$$[0, -1] + x0 = [2.1, 0.7] \ ; \ f(1.1, 1.7) = 3.6347$$

Figure 94: Polling in iteration 1 (Modified from [41]*).*

The algorithm polls the mesh points by calculating the value of the objective function until it finds one whose value is smaller than 4.6347 (the value of the objective function at the initial point). In this case, the first point it finds is [1.1, 1.7], were the value of the objective function is 4.5146 (this value is not necessarily the smallest one in the whole mesh, but is the first one found by the algorithm); Thus, the poll at iteration 1 was successful. Now, the algorithm sets the next point in the sequence equal to $x1 = [1.1, 1.7]$ (the first successful poll in iteration 1).

Iteration 2:

After a successful poll in iteration 1, the algorithm multiplies the current mesh size by the value of the expansion factor (by default this value is equal to 2 in MATLAB; can be modified by the user). Given that the initial mesh size is 1, in the second iteration the mesh size is 2. The mesh points in iteration 2 are:

$$2 * [1,0] + x1 = [3.1, 1.7]; f(3.1, 1.7) = 4.7282$$

135

$$2 * [0, 1] + x1 = [1.1, 3.7]; f(1.1, 3.7) = 6.5416$$

$$2 * [-1, 0] + x1 = [-0.9, 1.7]; f(-0.9, 1.7) = 3.25$$

$$2 * [0, -1] + x1 = [1.1, -0.3]; f(1.1, -0.3) = 3.11$$
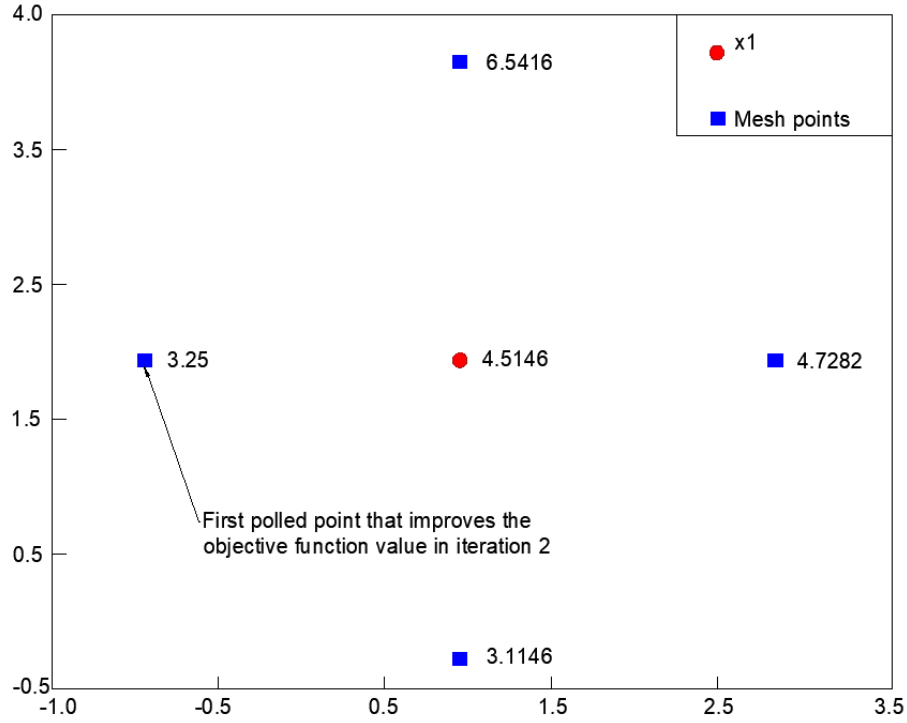

Figure 95: Polling in iteration 2.

The algorithm polls the mesh points until it finds one whose value is smaller than 4.5146 (objective function value at x1). The first point it finds is [-0.9, 1.7], were the value of the objective function is 3.25. Thus, the second point in the sequence is $x2 = [-0.9\ 1.7]$ and the current mesh size is multiplied by the value of expansion factor to get the new mesh for the third iteration.

If there is an unsuccessful poll in the iteration, the algorithm multiplies the current mesh by the value of the contraction factor (by default this value is equal to 0.5, can be changed by the user in MATLAB) instead of the expansion factor (with a value equal to 2) to calculate the new mesh in the next iteration. This process is repeated until the difference of objective function value

is less that the tolerance defined by the user $(F(i+1) - F(i) < tolerance)$, or a maximum number of iterations defined by the user as well. The following flowchart presents how the method works:
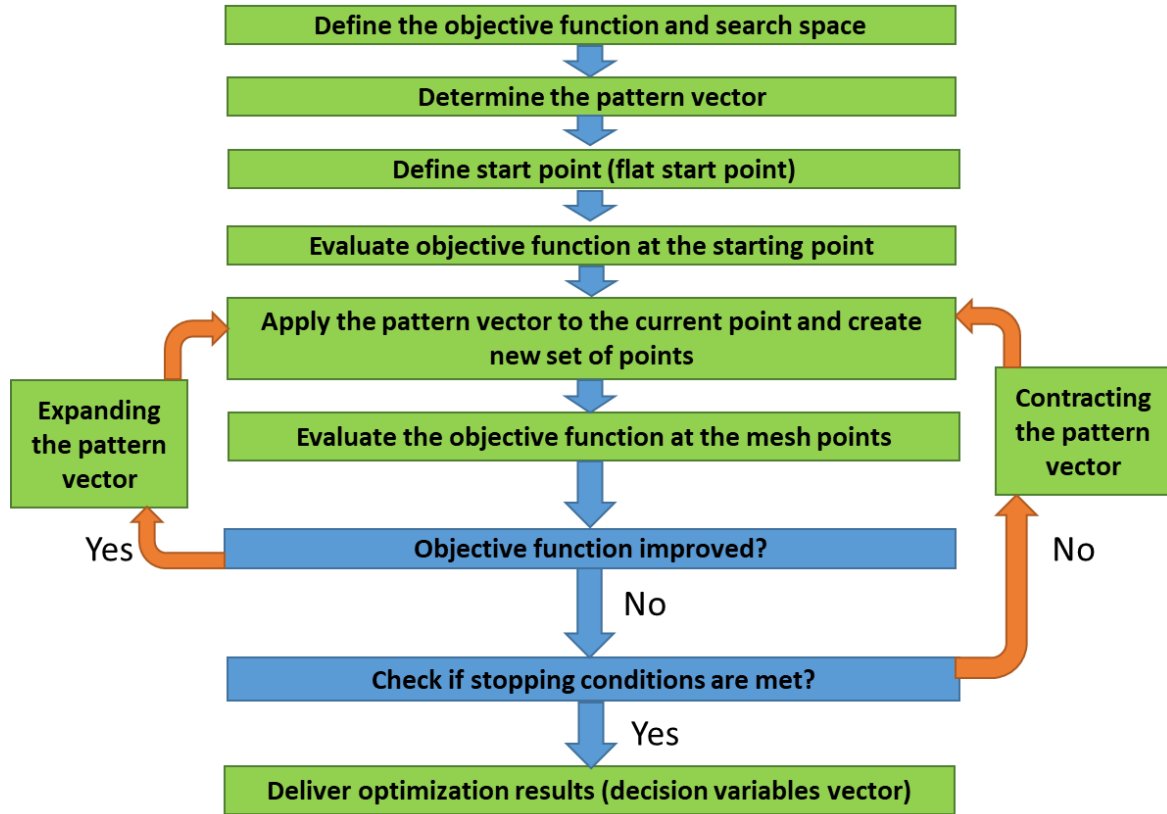

Figure 96: GPS algorithm flowchart (Modified from [65]*).*

The same process, as shown in the previous flowchart, is performed for problems with multiple decision variables. For problems with more than three decision variables a graphical representation, as shown in the previous example with the mesh points, cannot be done because there are more than three dimensions and cannot be seen graphically. It is important to emphasize that GPS in this thesis stands for General Pattern Search (Optimization routine/algorithm) and not Global Positioning System (satellite-based radio-navigation system); both are different things. As

well, it is important to emphasize that a global solution cannot be guaranteed due to the nature of the problem being solved with a heuristic method.

E.1.1 Methods comparison

The following table presents a method comparison. The methods presented below were used in the MOPF algorithm to see the results and to choose the best one to perform the optimization for a whole day with a time step of 15 minutes.

Table 5: Optimization Methods Comparison

Method	Utility/Slack P injection (kW)	Convergence time	Cost	Estimated time for a day-ahead optimization	Penalty value
GPS	90.000-kW	100.238 seconds	$ 62.958	9,600 seconds (2.667 hours)	1.11E-2
GA	89.88- kW	766.253 seconds	$ 63.757	73,500 seconds (20.417 hours)	3.11E-2
PSO	89.994-kW	174.531 seconds	$ 65.721	16,800 seconds (4.66 hours)	1.39E-2
Interior-Point	90.733-kW	22.407 seconds	$ 57.882	2,112 seconds (35.2 minutes)	43.88
SQP	90.000-kW	74.694 seconds	$ 67.366	7,200 seconds (2.0 hours)	6.75E-5
Active-Set	90.000-kW	584.84 seconds	$ 62.244	56,160 seconds (15.60hours)	2.495-6

With these results, the following conclusions where done:

▪ The GPS, SQP and the Active Set methods found a solution were the utility/slack delivers exactly 90 kW; the others are slightly different but they are very close.

- The method who achieved the lowest cost was the Interior-Point method, followed by the Active set and then the GPS methods.

- The algorithm who converged faster was the Interior-point, followed by SQP and then the GPS methods. The Interior-point method was the fastest one, but the solutions obtained are slightly different that the desired value (90 kW). In a longer simulation (e.g., a whole day optimization), this error is accumulated, thus, it is desired to obtain a value as close as possible to 90 kW on each time step; In addition, this method yielded the highest penalty value (43.88), thus, it is not reaching the best solution to the problem (the penalty value should be close to zero).

- The GPS method yielded very good results. The power delivered by the utility/slack was exactly 90 kW, the penalty value was low, and the simulation for a whole day optimization can take around 2.66 hours, which is reasonable.

- The Genetic Algorithm (GA) yielded good results, but it takes a very long computational time. If this simulation is performed for a whole day, the algorithm will take around 20.42 hours; the same happens with the Active-Set method.

- The Particle Swarm (PSO) yielded very good results, but the simulation for a whole day optimization can take around 4.66 hours, almost the double as the GPS method (2.66 hours).

- The SQP yielded very good results as well, but the cost is a little bit higher than the ones obtained with GPS and Particle Swarm.

All of the methods presented above serve to solve an optimal power flow (OPF) problem, but based on the results and comparisons made, the method that was selected to develop the

MOPF algorithm was the GPS method because it achieved a 90-kW from the utility/slack, it has a reasonable computational time, it achieved a low cost and the penalty value was low; nevertheless, the other ones can be used as well.

E.2 How the Back/Forward Sweep algorithm works

The back/forward sweep is one of the most effective methods to perform load flow analysis of unbalanced and radial distribution systems. Thus, it is commonly used to do load flow analyses in the power systems field. This method is popular because it considers the following [43], [66]–[73]:

- Radial and/or weak mesh networks

- High R/X ratios

- Phase unbalances

- Loads unbalances

- Distributed Generation (DG)

Traditional methods such as the Newton-Raphson method (and other ones) usually fell short; they often fail with distribution networks with a high integration of DERs and take long computational time. On the other hand, the back/forward sweep is a simple method and converge very fast. The load flow in a distribution system is calculated using the simplified recursive equations resented below (they could be modified) [43]:

$$P_{k+1} = P_k - P_{loss,k} - P_{lk+1}$$

$$Q_{k+1} = Q_k - Q_{loss,k} - Q_{lk+1}$$

$$P_{loss}(k, k+1) = R_k * \frac{P_k^2 + Q_k^2}{V_k^2}$$

$$Q_{loss}(k, k + 1) = X_k * \frac{P_k^2 + Q_k^2}{V_k^2}$$

Where:

- P_k is the real power flow output

- Q_k is the reactive power flow output

- P_{lk+1} is the real load power at busbar $k + 1$

- Q_{lk+1} is the reactive load power at busbar $k + 1$

- $P_{loss}(k, k + 1)$ is the real power loss in the line section; The total P loss is the sum of the individual line section losses.

- $Q_{loss}(k, k + 1)$ is the reactive power loss in the line section; The total Q loss is the sum of the individual line section losses.

The back/forward sweep method is a two-stage iterative process; the forward sweep and the backward sweep. The forward sweep is a voltage drop calculation with power flow updates. In this process, the busbar voltages are updated in a forward sweep starting from branches in the first layer toward those in the last. The backward sweep is a current flow solution with possible voltage updates, starting from the branches in the last layer and moving towards the branches connected to the root node. In this process, the voltages obtained in the forward sweep are maintained constant during the backward sweep [43]. The following flowchart presents how the back/forward sweep algorithm works:
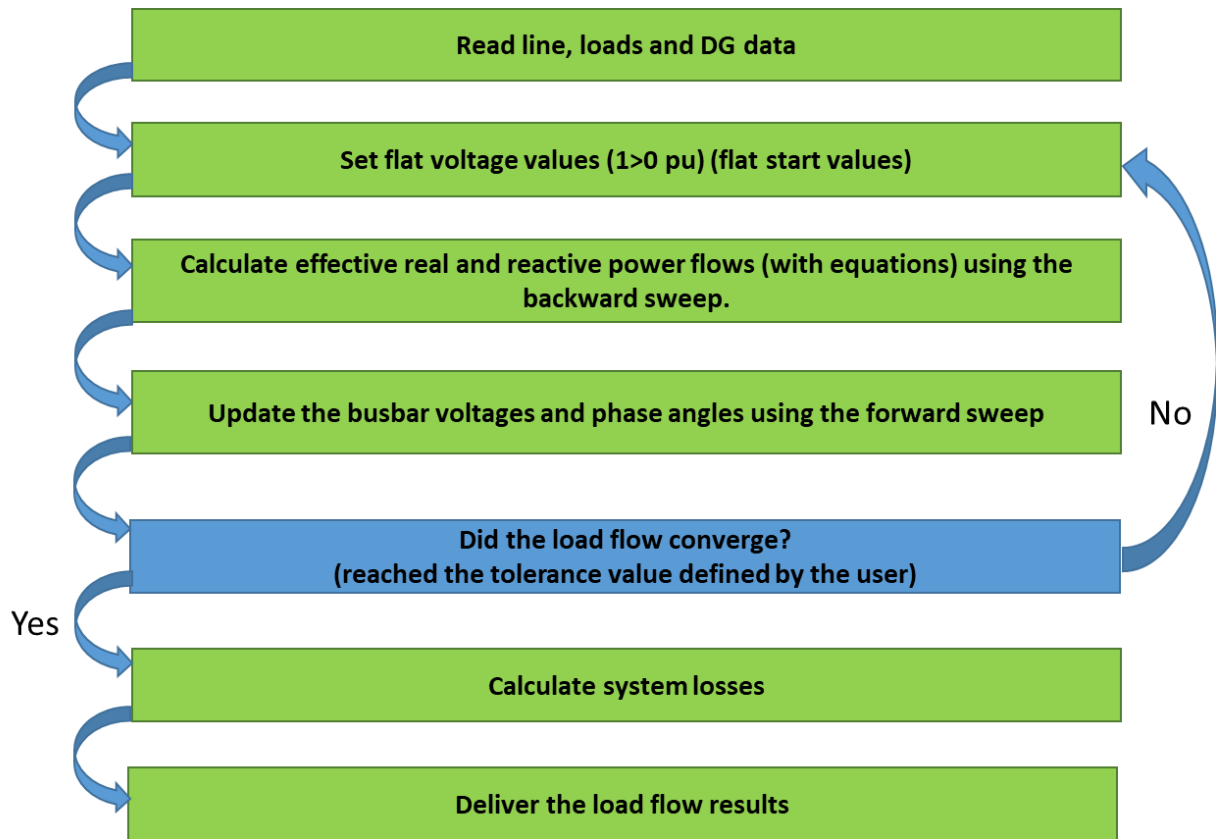
Figure 97: Back/forward sweep algorithm flowchart (Modified from [43]*).*

In other works, there might be some slight modifications to the algorithm, but the basic structure in the as one presented in the previous flowchart. This method has been used and validated in several works [42], [43], [66]–[73]; thus, it was used for the load flow calculation in the MOPF algorithm developed in this thesis work.
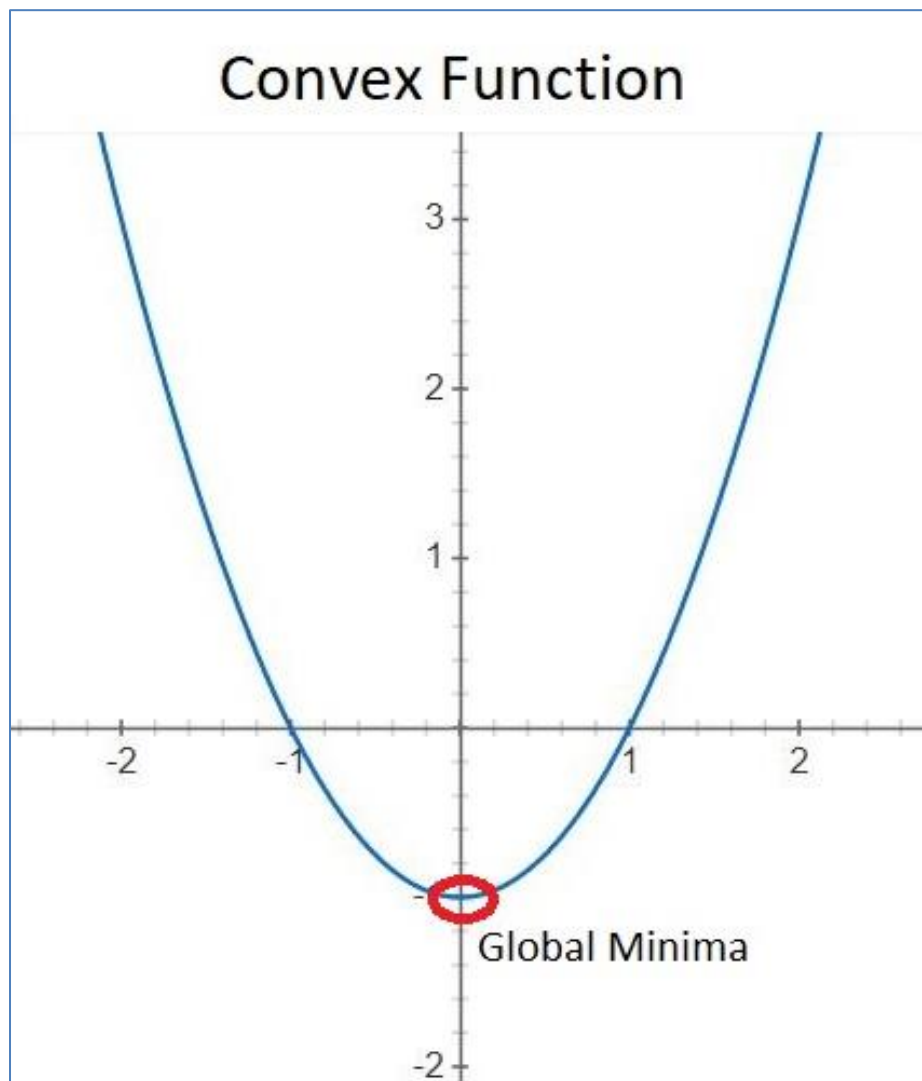
Appendix F: Convex and Non-Convex problems

F.1 Convex Problem

A convex problem is defined as a problem where its constraints, objectives and search space are convex functions; As an example, linear functions; which are considered to be convex. This kind of problems have a global solution (global minima). This problem could be solved using linear programming or methods such as the interior- point method (traditional methods). The

following figures illustrates an example of a convex function with its global minima [14], [74], [75].

Figure 98: Convex Function example

F.1 Non-Convex Problem

A non-convex problem is defined as a problem where its constraints, objectives and search space are non-convex functions. This kind of problem usually have multiple minima, known as local minima, but it only has one global minima. Due to the complexity of these kind of problems,

traditional methods usually fall short; they are solved with modern techniques such as modern methods of evolutionary programming (GPS, PSO, NSGA-2, etc.). In addition, since there may be more than one local solution, those methods cannot guarantee the global solution all the time; Sometimes they get caught on a local solution (which is a good solution). The achievability of a global or local solution depend on many factors, among them: the starting point, the constraints and the number of decision variables. The following figures illustrates an example of a non-convex function with its global and local minima [14], [74], [75].
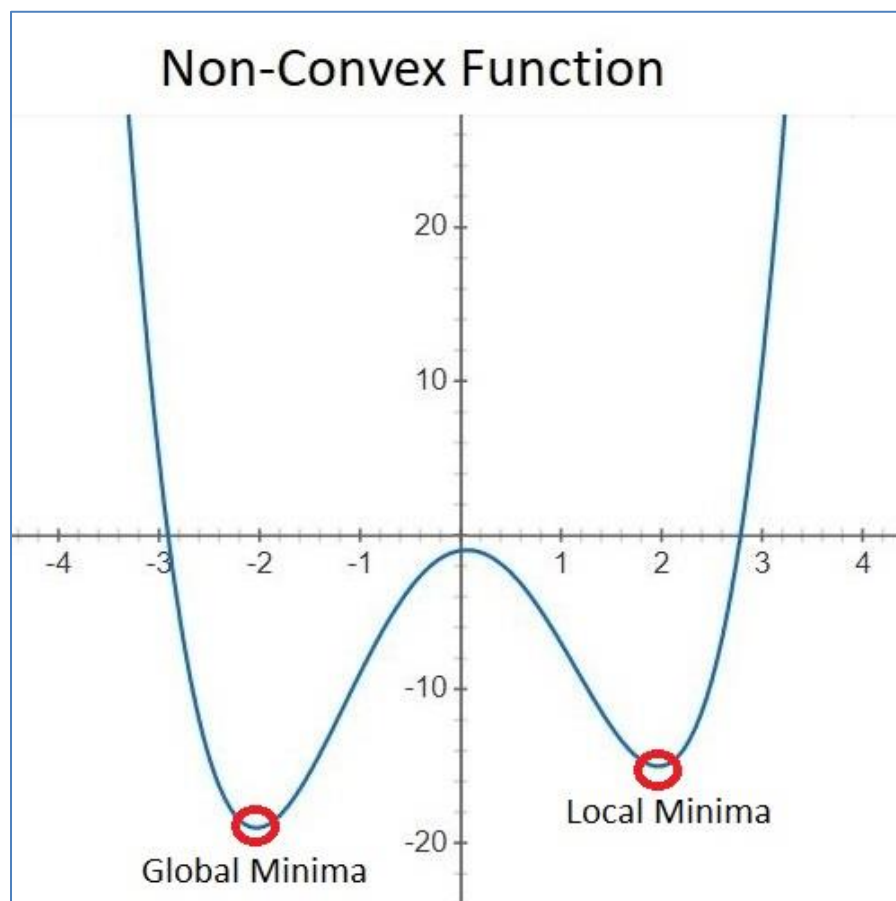
Figure 99: Non-Convex Function example

Appendix G: MG Life Cycle Assessment and Emission Costs

G.1 MG Life Cycle Assessment

On [76] it is presented a life cycle assessment of a MG, comparing three different systems; a PV-Battery system, a PV-Diesel system and a PV-Hybrid system. This assessment takes into account a wide range of considerations and detailed model for the systems and measures the impact based on several categories. The following table presents those categories and the results obtained for each system:

Table 6: Life cycle impacts of a PV-MG

Category	PV-Battery	PV-Diesel	PV-Hybrid
Climate change (kg CO2/kWh)	1.10E-01	9.71E-01	2.67E-01
Freshwater Eutrophication (kg P/kWh)	2.03E-04	4.13E-05	2.04E-04
Human toxicity (kg 1,4-DB/kWh)	4.46E-01	7.65E-02	4.44E-01
Particulate matter formation (kg PM10//kWh)	4.25E-04	5.74E-03	1.34E-03
Photochemical Oxidant Formation (kg NMVOC//kWh)	5.13E-04	1.75E-02	3.26E-03
Terrestrial Acidification (kg SO2/kWh)	1.34E-03	1.06E-02	3.02E-03
Terrestrial Ecotoxicity	1.27E-04	3.43E-04	1.82E-04

(kg 1,4-DB/kWh)			

The results obtained in this life cycle assessment concluded that PV-Battery systems produce lower impacts in the climate change, particulate matter formation, photochemical oxidant formation, and terrestrial acidification. Thus, a PV-Battery system provides a clean energy access solution. This was validated as well on the scenarios simulated in this thesis since the lowest emissions (kg CO_2) were obtained on the cases with DERs and optimization due to the MG is relying less on fossil-fuel resources. Sustainability has a cost, and so does the environmental impacts. If the total emissions are reduced, the MG cost could be reduced as well.

Based on the evaluation presented in [77], the relation between the monetary cost and CO_2 emissions is approximately $3.50 per Kg of CO_2 (evaluation made with a case study). This study showed a direct-proportion relation between the cost and the emissions, and also showed that the best way to encourage operators to limit emissions is to increase the cost fossil-fuel resources who produce those emissions. The following figure presents the cost of emissions per case using the previous cost-emission relation ($3.50 per Kg of CO_2).
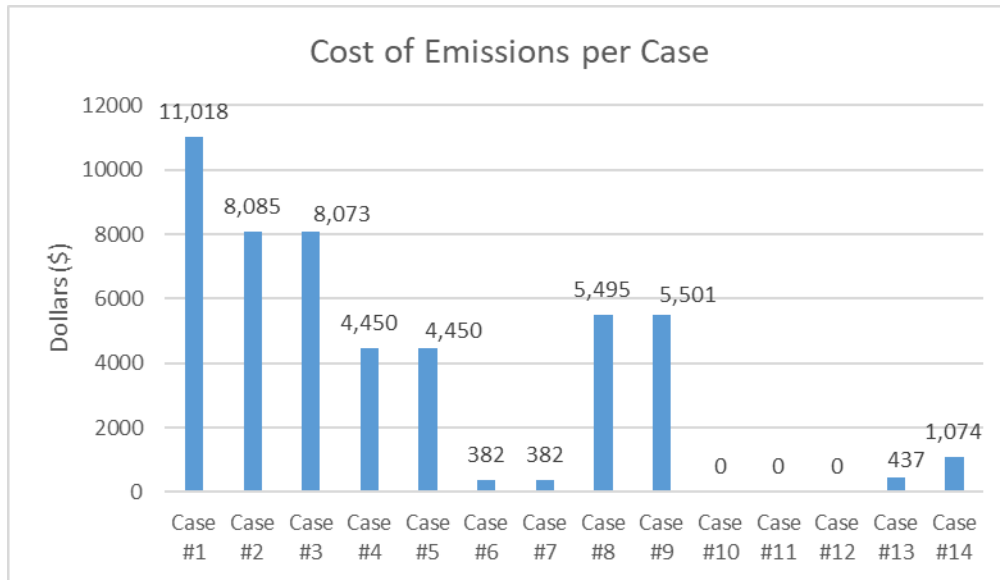
Figure 100: Cost of emissions per case.

Based on the previous figure, the cost of the cases with optimization (cases 4-14) were less, because those cases rely less on the utility (fossil-fuel generator). Thus, in terms of emission costs, a MG with DERs is less expensive than centralized generation; less dependent on the utility.

Appendix H: Resources Rates

H.1 Determination of PV rates

The average rate for residential customers with PVs is around $0.12 per kWh in the US. The range vary around the country and depends on different variables such as the availability of the solar resource; between $0.03 and $0.25 per kWh around the country [78]. On [79], a levelized cost of energy for various energy sources of is presented. It is basically the total life cycle cost of electricity, for a particular technology (e.g., PV solar, natural gas, etc.), divided by the total life cycle electricity produced in a 30-year period. From this study, the rate cost for a PV solar resource has been found to be around $0.0847 per kWh.

The solar resource in Puerto Rico is moderate (from 4.5 to 5.0 kWh/m^2/day) [80]. The rate per kWh could be variable, as in the US, and the value of this rate could also depend on how the customer obtained his/her system; If the system was paid by the customer (customer has made an initial inversion) or obtained through a PPA contract (customer has obtained the stem through a third-party entity). The levelized cost of energy ($\frac{\$}{kWh}$) in Puerto Rico, assuming a cost per watt of $3 for a PV system, was found to be around $0.08 and $0.17 per kWh; $0.08 per kWh for Cabo Rojo, $0.11 per kWh for Mayaguez, and $0.17 per kWh for Luquillo (El Yunque) [81].

For this thesis, a rate of $0.10 per kWh for a PV system was set; this value is close to the average rate for residential customers with PVs in the US ($0.12 per kWh), the rate cost for a PV solar resource obtained in the life cycle cost analysis for residential PV systems ($0.0847 per kWh; presented in [79]), and the levelized cost of energy range presented in [81]. Nevertheless, a more detailed and specific analysis could be done to determine this rate if detailed information for each

individual customer with a PV system is available (total system cost, installation costs, permits and certification fees, etc.)

H.2 Determination of BSS rates.

In [82] is presented a possible way to determine the cost per kWh for storage devices. Based on the discussion in this reference, the following expression could be used to determine this rate; considering the BSS cost, BSS capacity and number of cycles for a specific DoD.

$$BSS\ rate = \frac{BSS\ cost}{\#\ of\ cycles * DoD * BSS\ capacity}$$

A li-ion technology battery at 75% DoD could last around 2000 cycles [49]. Thus, assuming the cost range of $400-$750 per kWh of storage presented in [53], the BSS rate for a li-ion battery can be determined as follows:

$$BSS\ rate_1 = \frac{400}{2000 * 0.75 * 1} = \frac{\$0.267}{kWh}$$

$$BSS\ rate_2 = \frac{750}{2000 * 0.75 * 1} = \frac{\$0.50}{kWh}$$

Thus, the rate per kWh for a li-ion technology battery system could be between$0.267 and $0.50 per kWh. For the scenarios in this thesis, a rate of $0.30 per kWh was set for storage devices; this value is between the range presented in the previous calculation. Nevertheless, a more detailed analysis could be done to determine this rate if detailed information for each individual customer with a BSS is available (total system cost, installation costs, permits and certification fees, etc.)

H.3 Determination of reactive power rates.

A detailed analysis to estimate the cost of reactive power from a PV-DG is presented in [58]. Based on the results obtained in the case study, the cost of the reactive power injected by a PV system is way less that the cost of the real power injected; a fraction of the real power rates. The analysis of reactive power cost is more complex that the analysis on real power costs; reactive power costs are usually neglected in economic analysis of marginal prices. The values obtained in this analysis cannot be brought directly to the scenarios in this thesis since it is a different case study were the conditions and topology are not the same. But given that the reactive power rates are a fraction of the real power rates, this thesis will consider a ratio of 1/10 between the real power and reactive power rates from PV systems. Thus, if the real power rates for PVs are $0.10 per kWh, the reactive power rates will be $0.01 per kVarh.

H.4 Determination of DR rates.

The approach to determine the rates for DR in this thesis was a simple one. Since user with DR will respond based on price signals (as discussed in section 3.2), DR rates will be a fraction of the utility's price change percentage. If the utility's rate is $0.20 \frac{\$}{kWh}$ and there is a price change increase of 30%, which is equivalent to $0.06 \frac{\$}{kWh}$, the DR rates will be a fraction of this difference of $0.06 \frac{\$}{kWh}$. For example, instead of increasing the utility's rate from $0.20 \frac{\$}{kWh}$ to $0.26 \frac{\$}{kWh}$, DR customers can be incentivized with $0.05 \frac{\$}{kWh}$ (a fraction of this difference of $0.06 \frac{\$}{kWh}$) to achieve the balance between the energy generation with the demand. There are other approaches presented in literature such as paying local marginal price (LMP) for DR [83], but this approach requires a

151

more complex analysis and other several considerations that are out of the scope of this thesis. Since there are no regulations or platform for a DR program in Puerto Rico, a simple approach was used instead to set DR rates in this thesis; nevertheless, it could be modified or enhanced in the future.

Appendix I: Energy Market Scenario

For this scenario, an 11-bus distribution system consisting of five MGs (M1-M5), two sellers (S1 and S2), three buyers (B1-B3) and the utility (M0) was used, as presented in figure 101. The market optimization was performed for a 24-hourd period with a 15-minute time step. The goal was to achieve a low dispatch cost using the resources available. In this scenario the resources are fossil-fuel generators, large PV systems and microgrids (can sell or buy energy).
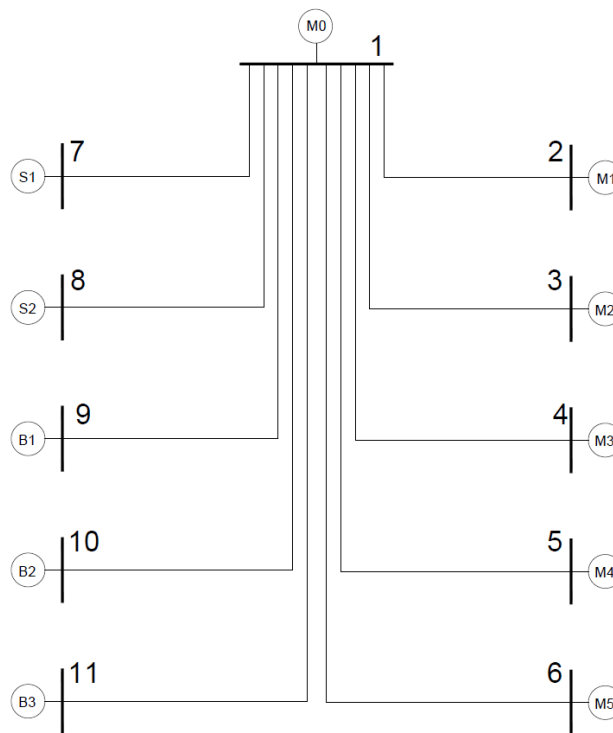
Figure 101: 11-Bus distribution system

I.1 Case #1: Seller #1 (Fossil-Gen), Seller #2 (Fossil-Gen), MGs with a sunny day.

On this case, both sellers (S1 and S2) are fossil-fuel generators (can deliver a maximum of 300-kW and 300-kVar) and the MGs inject/demand energy with a sunny day irradiance curve (using the optimized results obtained in cases #4, #6, #8, #10 and #12 from Chapter 6). Seller #1

is located at 2-km and seller #2 at 0.5-km from the MG; Both generators have a rate of $0.16 per

kWh. The following graphs were obtained after simulating case #1:
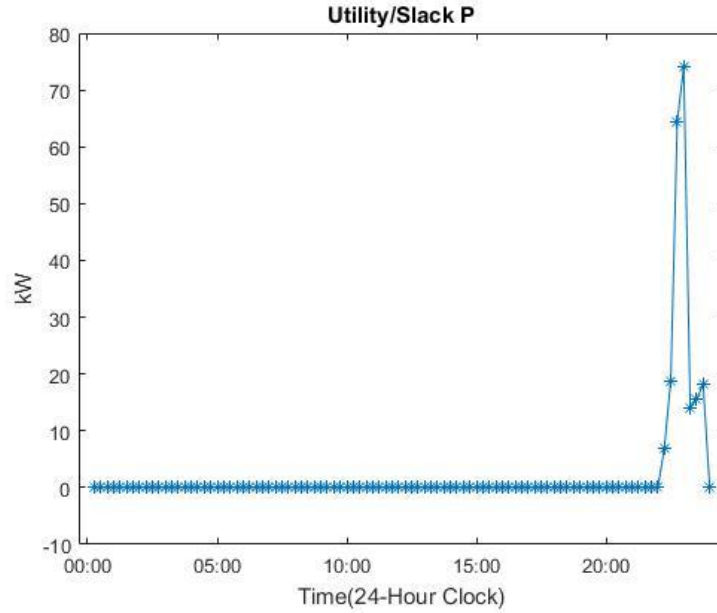
Figure 102:Utility/Slack real power injection (Case#1-energy market)
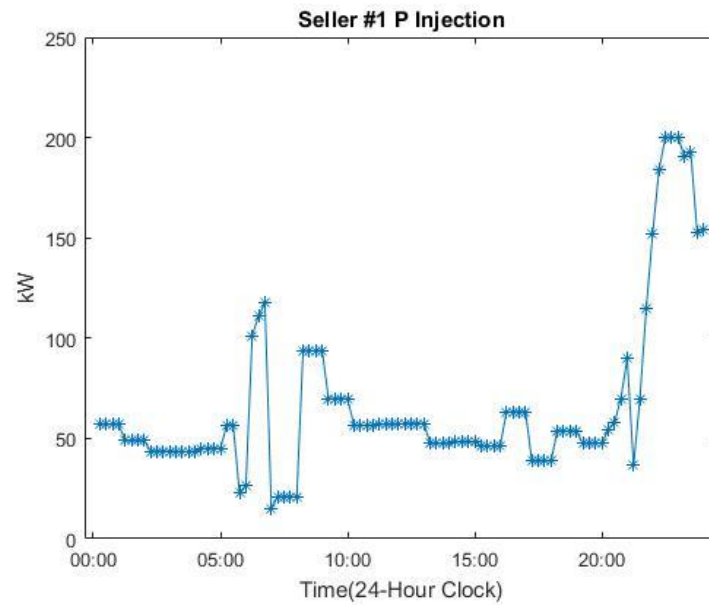
Figure 103: Seller #1 real power injection (Case#1-energy market)
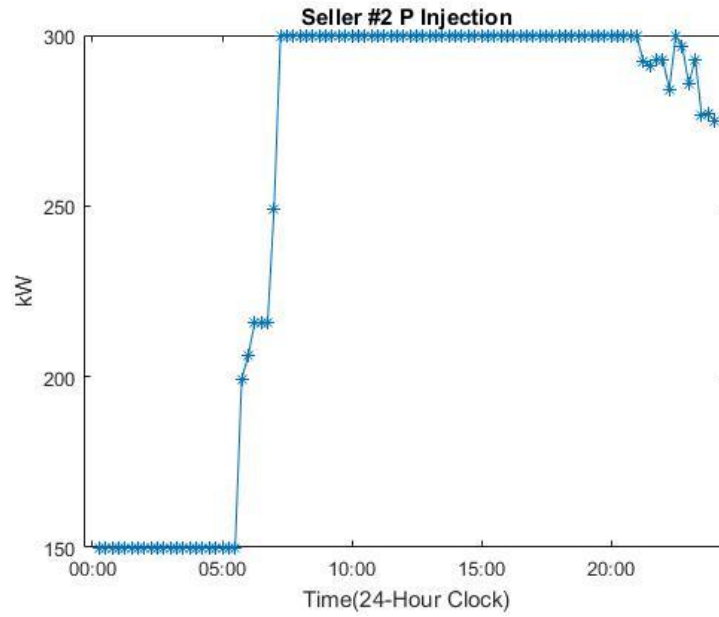
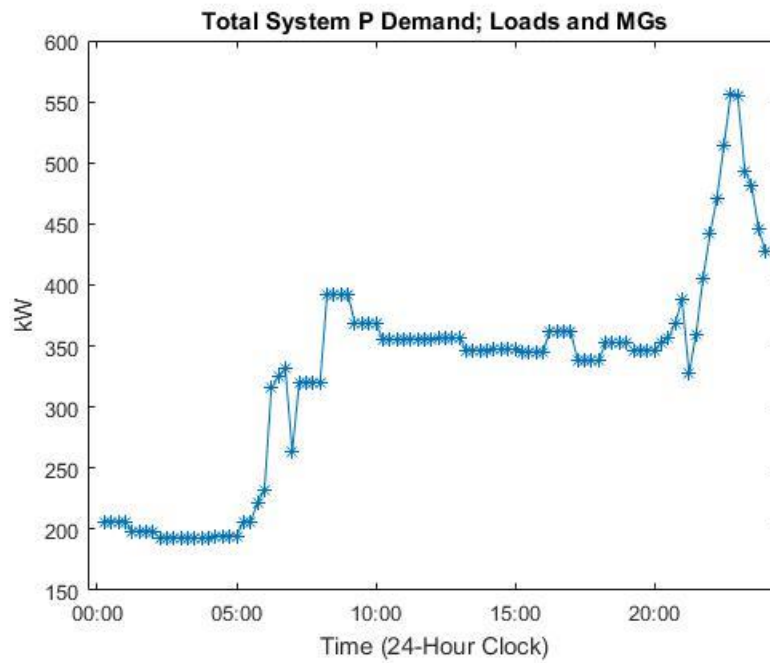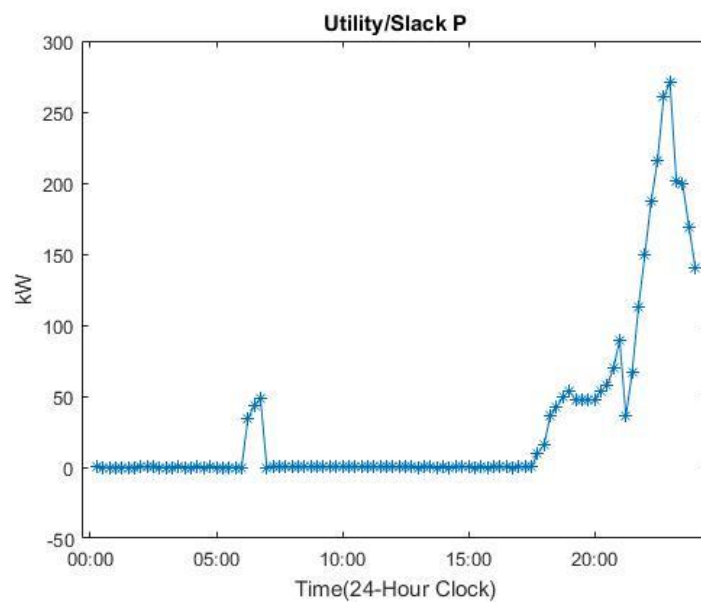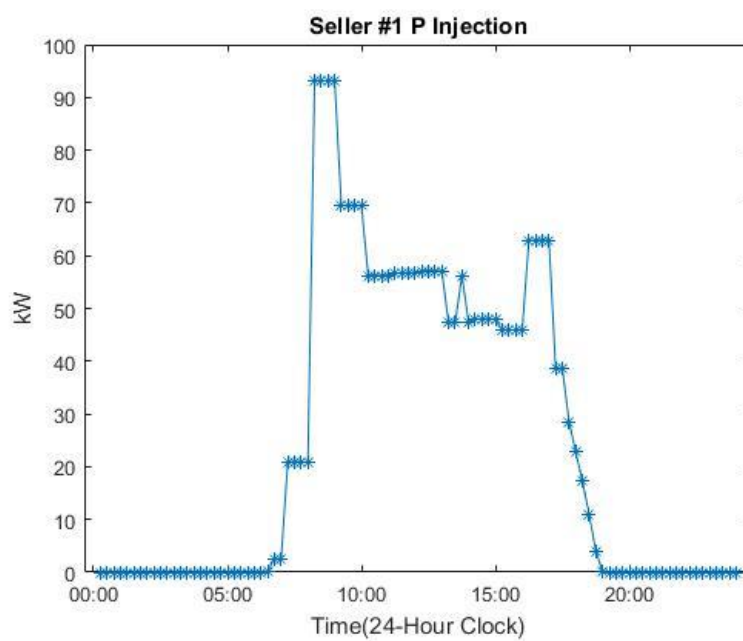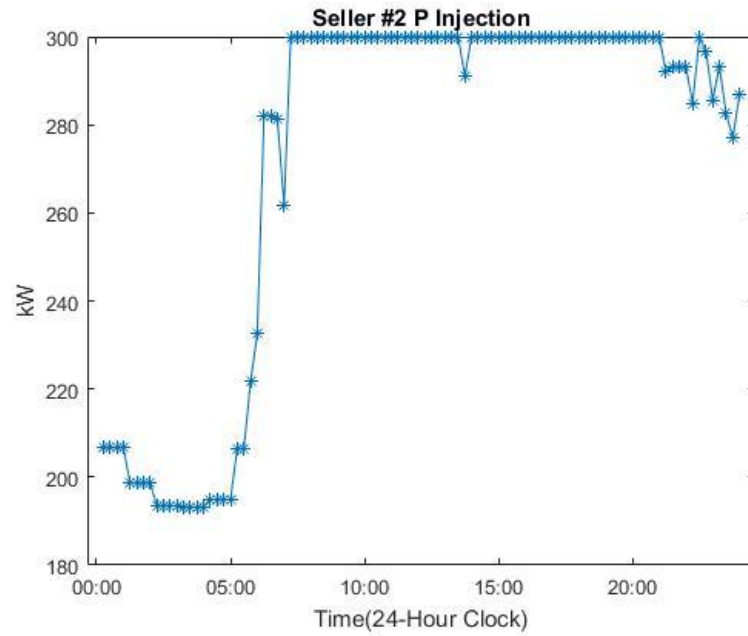*Figure 104: Seller #2 real power injection (Case#1-energy market)*

Figure 105: Total system demand (Including loads and MGs) (Case#1-energy market)

155

The results showed that the resources available were not enough to cover the whole demand. The utility had to deliver energy during the night, were the demand is higher. It can be noticed from figure 103 and figure 104 that seller #2 injected more power than seller #1. This makes sense because seller #2 is closer to the MG. Seller #1 is further than seller #2 and has to inject more power to supply the demand, which is more expensive and increases the dispatch cost in the market. For this case, the maximum power demanded from the utility was around 75-kW. Figure 105 shows the total system's demand, including the buyers and the MGs demand/injection.

I.2 Case #2: Seller #1 (Large PV system), Seller #2 (Fossil-Gen), MGs with a sunny day.

On this case, seller #1 is a large PV system (can deliver a maximum of 300-kW and 300-kVar but depends on a solar irradiation curve), seller #2 is a fossil-fuel generator (can deliver a maximum of 300-kW and 300-kVar) and the MGs inject/demand energy with a sunny day irradiance curve. Seller #1 is located at 2-km and seller #2 at 0.5-km from the MG. The PV system has a rate of $0.10 per kWh, and the fossil generator has a rate of $0.16 per kWh. The following graphs were obtained after simulating case #2:

Figure 106:Utility/Slack real power injection (Case#2-energy market)

Figure 107: Seller #1 real power injection (Case#2-energy market)

157

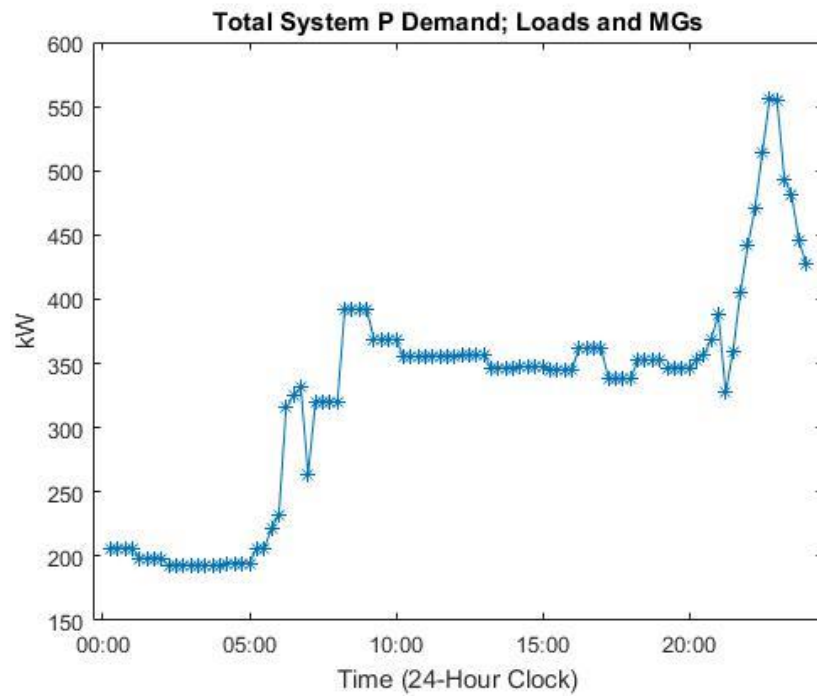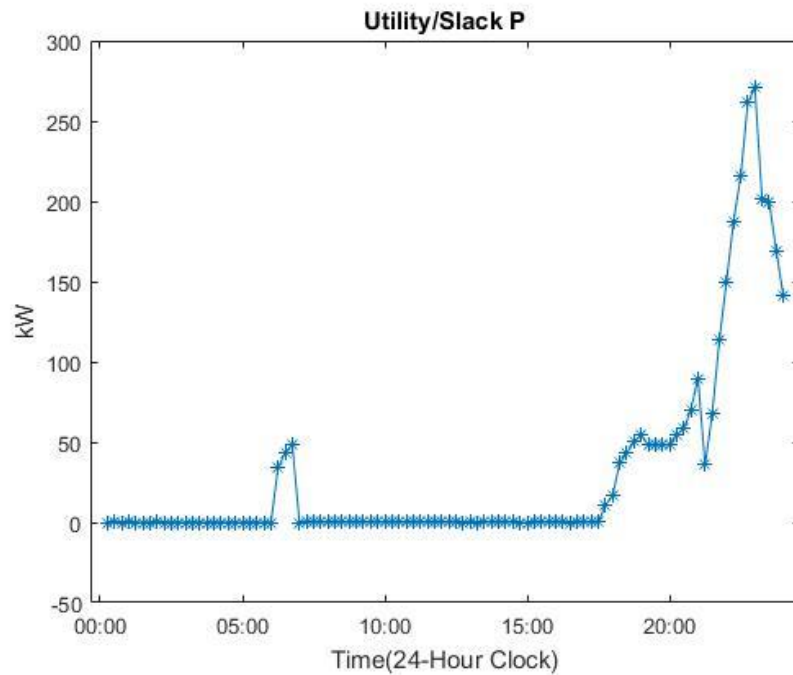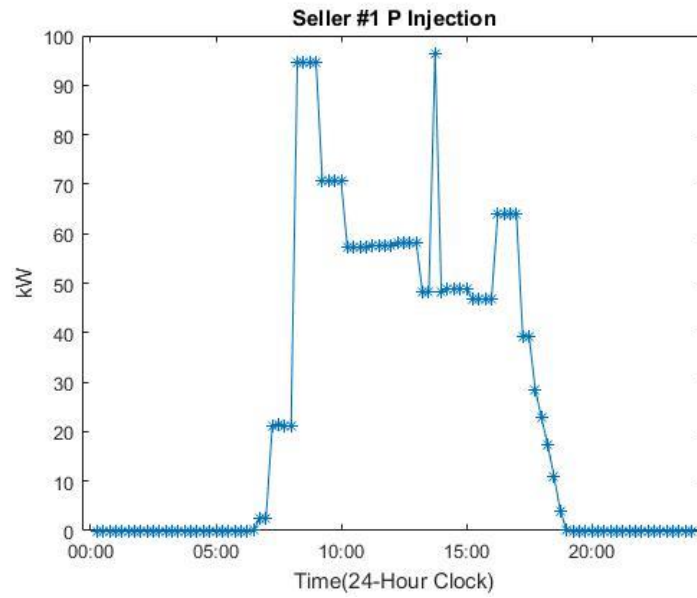*Figure 108: Seller #2 real power injection (Case#2-energy market)*

Figure 109: Total system demand (Including loads and MGs) (Case#2-energy market)

158

On this case, more power is being demanded from the utility because the seller #1 cannot provide a constant power like seller #2. Since seller #2 is closer to the MG, it delivered more power that seller #1. For this case, the maximum power demanded from the utility was around 275-kW, significantly higher than in case #1 (3.7-times higher).

I.3 Case #3: Seller #1 (Large PV system), Seller #2 (Fossil-Gen), MGs with a sunny day.

This case is the same as case #2, but now seller #1 (Large PV system) is located at 10km. The following graphs were obtained after simulating case #3:

Figure 110:Utility/Slack real power injection (Case#3-energy market)

159

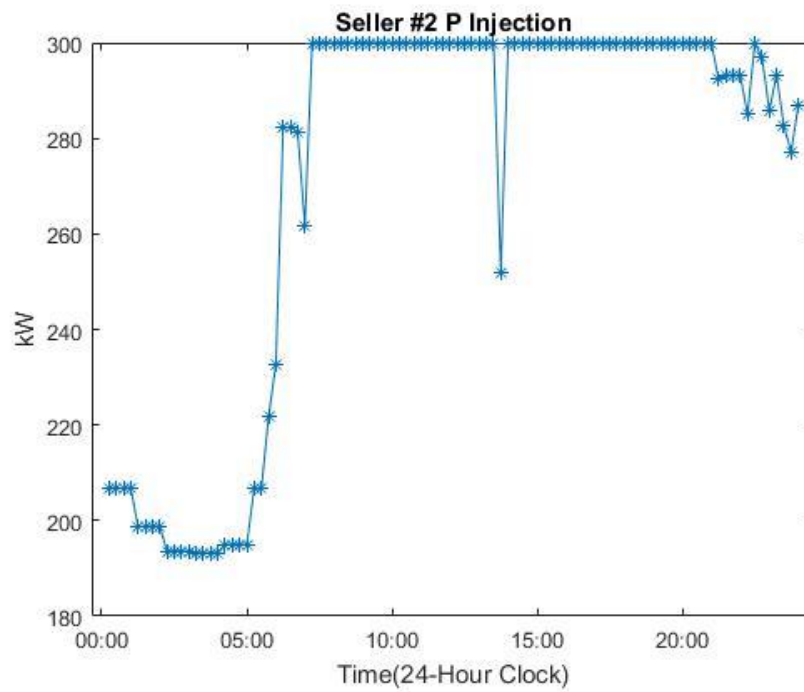*Figure 111: Seller #1 real power injection (Case#3-energy market)*

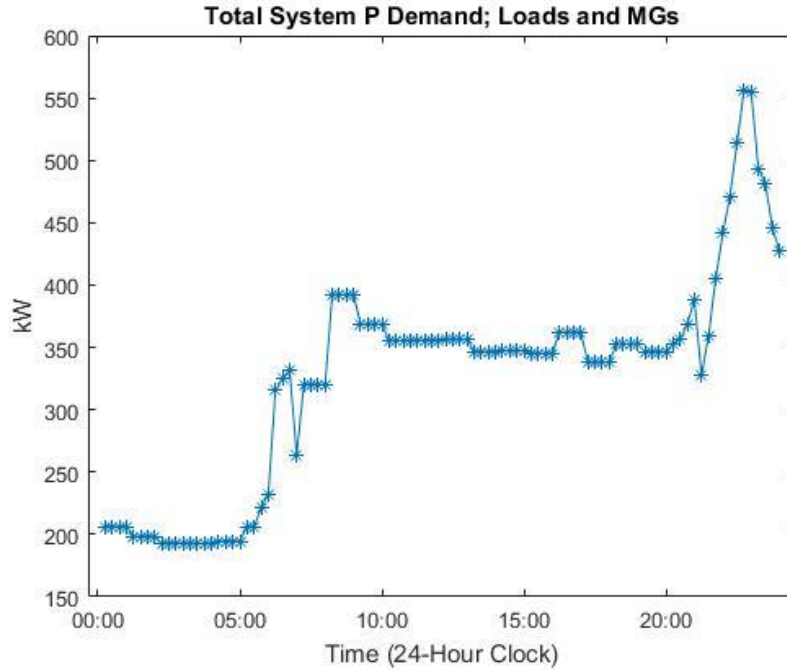*Figure 112: Seller #2 real power injection (Case#3-energy market)*

160

Figure 113: Total system demand (Including loads and MGs) (Case#3-energy market)

The results are very similar to case #2. Thus, placing seller #2 at 10-km did not change the optimization results significantly; Again, seller #2 dispatched more power because it was closer to the MG.

I.4 Case #4: Seller #1 (Large PV system), Seller #2 (Fossil-Gen), MGs with a cloudy day.

This case is the same as case #3, but now MGs inject/demand energy with a cloudy day irradiance curve. The following graphs were obtained after simulating case #4:
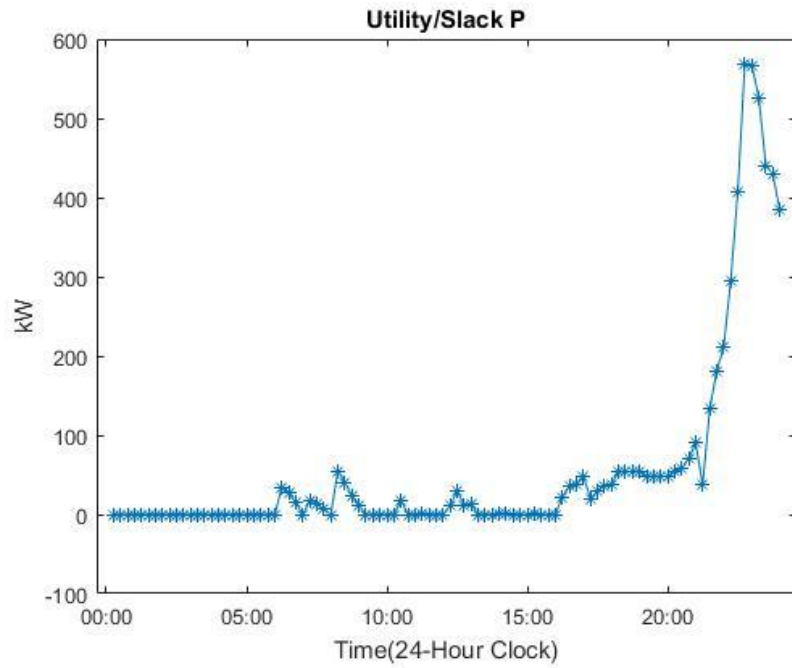
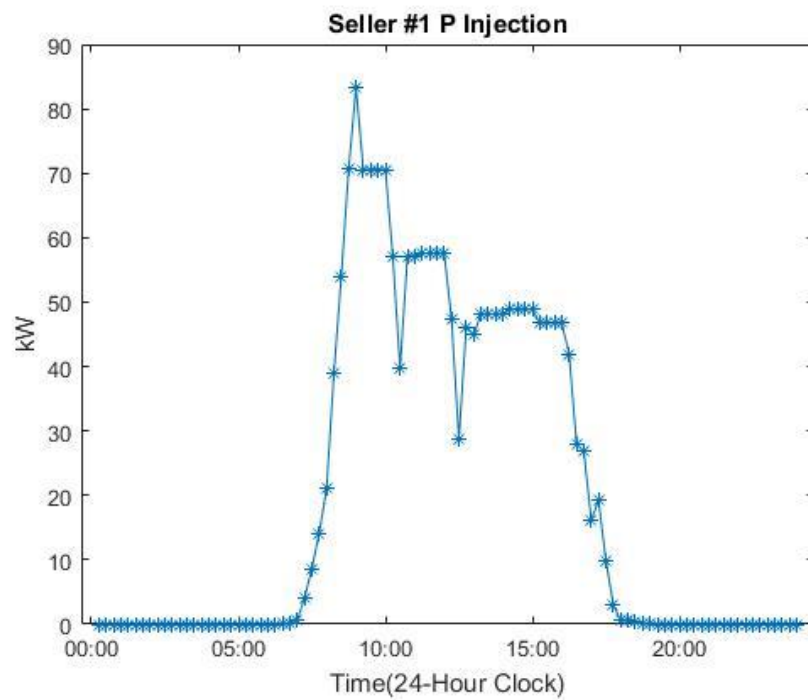*Figure 114:Utility/Slack real power injection (Case#4-energy market)*

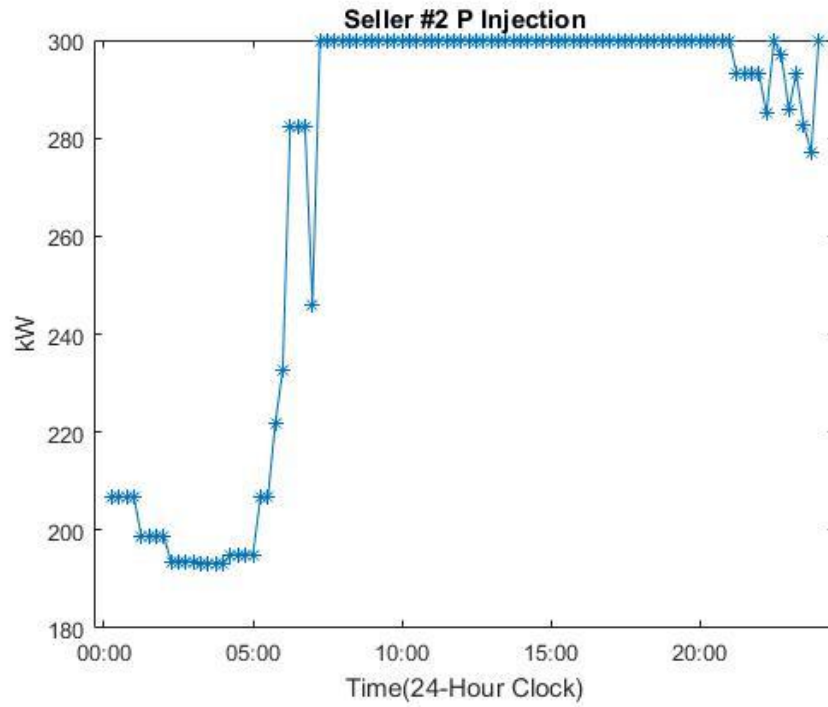*Figure 115: Seller #1 real power injection (Case#4-energy market)*

162

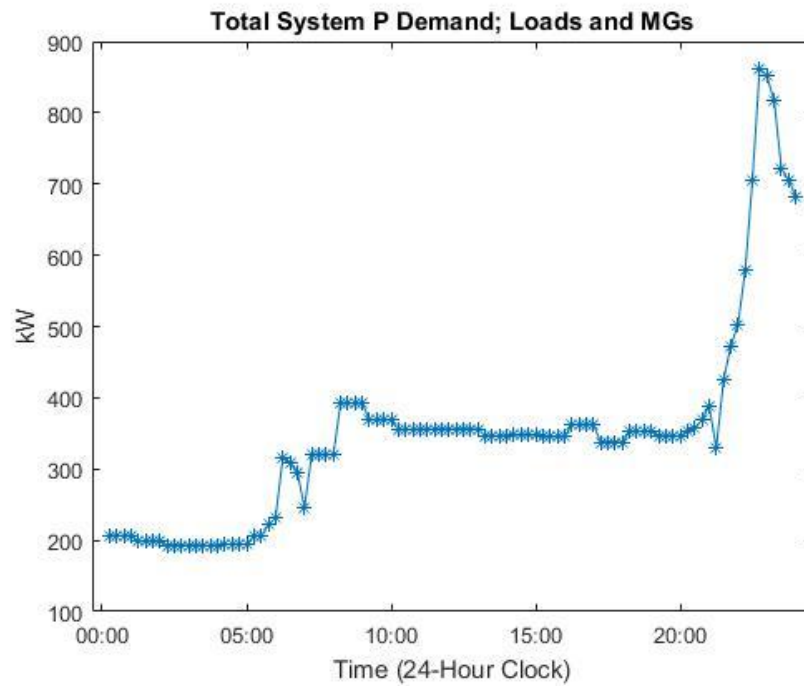*Figure 116: Seller #2 real power injection (Case#4-energy market)*

Figure 117: Total system demand (Including loads and MGs) (Case#4-energy market)

163

On this case, more energy was demanded from the Utility because the MGs demand/injection and seller #1 depend on the solar irradiation. Seller #1 and the MG's resources could not produce the same amount of energy with a cloudy day, thus the utility delivered the energy mismatch to the market.

I.5 Discussion (Energy Market)

This was a preliminary test to show the algorithm's flexibility to be modified and adapted to solve and optimize a particular problem desired by the user. In this case, an energy market at the distribution level with sellers, buyers and MGs. With this test, the market operator can determine how much energy each seller will deliver, how much energy the MGs will demand or how much will they deliver, how much energy will be required from the utility and the dispatch costs of each resource. The tool could be modified to consider other objectives, penalties and constraints in the market.